



**HAL**  
open science

# Catalysts for butadiene synthesis by Ostromyslensky process developed by surface organometallic chemistry

Pooja Gaval

► **To cite this version:**

Pooja Gaval. Catalysts for butadiene synthesis by Ostromyslensky process developed by surface organometallic chemistry. Other. Université de Lyon; Università degli studi (Bologne, Italie), 2018. English. NNT : 2018LYSE1315 . tel-02124491

**HAL Id: tel-02124491**

**<https://theses.hal.science/tel-02124491>**

Submitted on 9 May 2019

**HAL** is a multi-disciplinary open access archive for the deposit and dissemination of scientific research documents, whether they are published or not. The documents may come from teaching and research institutions in France or abroad, or from public or private research centers.

L'archive ouverte pluridisciplinaire **HAL**, est destinée au dépôt et à la diffusion de documents scientifiques de niveau recherche, publiés ou non, émanant des établissements d'enseignement et de recherche français ou étrangers, des laboratoires publics ou privés.



N°d'ordre NNT : xxx

## **THESE de DOCTORAT DE L'UNIVERSITE DE LYON**

opérée au sein de  
**l'Université Claude Bernard Lyon 1**

**Ecole Doctorale de Lyon**  
N° ED206

**Spécialité de doctorat : Chimie**  
**Discipline : Chimie Industrielle Durable**

Soutenue publiquement le 12/12/2018,  
par :

**Pooja GAVAL**

---

### **Catalyseurs pour la synthèse du butadiène via le procédé Ostromyslensky développés par Chimie organométallique de surface**

---

Devant le jury composé de :

*Prof. Stephane DANIELE*

*Prof. Susannah SCOTT*

*Dr. Regis GUAVIN*

*Prof. Francesco DI-RENZO*

*Prof. Stefania ALBONETTI*

*Dr. Elsje Alessandra QUADRELLI*

*Prof. Fabrizio Cavani*

Université Lyon 1

University of California, Santa  
Barbara

Université Lille - CNRS

CNRS-ICG Montpellier

Università di Bologna

CNRS-C2P2 Lyon

Università di Bologna

Président

Rapporteur

Rapporteur

Examineur

Examinatrice

Directrice de thèse

Co-directeur de thèse



ALMA MATER STUDIORUM  
UNIVERSITÀ DI BOLOGNA

Alma Mater Studiorum – Università di Bologna  
in cotutela con Université Claude Bernard Lyon 1

DOTTORATO DI RICERCA IN

**Chimica Industriale**

Ciclo XXXI

Settore Concorsuale di afferenza: 03/C2  
Settore Scientifico disciplinare: CHIM/04

Catalysts for butadiene synthesis by  
Ostromyslensky process developed by surface  
organometallic chemistry

**Presentata da:** Pooja GAVAL

**Coordinatore Dottorato**

*Dr. Elsje Alessandra Quadrelli*  
*Prof. Fabrizio Cavani*

**Relatore**

*Prof. Susannah Scott*  
*Dr. Regis Gauvin*

**Esame finale anno 2018**

# UNIVERSITE CLAUDE BERNARD - LYON 1

## Président de l'Université

Président du Conseil Académique

Vice-président du Conseil d'Administration

Vice-président du Conseil Formation et Vie Universitaire

Vice-président de la Commission Recherche

Directrice Générale des Services

**M. le Professeur Frédéric FLEURY**

M. le Professeur Hamda BEN HADID

M. le Professeur Didier REVEL

M. le Professeur Philippe CHEVALIER

M. Fabrice VALLÉE

Mme Dominique MARCHAND

## ***COMPOSANTES SANTE***

Faculté de Médecine Lyon Est – Claude Bernard

Faculté de Médecine et de Maïeutique Lyon Sud – Charles Mérieux

Faculté d'Odontologie

Institut des Sciences Pharmaceutiques et Biologiques

Institut des Sciences et Techniques de la Réadaptation

Département de formation et Centre de Recherche en Biologie Humaine

Directeur : M. le Professeur G.RODE

Directeur : Mme la Professeure C. BURILLON

Directeur : M. le Professeur D. BOURGEOIS

Directeur : Mme la Professeure C. VINCIGUERRA

Directeur : M. X. PERROT

Directeur : Mme la Professeure A-M. SCHOTT

## ***COMPOSANTES ET DEPARTEMENTS DE SCIENCES ET TECHNOLOGIE***

Faculté des Sciences et Technologies

Département Biologie

Département Chimie Biochimie

Département GEP

Département Informatique

Département Mathématiques

Département Mécanique

Département Physique

UFR Sciences et Techniques des Activités Physiques et Sportives

Observatoire des Sciences de l'Univers de Lyon

Polytech Lyon

Ecole Supérieure de Chimie Physique Electronique

Institut Universitaire de Technologie de Lyon 1

Ecole Supérieure du Professorat et de l'Education

Institut de Science Financière et d'Assurances

Directeur : M. F. DE MARCHI

Directeur : M. le Professeur F. THEVENARD

Directeur : Mme C. FELIX

Directeur : M. Hassan HAMMOURI

Directeur : M. le Professeur S. AKKOUCHE

Directeur : M. le Professeur G. TOMANOV

Directeur : M. le Professeur H. BEN HADID

Directeur : M. le Professeur J-C PLENET

Directeur : M. Y.VANPOULLE

Directeur : M. B. GUIDERDONI

Directeur : M. le Professeur E.PERRIN

Directeur : M. G. PIGNAULT

Directeur : M. le Professeur C. VITON

Directeur : M. le Professeur A. MOUGNIOTTE

Directeur : M. N. LEBOISNE



*“The world always seems a little brighter when you've just made something that was not there before.”*

*-Neil Gaiman*

# Acknowledgement

The pursuit of this PhD has as much been a journey in scientific exploration as it has been about self-discovery. In this I have been immensely fortunate to have had people around me, who both steered and supported me through this adventure.

My first and foremost thanks must go to my supervisor, Dr. Elsje Alessandra Quadrelli, whose scientific fervor and insight have been the guiding force behind this work. Her guidance has been instrumental not only in the pursuit of this research, but in the development of a sound rationale to conduct scientific inquiry. Our many interactions have shaped my work ethic and will continue to guide me in future. I take this opportunity to thank her also on personal note for always believing in me and helping me believe in myself during the tougher times.

I am most grateful to Prof. Fabrizio Cavani whose scientific expertise has shaped every aspect of this research. His insightful questions helped me explore new directions to conduct experiments. My mobility in Bologna will always remind me of his warm presence and concern for my well being in the new lab and city.

My deepest words of gratitude go to Dr. Mostafa Taoufik whose ideas and scientific inputs form the backbone of this work. I appreciate the intense discussions that boosted my scientific appetite to keep learning more about the field of surface organometallic chemistry and chemistry as whole.

I must also extend my thanks to Dr. Aimery DeMallmann who has been responsible for conducting and helping me interpret all of the EXAFS experiments that are a part of this thesis. I thank Dr. Kai Szeto for always extending a helpful hand whether it be in conducting experiments or in discussing the principle and workings of any and every instrument in our laboratory. I am also grateful to Dr. Clement Camp, Mrs. Christine Lucas, Dr. Nesrine Cherni and Mr. Laurent Veyre from CPE, Lyon for their timely help. I must thank Mr. Ruben Vera from University of Lyon 1 for XRD characterizations of the material, Prof. Silvia Bordiga and Dr. Alessandro Damin from University of Torino for UV-vis characterization and Dr. Mimoun Aouine from IRCELYON for the HRSTEM analysis.

SINCHEM is an administratively intense program. I must thank Mrs. Emmanuelle Foulhe (CPE, Lyon) and Mrs. Angela Maritato (UniBo) for being extremely kind and helpful in keeping me administratively up to date.

It is difficult for me to imagine the completion of this thesis without the help and support from Dr. Juliana Velasquez Ochoa. During the short time that was available in Bologna, it was her constant help and guidance that enabled successful completion and interpretation of experiments related to catalytic testing. I also thank my colleagues from Bologna-Francesco, Tomaso, Aisha, Valeria, Danilo and Giada for their complete support during the period of my mobility.

In Lyon I was found myself extremely lucky to have been surrounded by some extremely astute and insightful colleagues. I would specially like to mention Cherif and Marc for valuable discussions at a crucial time. A very special thanks to Vittoria and Iurii for their help regarding translations and more. I extend a warm thanks to all my other colleagues from Lyon- Jessica, Nicolas, Dominique, Marc, Pascal, Giuliana, Debora, Frederic, Anthony, Matthieu, Clement and Ravi for being such a marvelous support at all times. I extend a very special thanks to Tapish for being my go-to person throughout the three years in Lyon. To say the least it would have been a very different tenure without his constant support and assurance.

Being a part of the SINCHEM program has been an experience in being part of a global family. I will forever cherish fond memories from each of our interactions. I would like to express my warm regards to Prof. Stefania Albonetti for incredible effort on her part in establishing the program. I wish to give a special mention to Tin and Matilde for being a source of constant strength and support.

I was told every PhD is a different struggle and I realized nothing helps more but to seek help in times of distress. I am glad I found such a fantastic mentor in Ms. Shruti Chakravarti who lifted me up and steered me back into the arena every such time.

My thanks will never be complete without mentioning my friends from the other part of the globe who kept loving and nourishing me despite the time zones. I thank Puneet, Adwait, Mihir, Nikita, Radha, Anagha, Noopur, Rajashree, Divya, Priya, for being rock solid pillars of support and to Surahit for being a constant in this otherwise tumultuous journey.

My final words of gratitude are reserved for my parents. I must thank them for their continual love and support, but even more for inculcating the spirit of constant learning and unlearning, which has been the foundation for all my scientific endeavors.

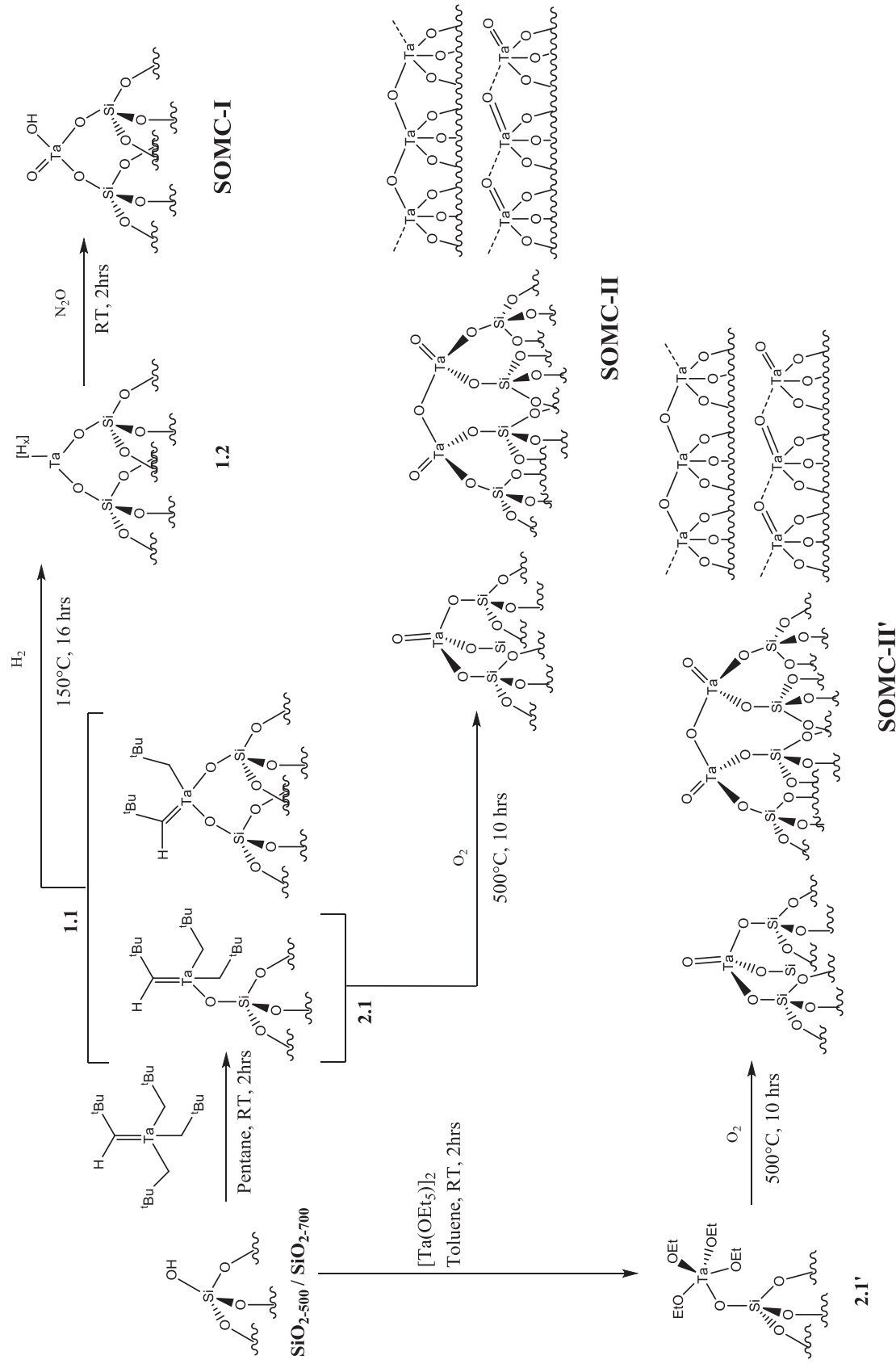
I am humbly aware that this thesis stands on the shoulders of all of the above and many more people. I extend my heartfelt gratitude to all of them.

# Abbreviations

$\delta$	chemical shift in NMR downfield from TMS, ppm
$\nu_{(A-B)}$ and $\delta_{(A-B)}$	stretching and bending frequencies of A-B bond
AA	acetaldehyde
BD	butadiene
BET	Brunauer–Emmett–Teller surface area
<sup>t</sup> Bu	tertbutyl, -CH(CH <sub>3</sub> ) <sub>3</sub>
DRIFT	diffuse reflectance infrared fourier transform
ETB	ethanol-to-butadiene
EtOH	ethanol
EXAFS	extended X-ray absorption fine structure
FTIR	fourier transform infrared spectroscopy
FWHM	full width at half maximum
GC	gas chromatography
HRSTEM	high resolution scanning tunneling microscopy
nm	nano meter
Np	neopentyl, -CH <sub>2</sub> C(CH <sub>3</sub> ) <sub>3</sub>
OEt	Ethoxy, -OC <sub>2</sub> H <sub>5</sub>
NMR	nuclear magnetic resonance
RT	room temperature
SBA	santa barbara amorphous
SOMC	surface organometallic chemistry
SSNMR	solid state nuclear magnetic resonance spectroscopy
TGA	thermogravimetry analysis
THF	tetrahydrofuran
TOS	time on stream
UHV	ultra-high vacuum
UV-vis-DRS	ultraviolet-visible-diffused reflectance spectroscopy
WHSV	weight hour space velocity
XANES	x-ray absorption near edge structure
XRD	x-ray diffraction



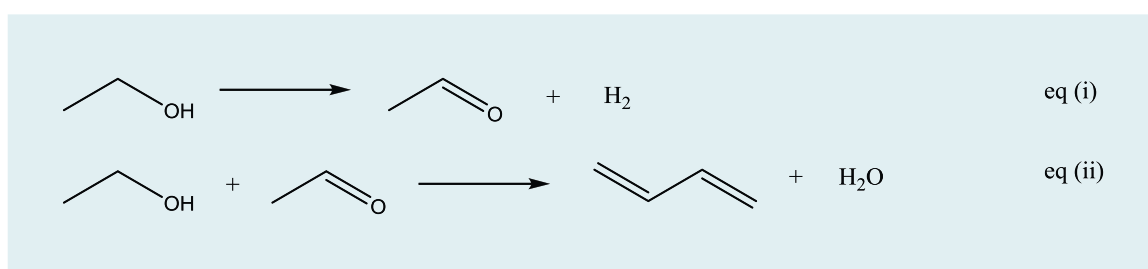
# Overall scheme and Nomenclature





# Summary

In the recent years, on-purpose synthesis of butadiene using bioethanol has gained unprecedented attention owing to rise in interest of bio-based building blocks along with steeply increasing demand for butadiene.<sup>1</sup> A relevant process in this context is the Ostromyslensky process, which proceeds via two steps, involving dehydrogenation of ethanol to acetaldehyde in a separate step (see eq. i), followed by butadiene production in the second stage by co-feeding ethanol and acetaldehyde (see eq. ii).<sup>2</sup>



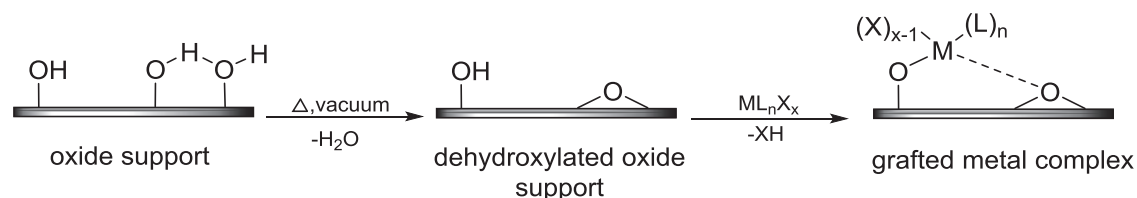
Although the economic viability and feasibility of this ethanol to butadiene (ETB) process is well-established, there is a room for better catalytic performances and selectivity.<sup>3</sup> The productivity of this transformation is marred by several parallel reactions generating a large number of side products. Additionally the process is known to have short catalyst regeneration cycle due the rapid deactivation of catalyst by coke formation.<sup>4</sup>

Following the original catalyst developed by Ostromyslensky, there has been a constant upsurge in the study of Ta/SiO<sub>2</sub> systems as catalysts for two step ETB transformations. A notable study is that by Jeong et al.<sup>5</sup> who prepared a series of ordered mesoporous silica (OMS) supported Tantalum oxide samples by wetness impregnation technique followed by calcination at high temperature. The catalysts showed better catalytic performances towards butadiene production compared to the earlier systems, indicating need for better dispersed tantalum on silica catalysts. The study primarily focused on effect of surface morphology on catalytic activity while no conclusive comment was made on the surface active species. A remarkable attempt to synthesize a well-defined active specie was recently made by Dzwigaj et al<sup>6,7</sup>. who reported Ta incorporation into vacant T-atom sites of the SiBEA zeolites framework as mononuclear Ta(V) allowing for the preparation of

highly selective catalysts for 1,3-butadiene synthesis. Though both these studies point towards the usefulness of well-dispersed tantalum oxide species on silica, there is no clear evidence on the nature of the species populating the surface of the catalyst or on that of the active species taking part in catalysis.

In general, the surface of Ta(V)/SiO<sub>2</sub> systems can be complex. It could include isolated tetrahedral moieties [(≡SiO)<sub>3</sub>Ta=O], oligo- and polymeric Ta<sub>x</sub>O<sub>y</sub> species presenting simultaneously bridging O atoms, tantalate (Ta=O) and Ta–O-support bonds, and particles of bulk Ta<sub>2</sub>O<sub>5</sub> formed at much higher Ta loading.<sup>8</sup> Then to be able to successfully develop structure activity relationship for these catalysts it will be imperative to be able to selectively tailor various model catalysts with isolated and oligomeric/polymeric species on the surface of the support. To this end, one of the powerful approaches can be surface organometallic chemistry (SOMC), which permits the preparation of well-defined surface species.

Surface Organometallic Chemistry is a technique developed to tailor well-defined heterogeneous catalysts by grafting organometallic complexes on surface sites of a support in a controlled fashion.<sup>9–11</sup> This approach is based on controlling the concentration of grafting sites per unit area of the support, which in turn controls the final density of organometallics grafted on the surface. Due to its ability to perform molecularly controlled grafting, SOMC produces surface sites with a known coordination sphere. This attribute is essential in developing a structure activity relationship for a catalyst and in turn for rational design of ideal catalysts for a process.<sup>12</sup>



**Scheme 1**-Schematic representation of preparation of a well-defined catalyst using SOMC

The main requirements for applying SOMC approach is the presence of a well-characterized support, and an organometallic complex - ML<sub>n</sub>X<sub>x</sub> (L= functional ligand, X= ancillary ligand).<sup>13</sup> Upon grafting the complex on the support, it can be used as a catalyst by itself or be subjected to post-treatments (calcination, hydrogenation, sulfidation) to

obtain a more stable structure or to attain a new functionality. **Figure 1** schematically represents an ideal SOMC catalyst with its key components.

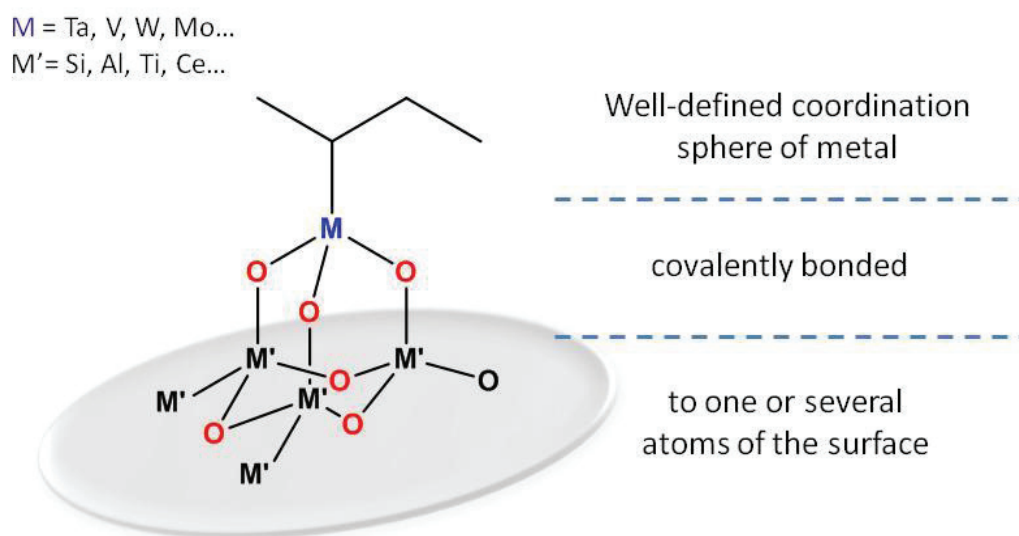


**Figure 1-** The general structure of surface organometallic compounds and the possibility of bearing different possible supports, transition metals, functional and spectator ligands

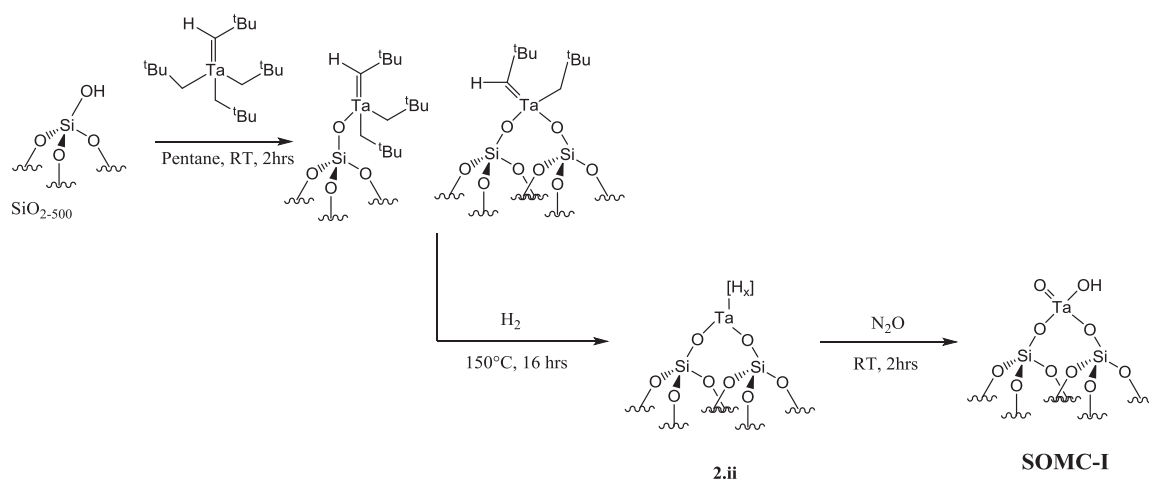
The primary aim of this work is to synthesize a family of well-defined silica-supported  $\text{TaO}_x$  catalysts with varying tantalum nuclearity and to study its effect on the second step of the Ostromyslensky process, i.e. transformation of EtOH/AA to butadiene. Secondly our aim is to use the above knowledge to build a meaningful structure activity relationship for the Ta (V)/ $\text{SiO}_2$  catalytic systems in the synthesis of BD from EtOH/AA.

As mentioned before, the grafting of tantalum alkyl complexes on partially dehydroxylated silica to obtain ‘single site’ catalysts with isolated tantalum centers has been well documented in the literature.<sup>14,15</sup> Thus, an evident strategy to synthesize single site  $\text{TaO}_x$  catalysts was via mild oxidation of these formerly studied well-defined silica supported tantalum species.

The first contribution of this thesis was to develop isolated single site  $\text{TaO}_x$  species was via mild oxidation of existing silica-supported tantalum hydrides  $[(\equiv\text{SiO})_2\text{Ta}(\text{H})_{x=1,3}]$  with  $\text{N}_2\text{O}$ . Well-defined tantalum hydride  $[(\equiv\text{SiO})_2\text{Ta}(\text{H})_{x=1,3}]$  species and their precursing tantalum alkyl  $[\equiv\text{SiOTa}(\text{=CH}^t\text{Bu})(\text{CH}_2^t\text{Bu})_2]$  species have been a model study in surface organometallic chemistry.<sup>9,10,16</sup> Materials with these species were synthesized according to the literature and their formation was monitored via IR, NMR spectroscopy and

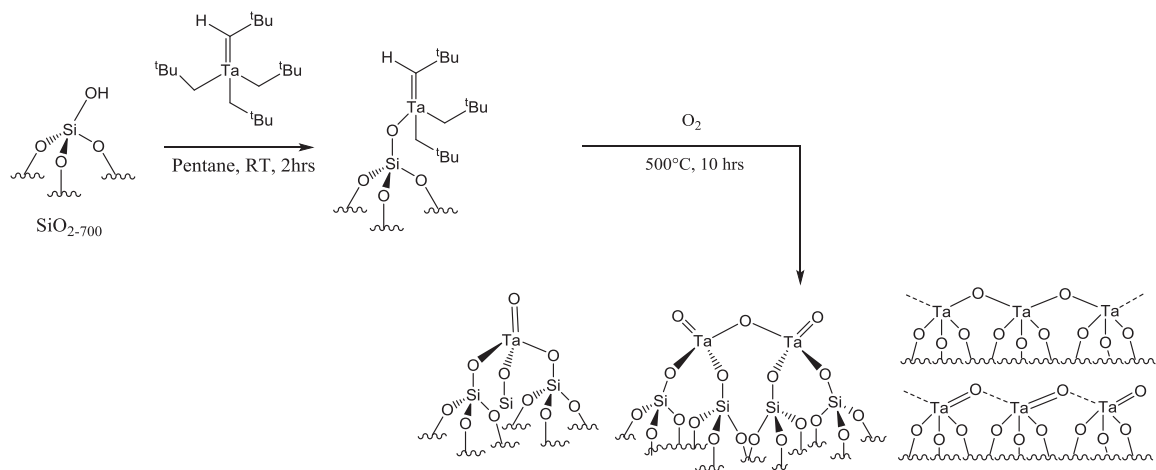
elemental analysis. Additionally, for the first time attempt was made to visualize their spatial arrangement on the surface of silica via HRSTEM.

Upon oxidative treatment of  $[(\equiv\text{SiO})_2\text{Ta}(\text{H})_{x=1,3}]$  with  $\text{N}_2\text{O}$  at room temperature, the material (**SOMC-I**) was characterized by IR, NMR spectroscopies, as well as elemental analysis. Formation of mostly well-defined isolated mono-tantalate specie  $[(\equiv\text{SiO})_2\text{Ta}(=\text{O})(\text{OH})]$  was established via EXAFS analysis. HRSTEM analysis of the material found largely isolated dispersion of Ta (V) center, with some degree of agglomeration.



**Scheme 1**

The second approach pursued in this thesis was to generate well-defined surface  $\text{TaO}_x$  species via calcination of silica supported peralkyl species  $[(\equiv\text{SiO})\text{Ta}(=\text{CH}^t\text{Bu})(\text{CH}_2^t\text{Bu})_2]$  at  $500^\circ\text{C}$  for 10 hrs under dry oxygen. The material so formed (**SOMC-II**), was characterized by IR, NMR spectroscopies, EXAFS analysis and HRSTEM microscopy. **Scheme 3** represents the scheme for synthesis of **SOMC-II** along with the representative HRSTEM micrographs of the surface species involved. The EXAFS spectroscopy confirmed the absence of  $\text{Ta}_2\text{O}_5$ , while suggesting the possibility of Ta-Ta interaction. The HRSTEM microscopy evidenced co-existence of isolated Ta (V) centers along with Ta species in a string like arrangement. This data together with the information from literature suggested the presence of a mixture of mononuclear, dinuclear and oligomer like species on the surface of **SOMC-II**.



**Scheme 2**

The family of catalysts synthesized by SOMC protocols was tested in the production of butadiene from ethanol and acetaldehyde in a lab scale continuous flow reactor under atmospheric pressure. A catalyst amount of 0.25 g was loaded in the reactor in the form of powder. Inlet feed molar ratios were always constant and were set at 2 mol% ethanol and acetaldehyde mixture with 98% nitrogen. Downstream products were fed to an automatic sampling system for gas-chromatography. **Figure 2** shows the schematic diagram for the lab scale reactor used in the catalytic testing.

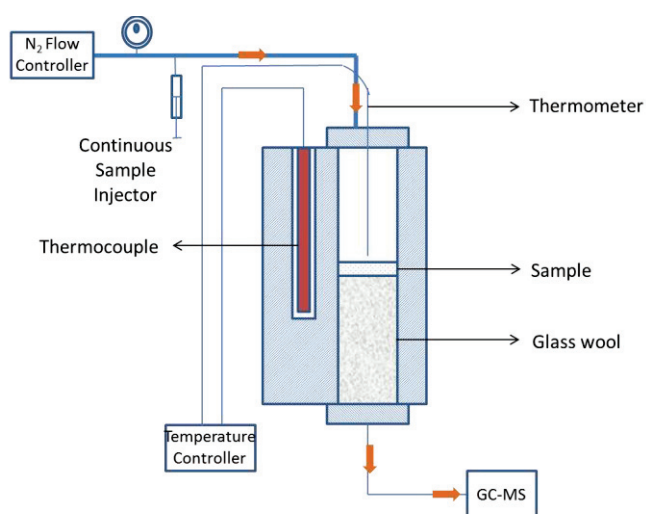


**Figure 2-** Reaction apparatus for synthesis of Butadiene from Ethanol and Aldehyde

**Figure 3** provides a comparison of the most performing catalysts from each of the two SOMC routes with the best performing tantalum based systems studied in literature. When tested under comparable catalytic testing conditions, SOMC based catalysts show excellent BD selectivity and yield as compared to the best performing Ta-based catalysts in literature. **SOMC-I** with isolated Ta(V) sites exhibits the best performance with BD selectivity of **86.9%** and BD yield of **48.2%**

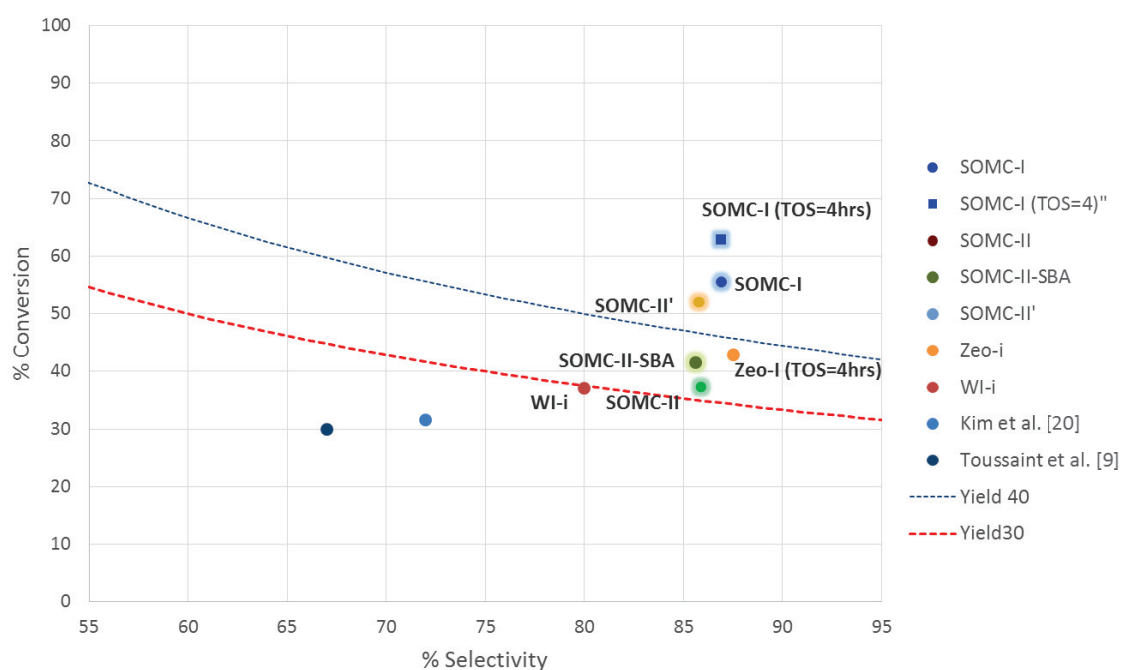


**Figure 3-** Catalytic activity of SOMC based catalysts compared to state-of-the-art tantalum based catalysts in conversion of EtOH/AA to BD

Notably, both **SOMC-I** and **SOMC-II** exhibit extremely narrow product distribution when compared with catalysts synthesized by conventional wetness impregnation techniques. The former three catalysts represent systems with relatively well-defined and homogeneous surface species. It can be anticipated that the presence of homogeneous surface species. In **Figure 4** shows the product distributions for the catalysts in consideration.

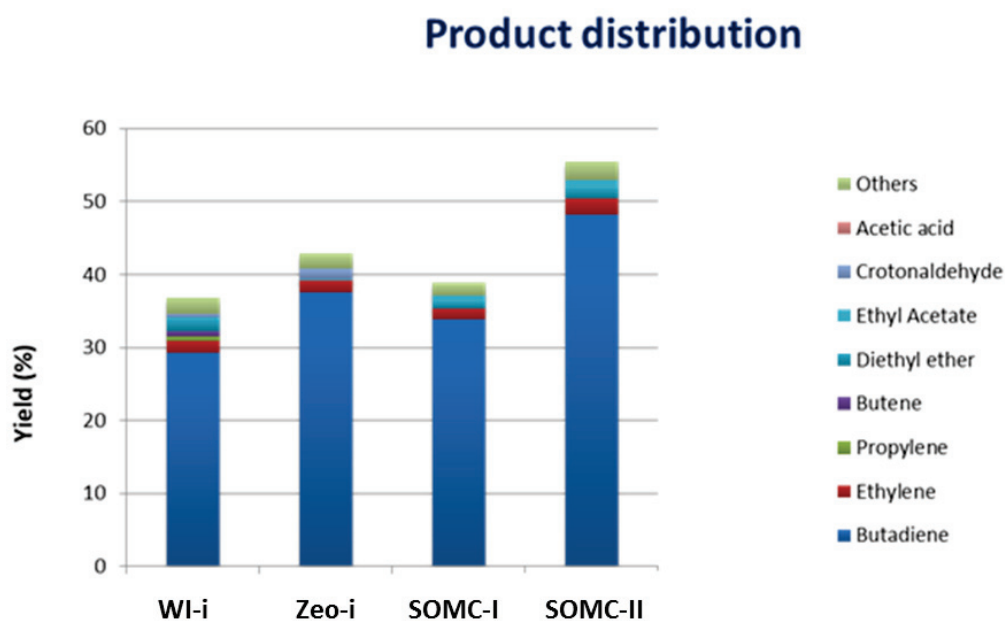


**Figure 4**-Product distribution of catalyst in consideration (i) WI-I (ii) Zeo-I (iii) SOMC-I (iv) SOMC-II

HRSTEM analysis of **SOMC-I**, pre-catalysis and post catalysis indicated evolution of isolated Ta(V) sites into string like arrangements similar to the surface of **SOMC-II**. This decrease in the concentration of isolated Ta (V) sites on the surface of **SOMC-I** also resulted in decrease in the overall conversion of EtOH/AA. Based on the combined information from catalytic activity tests and HRSTEM analysis it can be regarded probable that isolated Ta (V) centers act as the primary active sites in the conversion of EtOH/AA to BD while the Ta atoms in a string like organization show considerable but reduced activity in the same transformation.

Assuming isolated  $[(\equiv\text{SiO})_2\text{Ta}(=\text{O})(\text{OH})]$  to be the active site in the transformation of EtOH/AA to BD, an attempt was made to understand the mechanism of the reaction on the surface of SOMC-I. Based on the widely accepted Kagan mechanism, initially two molecules of acetaldehyde combine to form crotonaldehyde, which is then reduced by ethanol to form crotyl alcohol. This crotyl alcohol is ultimately dehydrated to butadiene. The Meerwein-Ponndorf-Verley reduction of crotonaldehyde is thought to be catalyzed by tantalum.<sup>17,18</sup> Based on in-situ DRIFT experiments for adsorption of (i) ethanol and (ii) a mixture of ethanol and acetaldehyde on the surface of the catalyst at 350°C, the following mechanism was hypothesized for the reduction step on the isolated Ta (V)

center (Figure 5).

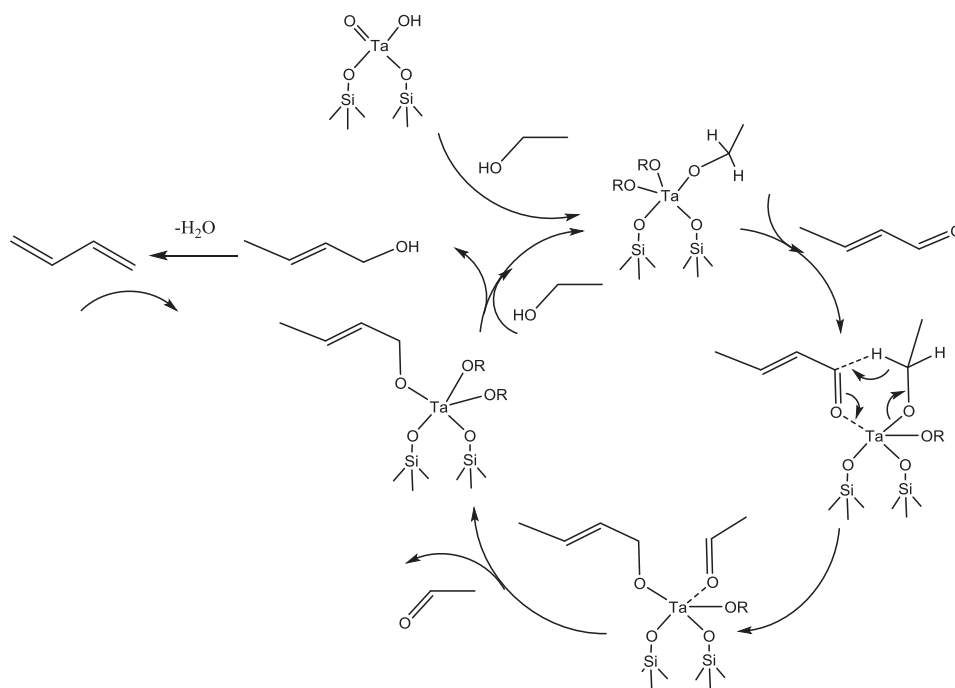


**Figure 5-** Proposed and hypothesized reaction mechanism for MPV reduction over the Ta (V) site of SOMC-I

Therefore, SOMC was found to be a successful approach in developing highly performing catalysts for the transformation of EtOH/AA to BD. Moreover the findings from this project illustrate the potential of SOMC technique in developing material with tunable surface properties via adjusting the nature and the number of surface active sites. This property can prove highly beneficial in developing multifunctional catalysts for various industrial processes.

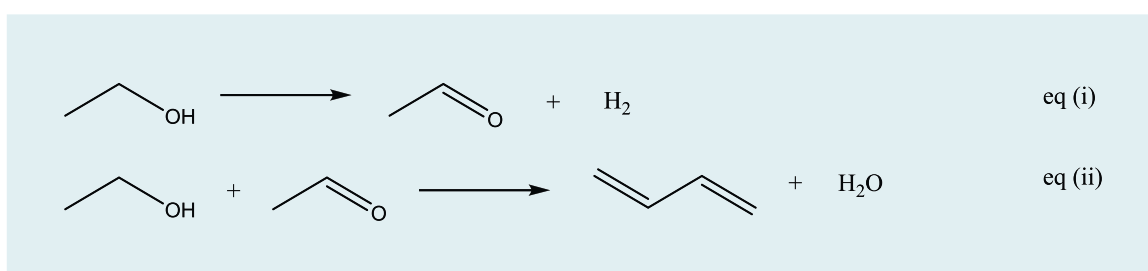
## References

1. Cavani, F., Albonetti, S., Basile, F. & Gandini, A. *Chemicals and fuels from bio-based building blocks*. (2016).
2. Makshina, E. V. *et al.* Review of old chemistry and new catalytic advances in the on-purpose synthesis of butadiene. *Chem. Soc. Rev.* **43**, 7917–7953 (2014).
3. Pomalaza, G., Capron, M., Ordonsky, V. & Dumeignil, F. Recent Breakthroughs in the Conversion of Ethanol to Butadiene. *Catalysts* **6**, 203 (2016).
4. Kim, T. W. *et al.* Butadiene production from bioethanol and acetaldehyde over tantalum oxide-supported spherical silica catalysts for circulating fluidized bed. *Chem. Eng. J.* **278**, 217–223 (2015).
5. Chae, H.-J. *et al.* Butadiene production from bioethanol and acetaldehyde over tantalum oxide-supported ordered mesoporous silica catalysts. *Applied Catal. B, Environ.* **150–151**, 596–604 (2014).
6. Kyriienko, P. I., Larina, O. V., Soloviev, S. O., Orlyk, S. M. & Dzwigaj, S. High selectivity of TaSiBEA zeolite catalysts in 1,3-butadiene production from ethanol and acetaldehyde mixture. *Catal. Commun.* **77**, 123–126 (2016).
7. Tielens, F., Shishido, T. & Dzwigaj, S. What Do Tantalum Framework Sites Look Like in Zeolites? A Combined Theoretical and Experimental Investigation. *J. Phys. Chem.* **114**, 9923–9930 (2010).
8. Barman, S. *et al.* Single-Site VO<sub>x</sub> Moieties Generated on Silica by Surface Organometallic Chemistry: A Way To Enhance the Catalytic Activity in the Oxidative Dehydrogenation of Propane. *ACS Catal.* **6**, 5908–5921 (2016).
9. Chabanas, M. *et al.* Molecular insight into surface organometallic chemistry through the combined use of 2D HETCOR solid-state NMR spectroscopy and silsesquioxane analogues. *Angew. Chemie - Int. Ed.* **40**, 4493–4496 (2001).
10. Le Roux, E. *et al.* Detailed structural investigation of the grafting of [Ta(=CHtBu)(CH<sub>2</sub>tBu)<sub>3</sub>] and [Cp\*TaMe<sub>4</sub>] on silica partially dehydroxylated at 700 °C and the activity of the grafted complexes toward alkane metathesis. *J. Am. Chem. Soc.* **126**, 13391–13399 (2004).
11. Pelletier, J. D. A. & Basset, J.-M. Catalysis by Design: Well-Defined Single-Site

- Heterogeneous Catalysts. *Acc. Chem. Res.* **49**, 664–677 (2016).
12. Quadrelli, A. & Basset, J.-M. On silsesquioxanes' accuracy as molecular models for silica-grafted complexes in heterogeneous catalysis. *Coord. Chem. Rev.* **254**, 707–728 (2010).
  13. Copéret, C. *et al.* Surface Organometallic and Coordination Chemistry toward Single-Site Heterogeneous Catalysts: Strategies, Methods, Structures, and Activities. *Chemical Reviews* (2016).
  14. Vidal, V., Théolier, A., Thivolle-Cazat, J., Basset, J.-M. & Corker, J. Synthesis, Characterization, and Reactivity, in the C–H Bond Activation of Cycloalkanes, of a Silica-Supported Tantalum(III) Monohydride Complex:  $(\equiv\text{SiO})_2\text{TaIII-H}$ . *J. Am. Chem. Soc.* **118**, 4595 (1996).
  15. P. Avenier, M. Taoufik, A. Lesage, Solans-Monfort, Baudouin, A. de M., L. Veyre, J.-M. B. & O. Eisenstein, L. Emsley, E. A. Q. Dinitrogen Dissociation on an Isolated Surface Tantalum Atom. *Science*, **317**, 1056–1060 (2007).
  16. Soignier, S. *et al.* Tantalum hydrides supported on MCM-41 mesoporous silica: Activation of methane and thermal evolution of the tantalum-methyl species. *Organometallics* **25**, 1569–1577 (2006).
  17. Corson, B. B., Jones, H. E., Welling, C. E., Hinckley, J. A. & Stahly, E. E. *Butadiene from Ethyl Alcohol. Catalysis in the One-and Two-Stop Processes. Industrial & Engineering Chemistry* **42**, (UTC, 1950).
  18. Müller, P. *et al.* Mechanistic Study on the Lewis Acid Catalyzed Synthesis of 1,3-Butadiene over Ta-BEA Using Modulated Operando DRIFTS-MS. *ACS Catal.* **6**, 6823–6832 (2016).

# Résumé

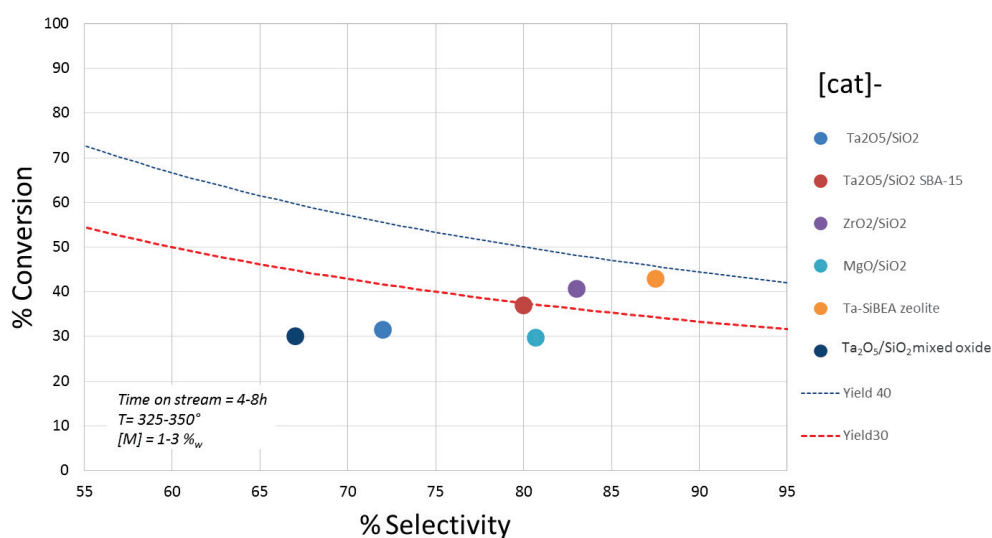
Au cours des dernières années, la synthèse ciblée du butadiène en utilisant le bioéthanol a suscité une attention sans précédent en raison de l'intérêt croissant aux matières premières biosourcées ainsi que de la demande croissante en butadiène.<sup>1</sup> Un processus pertinent dans ce contexte est le processus d'Ostromyslensky, qui s'effectue en deux étapes, comprenant la déshydrogénation de l'éthanol en acétaldéhyde en une étape séparée (eq. 1), suivie de la production de butadiène dans la deuxième étape par réaction d'acétaldéhyde avec de l'éthanol supplémentaire. (eq. 2)<sup>2</sup>



Bien que la viabilité économique et la faisabilité de cette transformation d'éthanol en butadiène (ETB) soient bien établies, de meilleures performances catalytiques et une meilleure sélectivité sont possibles.<sup>3</sup> La productivité de cette transformation est affectée par plusieurs réactions parallèles générant un grand nombre de produits secondaires. De plus, le procédé a un cycle de régénération du catalyseur court en raison de la désactivation rapide du catalyseur par formation de coke.<sup>4</sup>

À la suite du catalyseur original mis au point par Ostromyslensky, on observe une recrudescence constante dans l'étude des systèmes Ta/SiO<sub>2</sub> en tant que catalyseurs de transformations ETB en deux étapes. Une étude remarquable est celle de Jeong et al.<sup>5</sup> qui ont préparé une série d'échantillons d'oxyde de tantale supportés sur de la silice mésoporeuse ordonnée (OMS) par une technique d'imprégnation par voie humide suivie d'une calcination à haute température. Les catalyseurs ont montré de meilleures performances catalytiques vis-à-vis de la production de butadiène par rapport aux systèmes précédents, indiquant la nécessité de catalyseurs au tantale mieux dispersés sur de la silice. Ces études portaient principalement sur l'effet de la morphologie de surface sur l'activité catalytique, mais aucun commentaire concluant n'a été fait sur les espèces actives de surface. Une tentative remarquable de synthèse des espèces actives bien

définies a récemment été réalisée par Dzwigaj et al.<sup>6,7</sup> Ils ont rapporté l'incorporation de Ta dans des lacunes d'atomes T du réseau de zéolithes SiBEA en tant que Ta(V) mononucléaire, donnant lieu à des catalyseurs hautement sélectifs pour la synthèse de 1,3-butadiène. Bien que ces deux études mettent en évidence l'utilité d'espèces d'oxyde de tantale bien dispersées sur la silice, il n'existe aucun aperçu de la nature des espèces à la surface du catalyseur ou des espèces actives participant dans la catalyse.



Reaction Conditions: %Ta= 2wt %; Reaction Temperature 325 C, Flow rate 34mL/min

- Kim, T. *et al.*, *Chemical Engineering Journal* 278 (2015) 217–223
- Jeong, *et al.*, *S. Applied Catalysis B: Environmental*, 2014, 150– 151
- Gao M. *et al.*, *RSC Advances*, 2015, 5, 103982
- Zhang, M. *et al.*, *RSC Advances*, 2017, 7, 7140
- Dzwigaj, *et al.* *Catalysis Communications* , 2016, 77, 123–126
- W. J. Toussaint and J. T. Dunn, US 2,421,361, 1947

**Figure 1** – Etat de l'art des systèmes Ta/SiO<sub>2</sub> pour la transformation d'EtOH/AA en BD.

En général, la surface des systèmes Ta(V)/SiO<sub>2</sub> peut être complexe. Cela pourrait inclure des fragments tétraédriques isolés [(≡SiO)<sub>3</sub>Ta=O], des espèces Ta<sub>x</sub>O<sub>y</sub> oligo- et polymériques présentant simultanément des atomes O pontants, des liaisons Ta=O et Ta-O-support, ainsi que des particules de Ta<sub>2</sub>O<sub>5</sub> massif formées à une charge plus importante en Ta.<sup>8</sup> Pour pouvoir établir une relation entre la structure et l'activité pour ces catalyseurs, il sera impératif de synthétiser sélectivement divers catalyseurs modèles avec des espèces isolées et oligomères/polymères à la surface du support. À cet effet, une des

approches les plus puissantes peut être la chimie organométallique de surface (SOMC), qui permet d'obtenir des espèces bien définies à la surface d'un support.

La chimie organométallique de surface est une technique développée pour préparer des catalyseurs hétérogènes bien définis en greffant des complexes organométalliques sur des sites de surface d'un support de manière contrôlée.<sup>9-11</sup> Cette approche repose sur le contrôle de la concentration des sites de greffage par unité de surface du support, ce qui permet de contrôler la densité finale des espèces organométalliques greffées à la surface. Grâce à sa capacité à effectuer un greffage moléculaire contrôlé, SOMC permet d'obtenir des sites superficiels avec une sphère de coordination connue. Cet attribut est essentiel pour établir une relation entre la structure et l'activité d'un catalyseur et pour concevoir de manière rationnelle des catalyseurs idéaux pour un certain processus.<sup>12</sup>

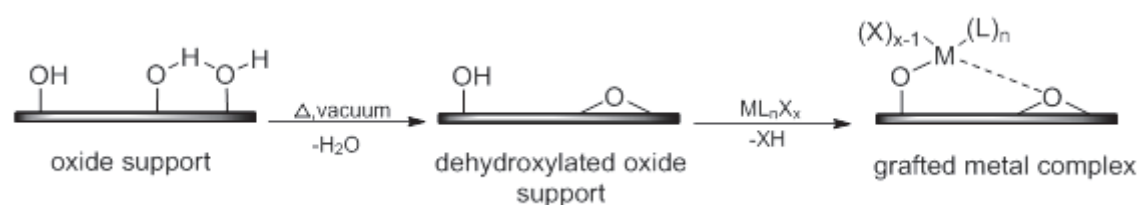


**Figure 2**-Représentation schématique de la préparation d'un catalyseur bien défini par SOMC

Le prérequis nécessaire pour pouvoir appliquer l'approche SOMC est la présence d'un support bien caractérisé et d'un complexe organométallique -  $ML_nX_x$  ( $L$  = ligand fonctionnel,  $X$  = ligand auxiliaire). Lors du greffage du complexe sur le support, celui-ci peut être utilisé en tant que catalyseur lui-même ou être soumis à des traitements postérieurs (calcination, hydrogénation, sulfuration) pour obtenir une structure plus stable ou pour lui redonner une nouvelle fonctionnalité. La **figure 2** représente schématiquement la préparation d'un catalyseur idéal par SOMC avec ses étapes principales.

Dans un premier temps, l'objectif de ce travail est de synthétiser une famille de catalyseurs  $TaO_x$  bien définis supportés sur de la silice avec une nucléarité du tantale variable et d'étudier son effet sur la deuxième étape du processus d'Ostromyslensky : la transformation d'un mélange éthanol/acétaldéhyde en butadiène. Nous avons également étudié l'effet du greffage de différents précurseurs de Ta de même que l'utilisation de différents supports. Deuxièmement, notre objectif est d'appliquer les connaissances susmentionnées pour établir un rapport pertinent entre la structure et l'activité pour les

systèmes catalytiques Ta(V)/SiO<sub>2</sub> dans la synthèse de butadiène à partir d'un mélange éthanol/acétaldéhyde.

M = Ta, V, W, Mo...

M' = Si, Al, Ti, Ce...

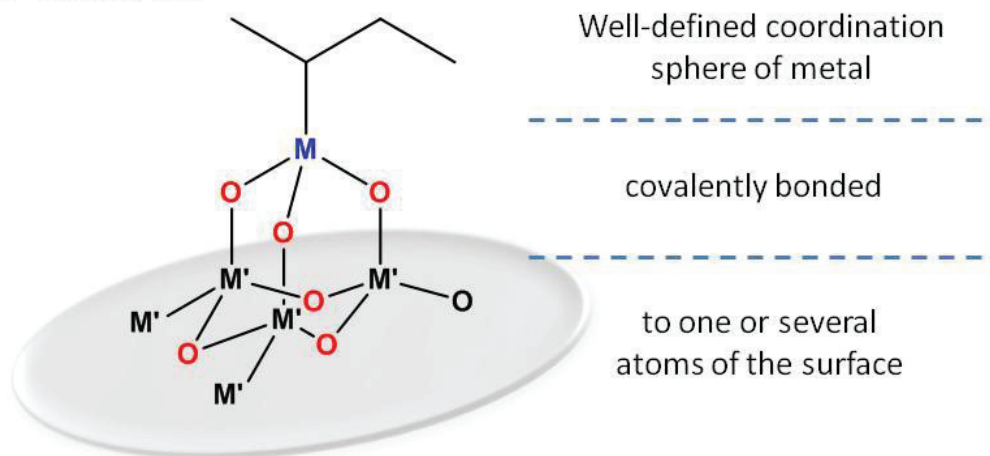


**Figure 3-** Structure générale des composés organométalliques de surface représentant différents supports, métaux de transition et ligands fonctionnels possibles

Comme mentionné précédemment, le greffage de complexes alkyliques de tantale sur de la silice partiellement déshydroxylée afin d'obtenir des catalyseurs «à site unique» avec des centres de tantale isolés a été bien rapporté dans la littérature.<sup>14-15</sup> De ce fait, une stratégie évidente pour synthétiser des catalyseurs TaO<sub>x</sub>«à site unique»a été choisie via l'oxydation douce de ces espèces de tantale bien définies supportées sur de la silice.

Les espèces TaO<sub>x</sub> isolée ont été obtenues par oxydation douce des hydrures de tantale sur silice [(≡SiO)<sub>2</sub>Ta(H)<sub>x=1,3</sub>] avec du N<sub>2</sub>O. Ces hydrures de tantale [(≡SiO)<sub>2</sub>Ta(H)<sub>x=1,3</sub>] ainsi que leur précurseur alkylique [≡SiOTa(=CH<sup>t</sup>Bu)(CH<sub>2</sub><sup>t</sup>Bu)<sub>2</sub>] ont été l'objet d'une étude modèle de la chimie organométallique de surface. Des matériaux contenant ces espèces ont été synthétisés conformément à la littérature et leur formation a été contrôlée par spectroscopie IR, RMN et analyse élémentaire. De plus, leur localisation à la surface de silice a été visualisée pour la première fois via HRSTEM.

Lors du traitement oxydant de [(SiO)<sub>2</sub>Ta(H)<sub>x=1,3</sub>] avec du N<sub>2</sub>O à la température ambiante, le matériau obtenu (**SOMC-I**) a été caractérisé par spectroscopies IR, RMN, ainsi que par analyse élémentaire. La formation exclusive d'une espèce isolée et bien définie

$[(\equiv\text{SiO})_2\text{Ta}(=\text{O})(\text{OH})]$  a été établie par EXAFS tandis que les clichés HRSTEM du matériau ont révélé principalement des centres de Ta(V) isolés avec un certain degré d'agglomération. (**Schéma 1**)

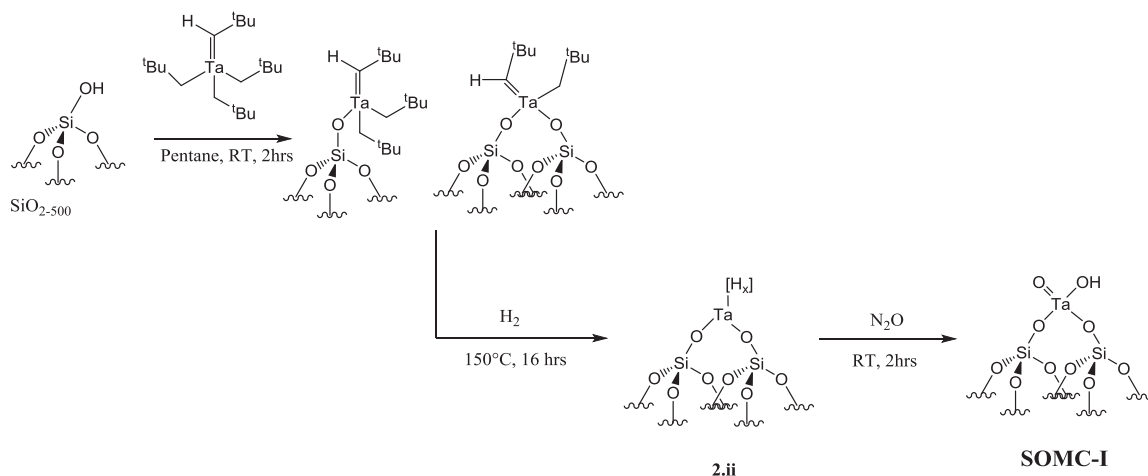


**Schéma 1**

Une autre approche pour générer des espèces de  $\text{TaO}_x$  bien définies consistait en calcination de complexe de tantalum peralkylique  $[\equiv\text{SiOTa}(=\text{CHtBu})(\text{CH}_2\text{tBu})_2]$ , greffé à la surface de silice, à  $500^\circ\text{C}$  pendant 10 heures sous oxygène sec. Le matériau ainsi formé (**SOMC-II**) a été caractérisé par spectroscopies IR, RMN, EXAFS et HRSTEM. Le **Schéma 2** représente le schéma de synthèse de **SOMC-II**. La spectroscopie EXAFS a confirmé l'absence de  $\text{Ta}_2\text{O}_5$ , tout en suggérant la possibilité d'une interaction Ta-Ta. L'analyse des clichés HRSTEM a mis en évidence la coexistence de centres de Ta(V) isolés avec des espèces de Ta arrangées en chaînes. Ces résultats, en tenant compte des données bibliographiques, suggèrent la présence d'un mélange des espèces mono-, di- et oligomériques à la surface de **SOMC-II**.

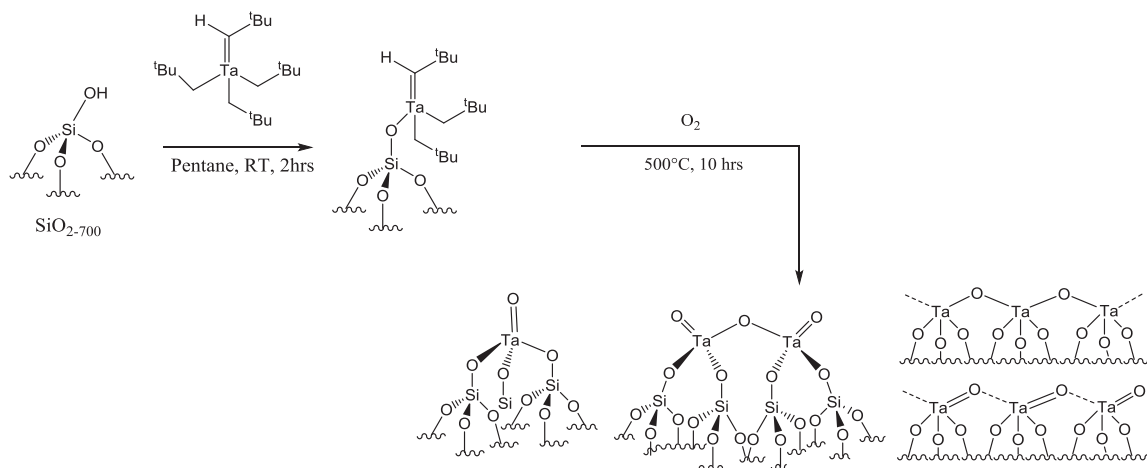


**Schéma 2**

La famille de catalyseurs synthétisés par protocole SOMC a été testée dans la production de butadiène à partir d'éthanol et d'acétaldéhyde dans un réacteur à flux continu à l'échelle du laboratoire et à pression atmosphérique. Dans un test typique, 0,25gde catalyseur sous forme de poudre a été chargé dans le réacteur. Le ratio molaire d'entrée est toujours constant et fixés à 2% molaire d'éthanol et d'acétaldéhyde avec 98% d'azote. Les produits de la réaction ont été introduits dans un système d'échantillonnage automatique pour être analysés par chromatographie en phase gazeuse. La **Figure 4** montre le diagramme schématique du réacteur à l'échelle du laboratoire utilisé pour les tests catalytiques.

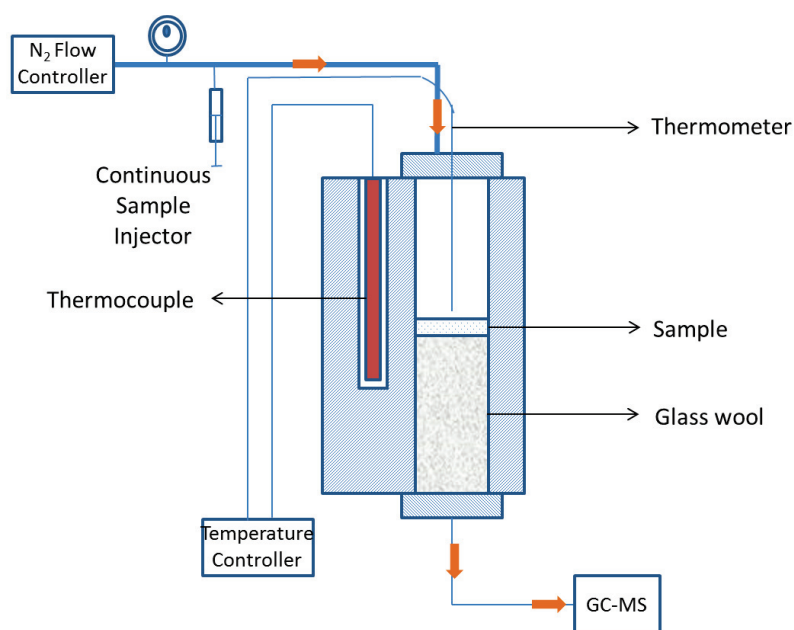


**Figure 4**-Représentation schématique du réacteur pour la synthèse de butadiène à partir d'éthanol et acétaldéhyde

La **Figure 5** permet de comparer les catalyseurs les plus performants de chacune des deux approches SOMC aux systèmes les plus performants rapportés jusqu'au présent dans la littérature. Lorsqu'ils sont testés dans des conditions comparables, les catalyseurs synthétisés par approche SOMC présentent une sélectivité et un rendement de butadiène excellents par rapport aux catalyseurs de Ta existants. **SOMC-I** avec des sites de Ta(V) isolés présente les meilleures performances avec une sélectivité de **86,9%** et un rendement de **48,2%** en butadiène.

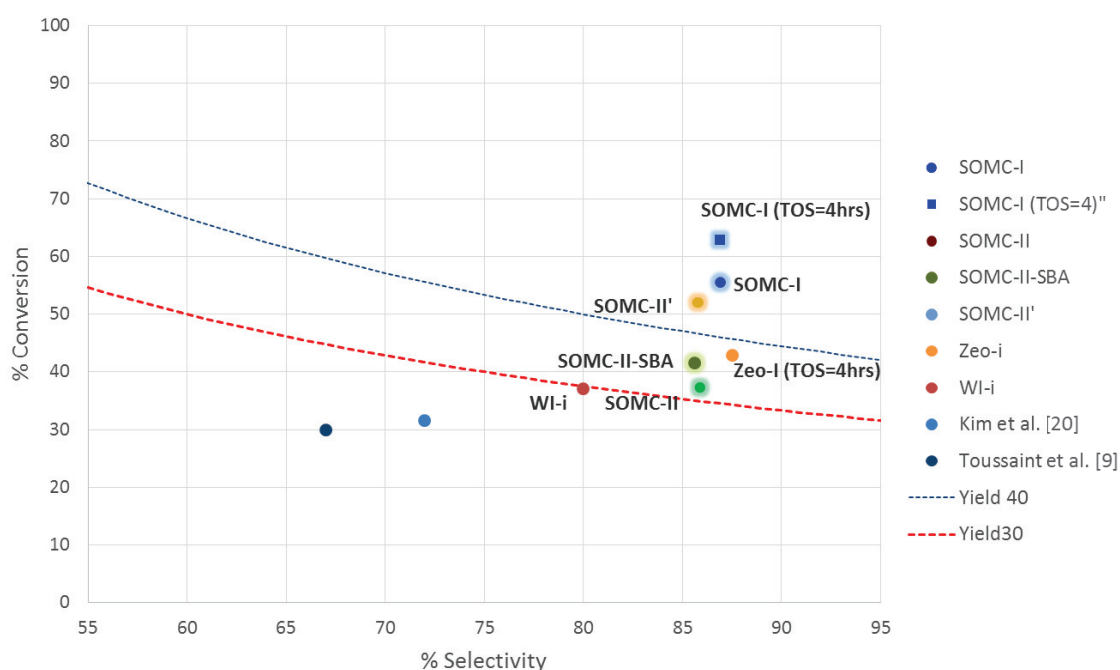


**Figure 5-** Activité catalytique de SOMC-I et SOMC-II comparée aux catalyseurs au tantale de l'état de l'art pour la conversion d'EtOH/AA en BD

Notamment, les deux matériaux **SOMC-I** et **SOMC-II** ainsi que **Zeo-I** présentent une distribution de produit extrêmement étroite par rapport aux catalyseurs synthétisés par les techniques d'imprégnation par voie humide classiques (**WI-I**). Les trois catalyseurs évoqués précédemment représentent des systèmes avec des espèces de surface

relativement bien définies et homogènes. On peut supposer que la présence d'espèces de surface homogènes peut limiter les réaction alternatives, diminuant ainsi le nombre de produits secondaires. Cette caractéristique est importante pour un catalyseur industriel dans la mesure de limiter la quantité de produits indésirables et, par conséquent, de réduire les étapes de séparation. La **figure 6** montre la distribution des produits pour les catalyseurs en question.

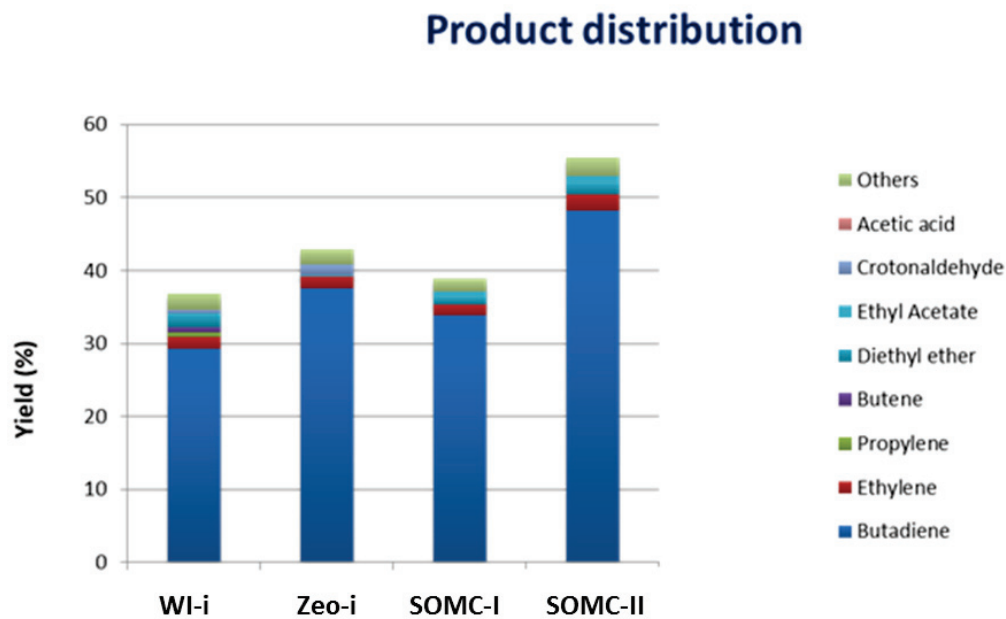


**Figure 6** - Répartition des produits de réaction pour chaque catalyseur : (i) WI-I (ii) Zeo-I (iii) SOMC-I (iv) SOMC-II

Les résultats de l'analyse HRSTEM du catalyseur **SOMC-I** avant et après la catalyse ont relevé une évolution des sites isolés de Ta(V) vers des chaînes semblables à celles présentes à la surface de **SOMC-II**. La baisse de la quantité de sites de Ta(V) isolés à la surface de **SOMC-I** a également entraîné une diminution de la conversion globale d'un mélange EtOH/AA. Prenant en compte les résultats des tests d'activité catalytique et de l'analyse HRSTEM, il paraît probable que les centres isolés de Ta(V) agissent comme les principaux sites actifs dans la conversion d'EtOH/AA en BD, alors que les atomes de Ta organisés en chaînes montrent une activité considérable, mais moins importante pour la même transformation.

En supposant que  $[(\equiv\text{SiO})_2\text{Ta}(=\text{O})(\text{H})]$  isolé soit le site actif dans la transformation d'EtOH/AA en BD, un mécanisme de cette réaction à la surface de **SOMC-I** a été proposé. Conformément au mécanisme de Kagan bien établi, deux molécules

d'acétaldéhyde réagissent pour donner une molécule de crotonaldéhyde, qui, par la suite, est réduite par éthanol en alcool de crotyle. L'alcool de crotyle se transforme finalement en butadiène. La réduction de Meerwein-Ponndorf-Verley de crotonaldéhyde, selon certaines études publiées, est censée être catalysée par tantale.<sup>17-18</sup> Sur la base des études de l'adsorption d'éthanol(i) et d'un mélange éthanol/acétaldéhyde(ii), suivies par DRIFT in-situ à la surface du catalyseur à 350 ° C, le mécanisme pour l'étape de réduction sur les centres de Ta(V) a été proposé (**Figure 7**).

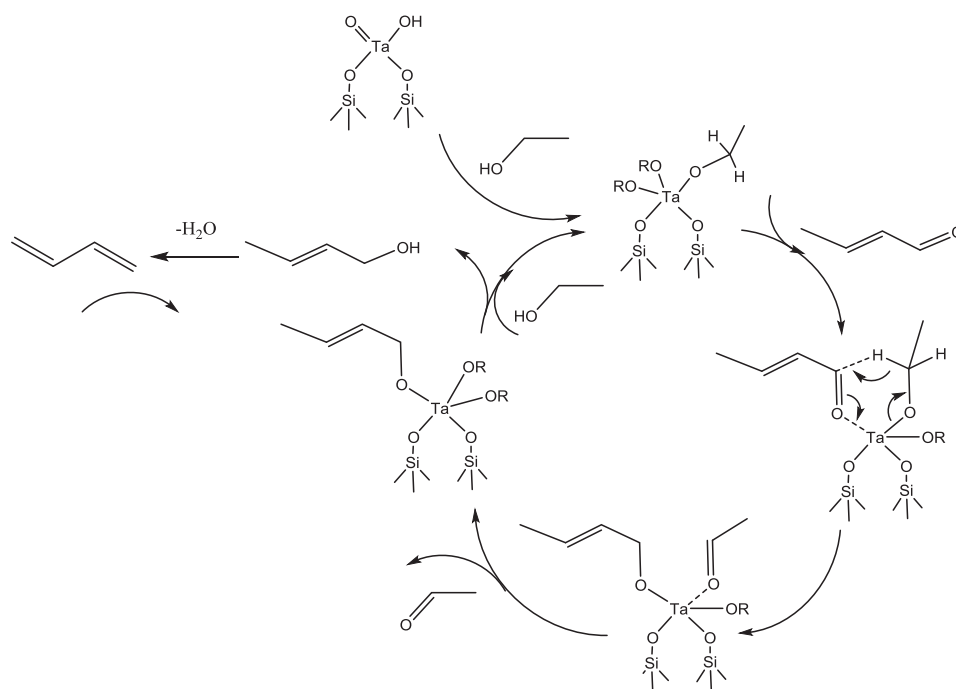


**Figure 7** - Mécanisme de la réaction de réduction de MPV proposé sur le site de Ta(V) de SOMC-I

En conclusion, la famille des catalyseurs au tantale supportés sur de la silice et synthétisés par le protocole SOMC a démontré une excellente activité dans la transformation d'un mélange EtOH/AA en BD. Les catalyseurs modèles avec des sites actifs bien définis se sont révélés efficaces pour la prédiction des sites actifs participant dans la transformation pour les systèmes Ta(V)/SiO<sub>2</sub>. Bien que cette étude soit une étape préliminaire dans la recherche sur ces systèmes catalytiques, elle la fait avancer et valorise l'utilisation de la chimie organométallique de surface en tant que technique de préparation de catalyseurs pour la synthèse de butadiène par le processus d'Ostromyslensky.

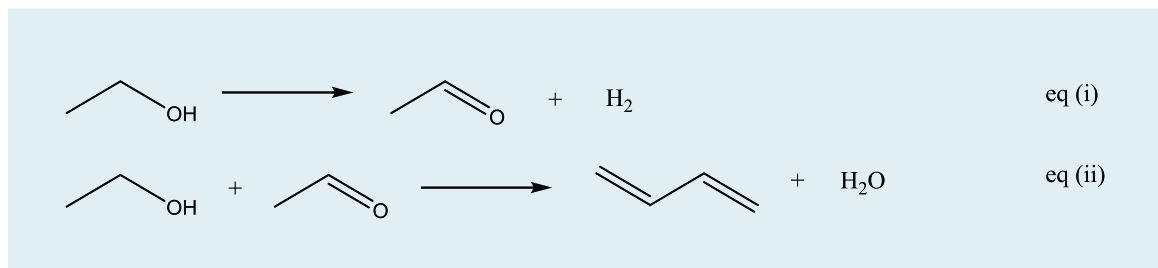
## References

1. Cavani, F., Albonetti, S., Basile, F. & Gandini, A. *Chemicals and fuels from bio-based building blocks*. (2016).
2. Makshina, E. V. *et al.* Review of old chemistry and new catalytic advances in the on-purpose synthesis of butadiene. *Chem. Soc. Rev.* **43**, 7917–7953 (2014).
3. Pomalaza, G., Capron, M., Ordonsky, V. & Dumeignil, F. Recent Breakthroughs in the Conversion of Ethanol to Butadiene. *Catalysts* **6**, 203 (2016).
4. Kim, T. W. *et al.* Butadiene production from bioethanol and acetaldehyde over tantalum oxide-supported spherical silica catalysts for circulating fluidized bed. *Chem. Eng. J.* **278**, 217–223 (2015).
5. Chae, H.-J. *et al.* Butadiene production from bioethanol and acetaldehyde over tantalum oxide-supported ordered mesoporous silica catalysts. *Applied Catal. B, Environ.* **150–151**, 596–604 (2014).
6. Kyriienko, P. I., Larina, O. V., Soloviev, S. O., Orlyk, S. M. & Dzwigaj, S. High selectivity of TaSiBEA zeolite catalysts in 1,3-butadiene production from ethanol and acetaldehyde mixture. *Catal. Commun.* **77**, 123–126 (2016).
7. Tielens, F., Shishido, T. & Dzwigaj, S. What Do Tantalum Framework Sites Look Like in Zeolites? A Combined Theoretical and Experimental Investigation. *J. Phys. Chem.* **114**, 9923–9930 (2010).
8. Barman, S. *et al.* Single-Site VO<sub>x</sub> Moieties Generated on Silica by Surface Organometallic Chemistry: A Way To Enhance the Catalytic Activity in the Oxidative Dehydrogenation of Propane. *ACS Catal.* **6**, 5908–5921 (2016).
9. Chabanas, M. *et al.* Molecular insight into surface organometallic chemistry through the combined use of 2D HETCOR solid-state NMR spectroscopy and silsesquioxane analogues. *Angew. Chemie - Int. Ed.* **40**, 4493–4496 (2001).
10. Le Roux, E. *et al.* Detailed structural investigation of the grafting of [Ta(=CHtBu)(CH<sub>2</sub>tBu)<sub>3</sub>] and [Cp\*TaMe<sub>4</sub>] on silica partially dehydroxylated at 700 °C and the activity of the grafted complexes toward alkane metathesis. *J. Am. Chem. Soc.* **126**, 13391–13399 (2004).
11. Pelletier, J. D. A. & Basset, J.-M. Catalysis by Design: Well-Defined Single-Site Heterogeneous Catalysts. *Acc. Chem. Res.* **49**, 664–677 (2016).
12. Quadrelli, A. & Basset, J.-M. On silsesquioxanes' accuracy as molecular models

- for silica-grafted complexes in heterogeneous catalysis. *Coord. Chem. Rev.* **254**, 707–728 (2010).
13. Copéret, C. *et al.* Surface Organometallic and Coordination Chemistry toward Single-Site Heterogeneous Catalysts: Strategies, Methods, Structures, and Activities. *Chemical Reviews* (2016).
  14. Vidal, V., Théolier, A., Thivolle-Cazat, J., Basset, J.-M. & Corker, J. Synthesis, Characterization, and Reactivity, in the C–H Bond Activation of Cycloalkanes, of a Silica-Supported Tantalum(III) Monohydride Complex:  $(\equiv\text{SiO})_2\text{TaIII-H}$ . *J. Am. Chem. Soc.* **118**, 4595 (1996).
  15. P. Avenier, M. Taoufik, A. Lesage, Solans-Monfort, Baudouin, A. de M., L. Veyre, J.-M. B. & O. Eisenstein, L. Emsley, E. A. Q. Dinitrogen Dissociation on an Isolated Surface Tantalum Atom. *Science*, **317**, 1056–1060 (2007).
  16. Soignier, S. *et al.* Tantalum hydrides supported on MCM-41 mesoporous silica: Activation of methane and thermal evolution of the tantalum-methyl species. *Organometallics* **25**, 1569–1577 (2006).
  17. Corson, B. B., Jones, H. E., Welling, C. E., Hinckley, J. A. & Stahly, E. E. *Butadiene from Ethyl Alcohol. Catalysis in the One-and Two-Stop Processes. Industrial & Engineering Chemistry* **42**, (UTC, 1950).
  18. Müller, P. *et al.* Mechanistic Study on the Lewis Acid Catalyzed Synthesis of 1,3-Butadiene over Ta-BEA Using Modulated Operando DRIFTS-MS. *ACS Catal.* **6**, 6823–6832 (2016).

# Riassunto

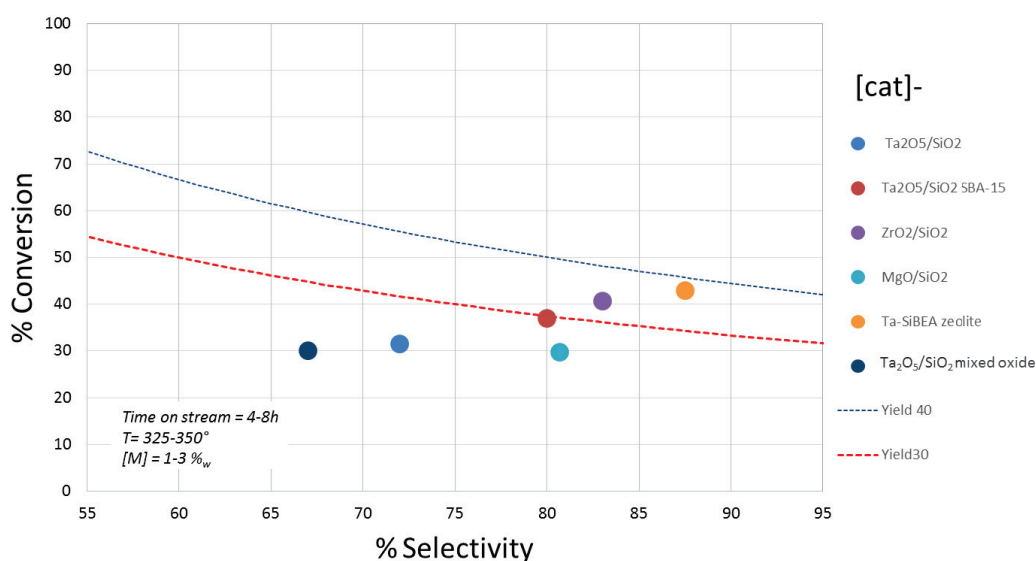
Negli ultimi anni, la sintesi specifica del butadiene a partire dal bio-etanolo ha ottenuto un'attenzione mai riscontrata precedentemente a causa dell'aumento dell'interesse sia verso building blocks a base biologica, che al rapido aumento della domanda per il butadiene stesso.<sup>1</sup> Un processo rilevante in questo ambito è quello Ostromysensky, costituito da due step: la deidrogenazione dell'etanolo ad acetaldeide in una prima fase, seguita dalla produzione del butadiene in un secondo stadio della reazione dove è previsto un co-feeding di etanolo ed acetaldeide.<sup>2</sup>



Nonostante questo processo di produzione da etanolo a butadiene (ETB) sia attualmente assestato sia da un punto di vista economico che operativo, c'è ancora spazio di miglioramento sia dal punto di vista delle performance catalitiche che da quello della selettività dei prodotti ottenuti.<sup>3</sup> Infatti la selettività del processo è inficiata dalla presenza di numerose reazioni parallele che danno vita a un gran numero di sottoprodotti di reazione. Inoltre è noto che il processo è caratterizzato da un ciclo di rigenerazione catalitica corto, a causa della rapida deattivazione per formazione di carbone.<sup>4</sup>

In seguito al primo sviluppo del catalizzatore di Ostromyslenky, c'è stato un costante aumento nello studio di sistemi Ta/SiO<sub>2</sub> come catalizzatori per le trasformazioni ETB in due step catalitici. Un importante studio è stato svolto da Jeon et al.<sup>5</sup> i quali hanno preparato una serie ossidi di Tantalio supportati su silice mesoporosa ordinata (OMS) tramite impregnazione liquida seguita da calcinazione ad alta temperatura. I catalizzatori hanno mostrato performance catalitiche verso la produzione di butadiene migliori rispetto ai precedenti sistemi, indicando la necessità di avere una migliore dispersione delle specie di tantalio sulla superficie dei catalizzatori. Lo studio da loro condotto si focalizza principalmente sull'effetto della morfologia della superficie sull'attività catalitica, mentre non sono riportati commenti conclusivi sul tipo di specie attive presenti sulla superficie.

Un tentativo rimarchevole verso la sintesi di specie attive ben definite è stato recentemente effettuato da Dzwagaj et al., i quali hanno riportato l'incorporazione del Ta nelle vacanze di ipo T-atom nella struttura di zeoliti SiBEA come Ta(V) mononucleare, permettendo la preparazione di catalizzatori altamente selettivi per la produzione di 1,3-butadiene. Nonostante entrambi questi studi dimostrino l'utilità di una buona dispersione degli ossidi di tantalio sulla superficie della silice, non ci sono chiare prove della natura delle specie che popolano la superficie del catalizzatore o di quella delle specie attive che prendono parte al processo catalitico.



Reaction Conditions: %Ta= 2wt %; Reaction Temperature 325 C, Flow rate 34mL/min

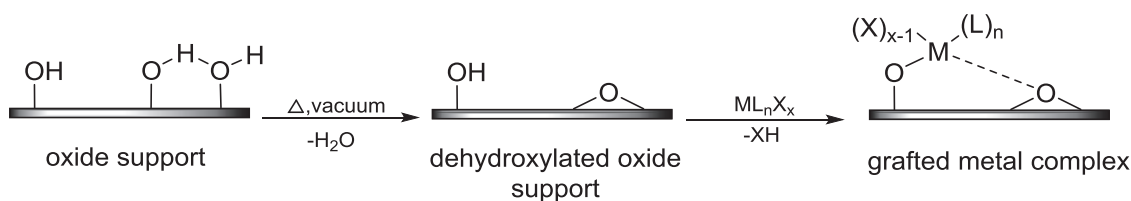
- Kim, T. *et al.*, Chemical Engineering Journal 278 (2015) 217–223
- Jeong, *et al.*, S. Applied Catalysis B: Environmental, 2014, 150– 151
- Gao M. *et al.*, RSC Advances, 2015, 5, 103982
- Zhang, M. *et al.*, RSC Advances, 2017, 7, 7140
- Dzwigaj, *et al.* Catalysis Communications , 2016, 77, 123–126
- W. J. Toussaint and J. T. Dunn, US 2,421,361, 1947

**Figura 1** - Sistemi Ta/SiO<sub>2</sub> riportati in letteratura per la trasformazione di EtOH/AA a BD.

In generale, la superficie dei sistemi Ta(V)/SiO<sub>2</sub> può essere complessa. Può includere frammenti tetraedrici isolati [(≡SiO)<sub>3</sub>Ta=O], specie del tipo Ta<sub>x</sub>O<sub>y</sub> di natura oligomerica e polimerica che presentino allo stesso tempo atomi di ossigeno a ponte, tantalati (Ta=O) e legami il Ta e l'O del supporto, e particelle bulk di Ta<sub>2</sub>O<sub>5</sub> formati a loading di Ta molto

più elevati.<sup>6</sup> È quindi necessario, per poter sviluppare con successo una relazione struttura-attività per questi catalizzatori, essere in grado di sintetizzare selettivamente catalizzatori modello per le specie isolate e quelle oligo/polimeriche sulla superficie del supporto. A questo fine, un approccio efficace è la chimica organometallica di superficie (SOMC), che permette la preparazione di specie di superficie strutturalmente ben definite.

La chimica organometallica di superficie è una tecnica sviluppata per la sintesi catalizzatori eterogenei ben definiti da un punto di vista strutturale tramite grafting in maniera controllata di complessi organometallici su siti attivi di un supporto. Questo approccio è basato sul controllo della concentrazione dei siti di grafting per unità di area del supporto, che a sua volta controlla la densità finale delle specie organometalliche graffate sulla superficie. Grazie all'abilità di effettuare un grafting controllato da un punto di vista molecolare, la SOMC produce siti di superficie con una sfera di coordinazione nota. Questo attributo è essenziale nello sviluppo di una relazione struttura-attività per un catalizzatore e in seguito per il design razionale di un catalizzatore ideale per un



determinato processo.

**Figura 2** - Rappresentazione schematica della preparazione di un catalizzatore definite da un punto di vista strutturale tramite SOMC.

I requisiti principali per l'applicazione dell'approccio SOMC è la presenza di un supporto ben caratterizzato, e di un complesso organometallico  $\text{-ML}_n\text{X}_x$  (L= legando funzionale, X=legando ancillare). Una volta che il complesso organometallico è stato graffato sul supporto, può essere utilizzato direttamente come catalizzatore o essere sottoposto a trattamenti successivi (calcinazione, idrogenazione, sulfidazione) per ottenere una struttura più stabile o per ottenere una nuova funzionalità. La **Figura 2** rappresenta schematicamente un ideale catalizzatore SOMC con le sue componenti chiave.

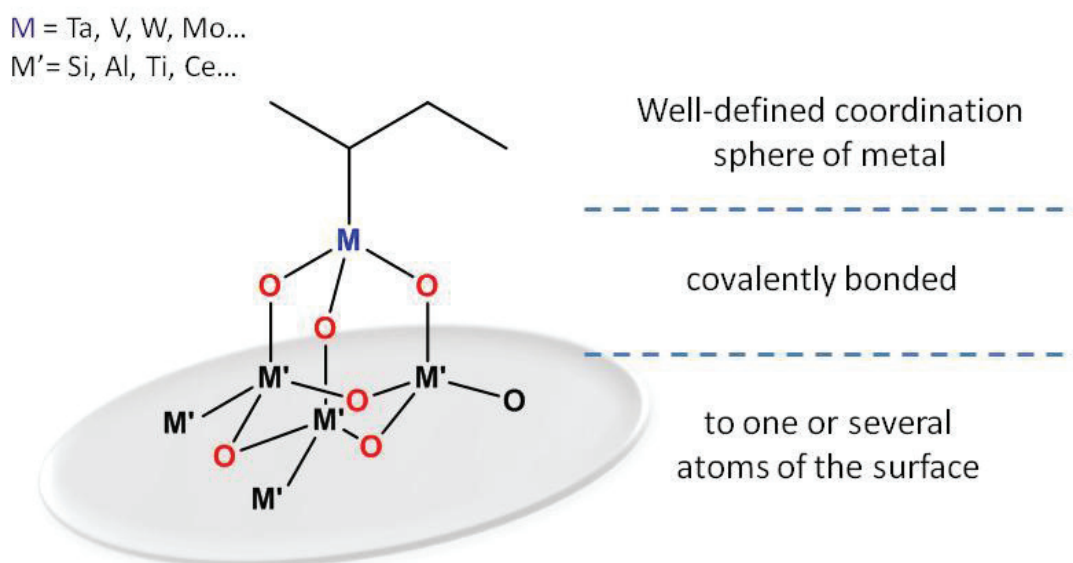


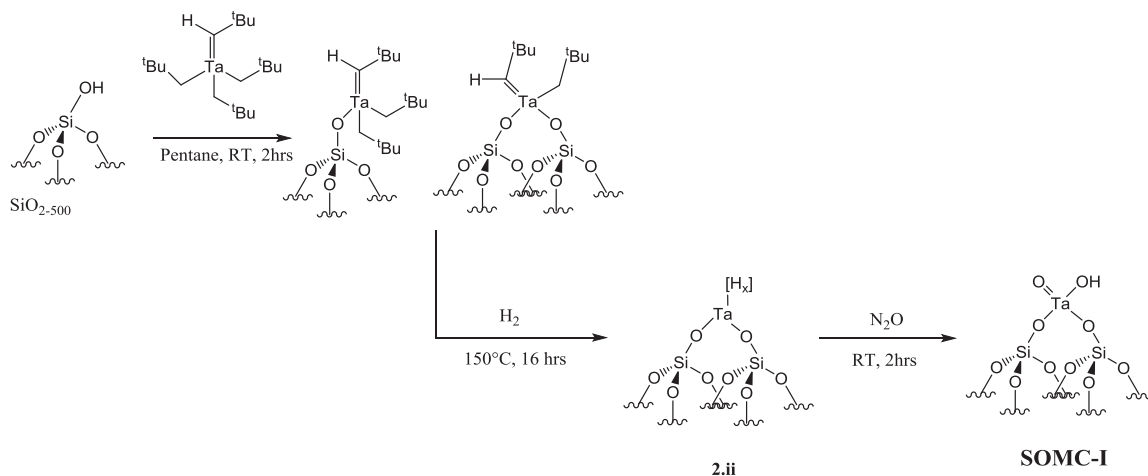
**Figura 3** - Tipica struttura dei composti organometallici di superficie mostrante la possibilità di utilizzo di diversi supporti, metalli di transizione e legandi funzionali e spettatori.

Lo scopo principale di questo lavoro è sintetizzare una famiglia di catalizzatori ben definiti basati su specie  $TaO_x$  supportate su silice con il tantalio in forma sia monomerica che oligo/polimerica e di studiare l'effetto dell'intorno del tantalio sul secondo step del processo Ostromyslensky, ossia la trasformazione del EtOH/AA a butadiene. Abbiamo anche investigato l'effetto del grafting di differenti precursori di tantalio e l'uso di diversi supporti per il grafting stesso. In secondo luogo il nostro scopo è quello di utilizzare le conoscenze acquisite per costruire una relazione struttura-attività per i sistemi catalitici Ta(V)/SiO<sub>2</sub> nella sintesi del BD da EtOH/AA.

Come detto precedentemente il grafting di alchili di tantalio su silice parzialmente deidrossilata per ottenere catalizzatori 'single site' (a sito singolo) con centri di Ta isolati è ben documentata in letteratura. Così, una strategia evidente per la sintesi di catalizzatori 'single site' del tipo TaO<sub>x</sub>, è quella che preveda una mite ossidazione di queste specie supportate di tantalio precedentemente già ampiamente studiate.

La specie isolata  $\text{TiO}_x$  è stata ottenuta tramite mite ossidazione di idruri di tantalio supportati su silice  $[(\equiv\text{SiO})_2\text{Ta}(\text{H})_{x=1,3}]$  con  $\text{N}_2\text{O}$ . Gli idruri di tantalio ben definiti strutturalmente  $[(\equiv\text{SiO})_2\text{Ta}(\text{H})_{x=1,3}]$  e i tantalio alchili loro precursori,  $[\equiv\text{SiOTa}(\text{=CH}^t\text{Bu})(\text{CH}^t\text{Bu})_2]$ , sono stati un modello di studio in chimica organometallica di superficie. Materiali che presentino queste specie sono stati sintetizzati seguendo la letteratura e la loro formazione è stata monitorata tramite IR, spettroscopia NMR e analisi elementare. Inoltre, è stato effettuato un primo tentativo di visualizzare il loro arrangiamento spaziale sulla superficie della silice tramite HRSTEM.

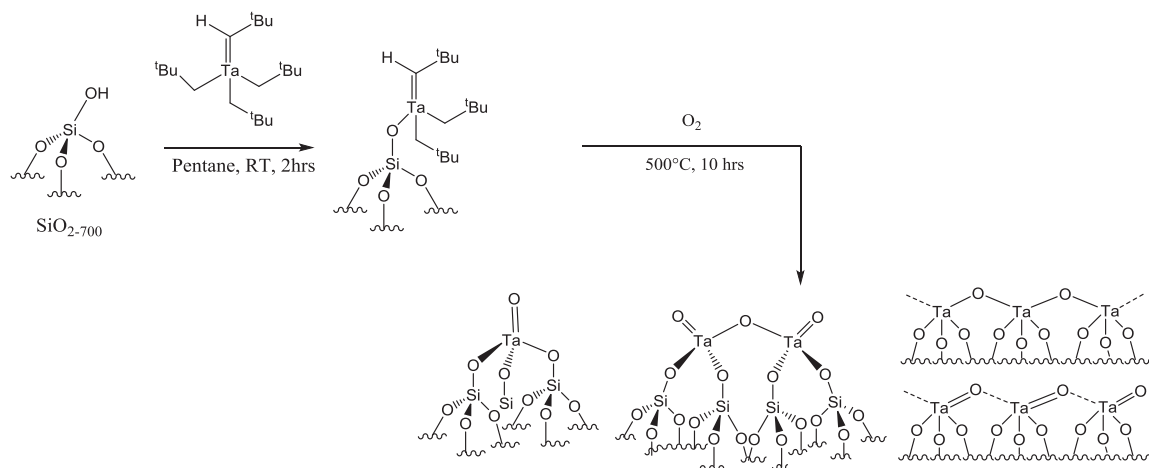
In seguito al trattamento ossidativo di  $[(\equiv\text{SiO})_2\text{Ta}(\text{H})_{x=1,3}]$  con  $\text{N}_2\text{O}$  a temperatura ambiente, il materiale **(SOMC-I)** è stato caratterizzato tramite IR, spettroscopia NMR e analisi elementare. La formazione di unicamente specie isolate e ben definite di monotantalato  $[(\equiv\text{SiO})_2\text{Ta}(\text{=O})(\text{OH})]$  è stata confermata tramite analisi EXAFS mentre l'analisi HRSTEM del materiale ha mostrato una dispersione per lo più isolata dei centri di Ta(V), con un grado di agglomerazioni minoritario.



**Schema 1**

Un altro approccio utilizzato per la sintesi di specie di  $\text{TaO}_x$  sulla superficie strutturalmente ben definite è stata la calcinazione a  $500^\circ\text{C}$  per 10 ore sotto ossigeno secco di specie peralchiliche supportate su silice del tipo  $[\equiv\text{SiOTa}(\text{=CH}^t\text{Bu})(\text{CH}_2^t\text{Bu})_2]$ . Il materiale così ottenuto (**SOMC-II**), è stato caratterizzato tramite spettroscopia IR e

NMR, analisi EXAFS e microscopia HRSTEM. La **Figura 4** rappresenta lo schema per la sintesi di **SOMC-II** insieme ai micrografici HRSTEM rappresentativi delle specie di superficie coinvolte.



**Schema 2**

La spettroscopia EXAFS ha confermato l'assenza di  $\text{Ta}_2\text{O}_5$ , mentre suggerisce la presenza di possibili interazioni Ta-Ta. La spettroscopia HRSTEM ha evidenziato la coesistenza di centri di Ta(V) isolati ed atomi di Ta in disposizione di tipo stringa. Questi risultati insieme alle informazioni di letteratura suggeriscono la presenza sulla superficie di **SOMC-II** di un misto di specie mononucleari, dinucleari e oligomeriche.

La famiglia di catalizzatori sintetizzata tramite protocollo SOMC è stata testata nella produzione di butadiene da etanolo e acetaldeide a pressione atmosferica in un reattore da laboratorio a flusso continuo. 0.25 g di catalizzatore sono stati caricati all'interno del reattore sotto forma di polvere. I rapporti molarli di alimentazione in ingresso del reattore sono stati mantenuti sempre costanti e la miscela utilizzata era costituita al 2% di etanolo e acetaldeide ed al 98% azoto. I prodotti in uscita dal reattore sono stati analizzati tramite un gascromatografo munito di autocampionatore. La **Figura 4** mostra un diagramma schematico del reattore da laboratorio utilizzato nelle prove catalitiche.

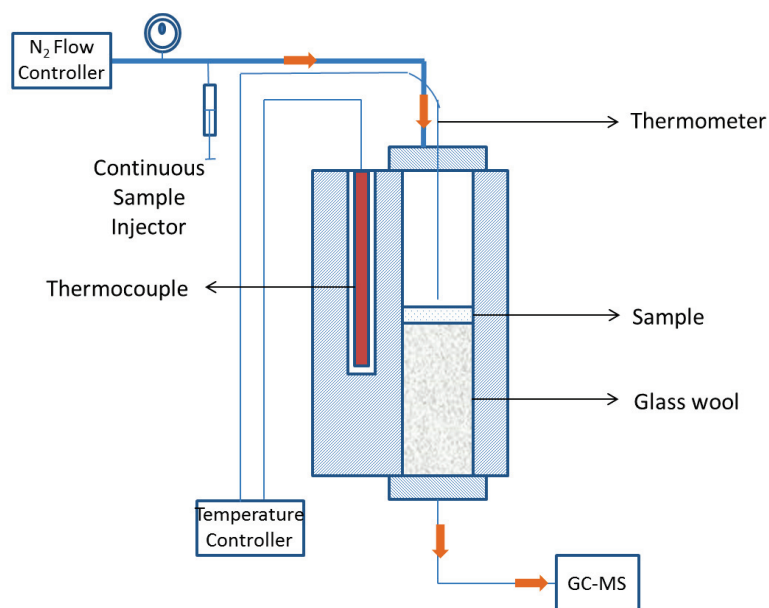


**Figura 1** - Apparato di reazione per la sintesi di butadiene a partire da etanolo e acetaldeide.

La **Figura 5** mostra un confronto tra i catalizzatori più performanti ottenuti tramite l'approccio SOMC e i sistemi a base di tantalio più performanti studiati in letteratura. Quando testati in condizioni catalitiche comparabili, i catalizzatori ottenuti tramite SOMC mostrano un'eccellente selettività e resa nei confronti del BD rispetto ai migliori catalizzatori a base di Ta presenti in letteratura. **SOMC-I**, con siti Ta(V) isolati si è dimostrato il più performante, con una selettività del **86.9%** e una resa del **48.2%** nei confronti del BD.

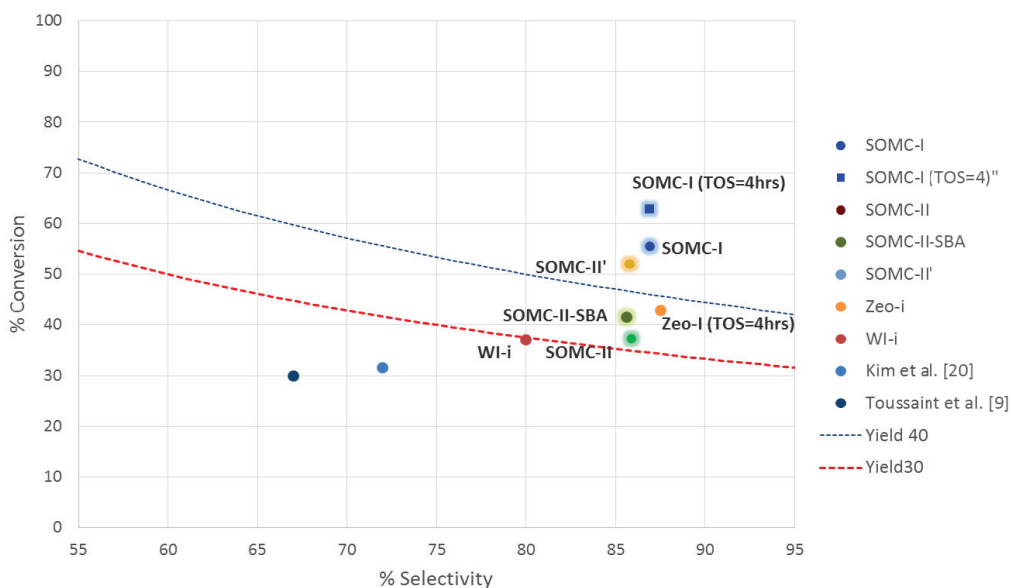


**Figura 2** – Attività catalitica di SOMC-I and SOMC-II paragonata allo stato dell'arte dei catalizzatori a base di tantalio nella conversione di EtOH/AA a BD.

Da notare è che sia **SOMC-I** sia **SOMC-II**, come anche **Zeo-I**, mostrano una distribuzione dei prodotti di reazione alquanto stretta se paragonata a quelle ottenute con i catalizzatori sintetizzati tramite tecniche di impregnazione liquida tradizionali (**WI-I**). I primi tre catalizzatori rappresentano sistemi con specie di superficie relativamente ben definite e omogenee. Possiamo anticipare che la presenza di specie omogenee sulla superficie può limitare il numero di percorsi di reazione collaterali, abbattendo così il numero di sottoprodotti di reazione. Questa caratteristica è importante per un catalizzatore industriale dal momento che permette di evitare lo spreco di carbonio in sottoprodotti indesiderati e di ridurre il numero di fasi nella separazione dei prodotti. Nella **Figura 7** sono mostrate le distribuzioni dei prodotti per i catalizzatori presi in considerazione.

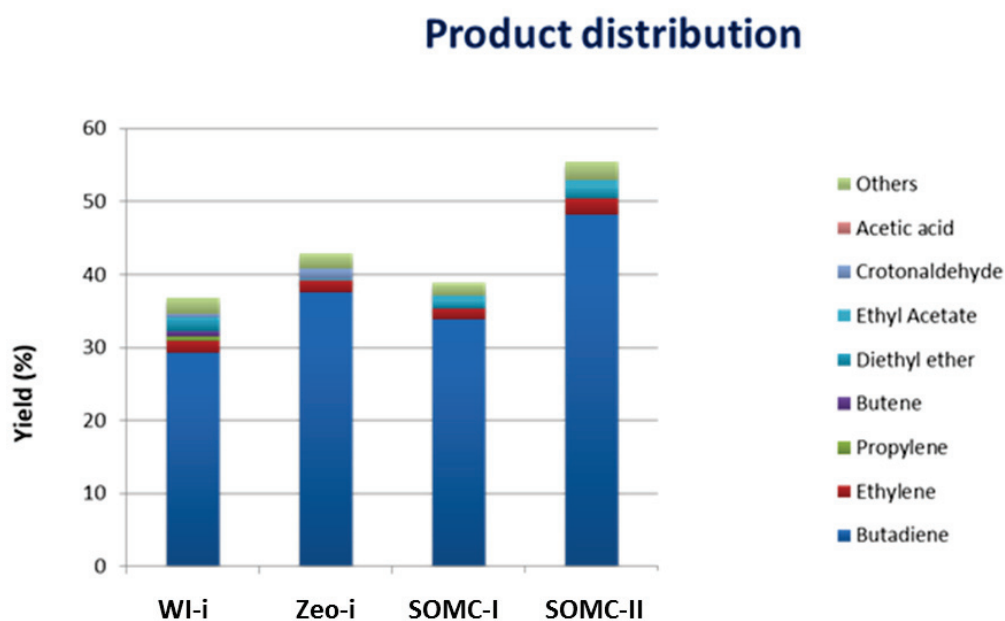


**Figura 3** – Distribuzione dei prodotti dei catalizzatori considerati (i) WI-I (ii) Zeo-I (iii) SOMC-I (iv) SOMC-II .

L'analisi EXAFS di **SOMC-I**, prima e dopo la catalisi indica un'evoluzione dei siti isolati di Ta(V) in arrangiamenti tipo stringa simili alla superficie di **SOMC-II**. Questa diminuzione della concentrazione delle specie isolate di Ta(V) sulla superficie di **SOMC-I** ha portato anche a una diminuzione della conversione totale di EtOH/AA. Basandosi sulle informazioni combinate fornite dai test di attività catalitica e le analisi HRSTEM si può ritenere probabile che i centri Ta(V) isolati agiscano come siti attivi primari nella conversione di ETOH/AA in BD, mentre gli atomi di Ta che si trovano in un'organizzazione di tipo stringa mostrano un'attività inferiore nel medesimo processo, seppur ancora notevole.

Assumendo che le specie isolate del tipo  $[(\equiv\text{SiO})_2\text{Ta}(=\text{O})(\text{H})]$  siano i siti attivi nella trasformazione di EtOH/AA in BD, è stato effettuato un tentativo per comprendere il meccanismo di reazione alla superficie di **SOMC-I**. Si pensa che il tantalio possa catalizzare la Reazione Meerwin-Ponndorf-Verley tra la crotonaldeide e l'etanolo. Basandosi su esperimenti di DRIFT in-situ di adsorbimento di (i) etanolo e (ii) una miscela di etanolo e acetaldeide sulla superficie del catalizzatore a 350°C , è stato

ipotizzato il seguente meccanismo per lo step di riduzione al cento isolato di Ta(V) (Figura 7).

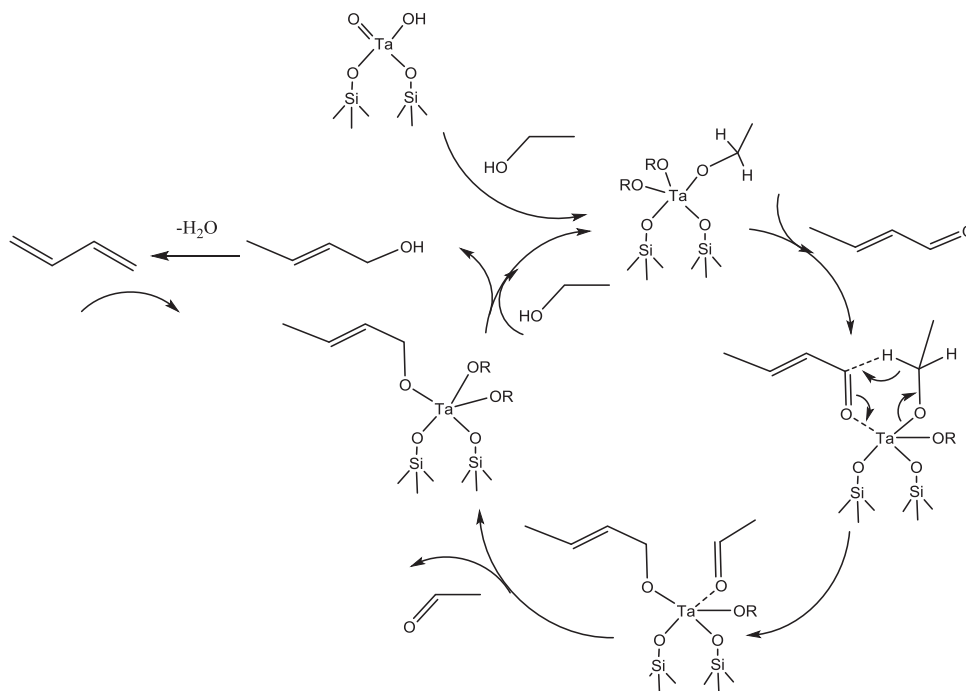


**Figure 4** – Meccanismo di reazione proposto ed ipotizzato per la riduzione MPV sui siti di Ta(V) di SOMC-I.

Per concludere, la famiglia di catalizzatori a base di tantalio supportato su silice sintetizzati seguendo il protocollo SOMC ha mostrato un'eccellente attività nella trasformazione di EtOH/AA a BD. I catalizzatori modello con siti di superficie designati appositamente si sono rivelati incisive nella predizione quali siti attivi partecipino alla trasformazione per i sistemi Ta(V)/SiO<sub>2</sub>. Anche se è chiaro che questo studio sia uno step preliminare nell'investigazione di questi sistemi catalitici, i risultati forniscono un notevole impulso verso l'investigazione della chimica organometallica di superficie come tecnica sintetica dei catalizzatori della sintesi specifica del butadiene tramite processo Ostromyslensky.

## Riferimenti

1. Cavani, F., Albonetti, S., Basile, F. & Gandini, A. *Chemicals and fuels from bio-based building blocks*. (2016).
2. Makshina, E. V. *et al.* Review of old chemistry and new catalytic advances in the on-purpose synthesis of butadiene. *Chem. Soc. Rev.* **43**, 7917–7953 (2014).
3. Pomalaza, G., Capron, M., Ordonsky, V. & Dumeignil, F. Recent Breakthroughs in the Conversion of Ethanol to Butadiene. *Catalysts* **6**, 203 (2016).
4. Kim, T. W. *et al.* Butadiene production from bioethanol and acetaldehyde over tantalum oxide-supported spherical silica catalysts for circulating fluidized bed. *Chem. Eng. J.* **278**, 217–223 (2015).
5. Chae, H.-J. *et al.* Butadiene production from bioethanol and acetaldehyde over tantalum oxide-supported ordered mesoporous silica catalysts. *Applied Catal. B, Environ.* **150–151**, 596–604 (2014).
6. Kyriienko, P. I., Larina, O. V., Soloviev, S. O., Orlyk, S. M. & Dzwigaj, S. High selectivity of TaSiBEA zeolite catalysts in 1,3-butadiene production from ethanol and acetaldehyde mixture. *Catal. Commun.* **77**, 123–126 (2016).
7. Tielens, F., Shishido, T. & Dzwigaj, S. What Do Tantalum Framework Sites Look Like in Zeolites? A Combined Theoretical and Experimental Investigation. *J. Phys. Chem.* **114**, 9923–9930 (2010).
8. Barman, S. *et al.* Single-Site VO<sub>x</sub> Moieties Generated on Silica by Surface Organometallic Chemistry: A Way To Enhance the Catalytic Activity in the Oxidative Dehydrogenation of Propane. *ACS Catal.* **6**, 5908–5921 (2016).
9. Chabanas, M. *et al.* Molecular insight into surface organometallic chemistry through the combined use of 2D HETCOR solid-state NMR spectroscopy and silsesquioxane analogues. *Angew. Chemie - Int. Ed.* **40**, 4493–4496 (2001).
10. Le Roux, E. *et al.* Detailed structural investigation of the grafting of [Ta(=CHtBu)(CH<sub>2</sub>tBu)<sub>3</sub>] and [Cp\*TaMe<sub>4</sub>] on silica partially dehydroxylated at 700 °C and the activity of the grafted complexes toward alkane metathesis. *J. Am. Chem. Soc.* **126**, 13391–13399 (2004).
11. Pelletier, J. D. A. & Basset, J.-M. Catalysis by Design: Well-Defined Single-Site Heterogeneous Catalysts. *Acc. Chem. Res.* **49**, 664–677 (2016).
12. Quadrelli, A. & Basset, J.-M. On silsesquioxanes' accuracy as molecular models

- for silica-grafted complexes in heterogeneous catalysis. *Coord. Chem. Rev.* **254**, 707–728 (2010).
13. Copéret, C. *et al.* Surface Organometallic and Coordination Chemistry toward Single-Site Heterogeneous Catalysts: Strategies, Methods, Structures, and Activities. *Chemical Reviews* (2016).
  14. Vidal, V., Théolier, A., Thivolle-Cazat, J., Basset, J.-M. & Corker, J. Synthesis, Characterization, and Reactivity, in the C–H Bond Activation of Cycloalkanes, of a Silica-Supported Tantalum(III) Monohydride Complex:  $(\equiv\text{SiO})_2\text{TaIII-H}$ . *J. Am. Chem. Soc.* **118**, 4595 (1996).
  15. P. Avenier, M. Taoufik, A. Lesage, Solans-Monfort, Baudouin, A. de M., L. Veyre, J.-M. B. & O. Eisenstein, L. Emsley, E. A. Q. Dinitrogen Dissociation on an Isolated Surface Tantalum Atom. *Science*. **317**, 1056–1060 (2007).
  16. Soignier, S. *et al.* Tantalum hydrides supported on MCM-41 mesoporous silica: Activation of methane and thermal evolution of the tantalum-methyl species. *Organometallics* **25**, 1569–1577 (2006).
  17. Corson, B. B., Jones, H. E., Welling, C. E., Hinckley, J. A. & Stahly, E. E. *Butadiene from Ethyl Alcohol. Catalysis in the One-and Two-Stop Processes. Industrial & Engineering Chemistry* **42**, (UTC, 1950).
  18. Müller, P. *et al.* Mechanistic Study on the Lewis Acid Catalyzed Synthesis of 1,3-Butadiene over Ta-BEA Using Modulated Operando DRIFTS-MS. *ACS Catal.* **6**, 6823–6832 (2016).

# Contents

## Chapter 1- Introduction

### Part A - Catalytic advances in on-purpose production of butadiene

<b>A1. General Introduction</b> .....	<b>7</b>
A1.1. Importance of Butadiene .....	7
A1.2. Present industrial processes for production of butadiene.....	7
A1.3. Emergence of bio-ethanol as a building block .....	10
<b>A2. Towards on purpose butadiene production</b> .....	<b>11</b>
A2.1. Routes in consideration for on-purpose butadiene production .....	11
A2.2. Butadiene synthesis by Ostromyslensky's two-step process .....	13
A2.3. Catalyst design .....	15
A2.4. State of the art catalytic systems .....	16
<b>A3. Towards better catalysis</b> .....	<b>19</b>

### Part B–Surface Organometallic Chemistry

<b>B1. General Introduction</b> .....	<b>23</b>
B1.1. Preparation and characterization of catalyst supports .....	23
B1.2. Grafting of organometallic complexes on catalyst support .....	24

B1.3. Evolution of well-defined surface sites upon post-treatment .....	25
B1.4. Characterization tools for studying the surface sites.....	28
<b>B2. Well defined silica supported Tantalum species .....</b>	<b>29</b>
B2.1. Grafting of Tantalum-alkyls on silica .....	29
B2.2. Grafting of Tantalum-alkoxys on silica .....	30
B2.3. Ta-H species supported on silica .....	31
<b>C. Aim of this work .....</b>	<b>32</b>
<b>D. References .....</b>	<b>33</b>

## Chapter 2-

### Tailoring ‘single site’ TaO<sub>x</sub> species on silica-support via mild oxidation with N<sub>2</sub>O

<b>A. Introduction.....</b>	<b>42</b>
<b>B. Results and Discussions .....</b>	<b>44</b>
B1. New insights into silica-supported tantalum alkyl [≡SiOTa(=CH <sup>t</sup> Bu)(CH <sub>2</sub> <sup>t</sup> Bu) <sub>2</sub> ] and tantalum hydride [(≡SiO) <sub>2</sub> Ta(H) <sub>x=1,3</sub> ] systems via HR-STEM analysis .....	44
B2. Tailoring single site TaO <sub>x</sub> species on the surface of SiO <sub>2-500</sub> via mild oxidation with N <sub>2</sub> O .....	48
B3. Evolution of surface TaO <sub>x</sub> species with temperature .....	51
B4. Towards di-nuclear tantalum surface species supported on silica .....	53
<b>C. Conclusions.....</b>	<b>56</b>

<b>D. Experimental details .....</b>	<b>57</b>
D1. General procedure for the preparation of starting materials .....	57
D2. Synthesis and characterization of catalyst supports .....	57
D3. Synthesis and characterization of [Ta(=CH <sup>t</sup> Bu)(CH <sub>2</sub> <sup>t</sup> Bu) <sub>3</sub> ].....	57
D4. Preparation of surface complexes by SOMC protocol.....	58
D5. Catalyst characterization by HRSTEM .....	59
D6. Catalyst characterization by EXAFS spectroscopy .....	59
 <b>D. Experimental details .....</b>	 <b>61</b>

## Chapter 3-

### Well defined TaO<sub>x</sub> species supported on silica with molecular O<sub>2</sub> as oxidant

<b>A. Introduction.....</b>	<b>67</b>
<b>B. Results and discussions .....</b>	<b>71</b>
B1. Synthesis of TaO <sub>x</sub> /SiO <sub>2</sub> catalysts via oxidation of known silica-supported tantalum alkyl species with molecular O <sub>2</sub> .....	71
B2. Characterization of surface species for TaO <sub>x</sub> /SiO <sub>2</sub> catalysts .....	74
B3. Synthesis and characterization of TaO <sub>x</sub> /SiO <sub>2</sub> catalysts via oxidation of silica- supported alkoxo tantalum species with molecular O <sub>2</sub> .....	77
<b>C. Conclusions .....</b>	<b>81</b>
<b>D. Experimental details .....</b>	<b>82</b>

D1. General procedure for the preparation of starting materials.....	83
D2. Preparation of surface complexes by SOMC protocol.....	83
D3. <i>In operando</i> FTIR spectroscopy experiments .....	84
D4. Catalyst characterization by EXAFS spectroscopy .....	84
<b>E. References .....</b>	<b>85</b>

## Chapter 4-

### Catalytic performance of SOMC catalysts compared to state of the art

<b>A. Introduction.....</b>	<b>89</b>
<b>B. Results and discussion .....</b>	<b>93</b>
B1. General description of catalytic tests and analytical methods.....	93
B2. Catalytic activity of catalysts synthesized by SOMC protocol .....	94
B2.1. Comparison of the [Ta(=CH <sup>t</sup> Bu)(CH <sub>2</sub> <sup>t</sup> Bu) <sub>3</sub> ] based catalysts .....	96
B2.1. Comparison of the [Ta(=CH <sup>t</sup> Bu)(CH <sub>2</sub> <sup>t</sup> Bu) <sub>3</sub> ] based catalysts with Ta(OEt <sub>5</sub> ) based catalysts .....	98
B3. Butadiene selectivity and product distribution .....	100
B4. Post-catalysis analysis .....	102
<b>C. Conclusions.....</b>	<b>103</b>
<b>D. Experimental details .....</b>	<b>104</b>
D1. General description of the catalytic reactor .....	105
D2. Analysis of coke formation by Thermo-gravimetric Analysis (TGA).....	106
<b>E. References.....</b>	<b>108</b>

## **Chapter 5-**

# **Towards catalyst structure activity relationship in transformation of ethanol and acetaldehyde to butadiene**

<b>A. Introduction.....</b>	<b>113</b>
<b>B. Results and discussion .....</b>	<b>116</b>
B1. Evaluation of surface acidity of SOMC catalysts and its effect on catalytic performance .....	116
B2. Studying the influence of reaction parameters on catalytic activity .	119
B2.1. Effect of feed composition on catalytic activity .....	119
B2.1 Effect of contact time on catalytic activity .....	120
B3. Proposed reaction mechanism for transformation of ethanol and acetaldehyde to butadiene .....	121
<b>C. Conclusions.....</b>	<b>124</b>
<b>D. Experimental details .....</b>	<b>125</b>
D1. Evaluation of surface acidity .....	125
D1.1. By Pyridine adsorption desorption .....	125
D1.1. By NH <sub>3</sub> Temperature programmed desorption (NH <sub>3</sub> -TPD).....	126
D2. Surface area by N <sub>2</sub> adsorption desorption isotherms .....	126
<b>E. References .....</b>	<b>130</b>

## Annex 1- Instrumental details

### B1.1. Infrared spectroscopy

B1.1 Fourier transform infrared spectroscopy in transmission

B1.2 Diffused reflectance infrared spectroscopy (DRIFTS)

B1.3 Attenuated total reflectance infrared spectroscopy (ATR)

### B1.2. Nuclear Magnetic Resonance (NMR) spectroscopy in liquid medium

B2.1 Nuclear Magnetic Resonance (NMR) spectroscopy in liquid medium

B2.2  $^1\text{H}$  and  $^{13}\text{C}$  Solid state nuclear magnetic resonance spectroscopy

B2.3  $^{17}\text{O}$  Solid state nuclear magnetic resonance spectroscopy (SSNMR)

### B1.3. Elementary microanalysis

### B1.4. Gas evolution analysis by Gas Chromatography

### B1.5. UV-Visible diffuse reflectance spectroscopy (UV-vis DRS)

### B1.6. Extended X-Ray absorption fine structure spectroscopy (EXAFS)

### B1.7. High Resolution Transmission Electron Microscope (HRTEM)

# Chapter 1

## Introduction

*The intent of this chapter is to summarize the developments in on-purpose production of butadiene, both from an industrial and academic point of view and to understand the limitations of the process with respect to the catalysis.*

*The second part of the chapter introduces the concept of surface organometallic chemistry (SOMC) as a technique to tailor well-defined heterogeneous catalysts and tries to explore its relevance in the production of butadiene from ethanol in Ostromyslensky's two-step process.*

*The last section delineates the objectives of this thesis*



# Contents

## Part A - Catalytic advances in on-purpose production of butadiene

<b>A1. General Introduction</b> .....	7
A1.1. Importance of Butadiene .....	7
A1.2. Present industrial processes for production of butadiene .....	7
A1.3. Emergence of bio-ethanol as a building block .....	10
<b>A2. Towards on purpose butadiene production</b> .....	11
A2.1. Routes in consideration for on-purpose butadiene production .....	11
A2.2. Butadiene synthesis by Ostromyslensky's two-step process .....	13
A2.3. Catalyst design .....	15
A2.4. State of the art catalytic systems .....	16
<b>A3. Towards better catalysis</b> .....	19

## Part B–Surface Organometallic Chemistry

<b>B1. General Introduction</b> .....	23
B1.1. Preparation and characterization of catalyst supports .....	23
B1.2. Grafting of organometallic complexes on catalyst support .....	24
B1.3. Evolution of well-defined surface sites upon post-treatment .....	25
B1.4. Characterization tools for studying the surface sites .....	28
<b>B2. Well defined silica supported Tantalum species</b> .....	29
B2.1. Grafting of Tantalum-alkyls on silica .....	29

B2.2. Grafting of Tantalum-alkoxys on silica .....	30
B2.3. Ta-H species supported on silica .....	31
<b>C. Aim of this work .....</b>	<b>32</b>
<b>D. References .....</b>	<b>33</b>

**Part A:**  
**Catalytic advances in on-purpose  
production of butadiene**



## A1. General Introduction

### A1.1. Importance of Butadiene

1,3-Butadiene is one of the most versatile and hence one of the most useful chemical building block<sup>1</sup>. Its largest use is in the production of synthetic elastomers such as Styrene–Butadiene Rubber (SBR), Styrene–Butadiene latex, Polybutadiene rubber, Nitrile rubber, and Chloroprene rubber<sup>2–4</sup>. (**Figure 1.1**) It also has some non-elastomeric uses, such as a raw material for making hexamethylenediamine, which is the precursor of nylon 6,6, and in the production of largest volume engineering thermoplastic resin, Acrylonitrile–Butadiene–Styrene (ABS). The global butadiene production for 2020 is predicted to be 15.91Mtonnes with an expected growth of 3%per annum from 2017-2024.

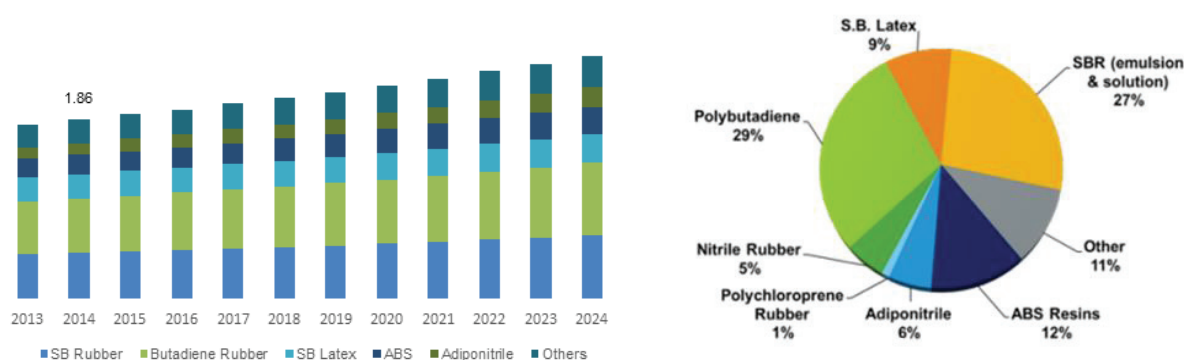


**Figure 1.1**-Global butadiene production forecast by application in billion USD (left) Major applications of butadiene (right)

### A1.2. Present industrial processes for production of butadiene

More than 95% of butadiene is currently obtained as a byproduct of steam cracking to produce ethylene<sup>4</sup>. This makes butadiene production highly dependent on the feedstock used to obtain ethylene.

With the recent developments in Shale gas technology, vast reservoirs of natural gas have opened up for chemical industry at cost effective prices<sup>5,6</sup>. In the wake of these changes, the production of ethylene has shifted from steam cracking of heavier feedstock like naphtha or gas oil to lighter starting material like the ethane obtained from shale gas.<sup>2</sup> However, the quantity of crude C4 hydrocarbons (and consequently the amount of

butadiene) in the lightened feedstock is much less than the heavier feedstock. (Figure 1.2) This is leading to restricted butadiene production and subsequent rise in its price.<sup>4</sup>

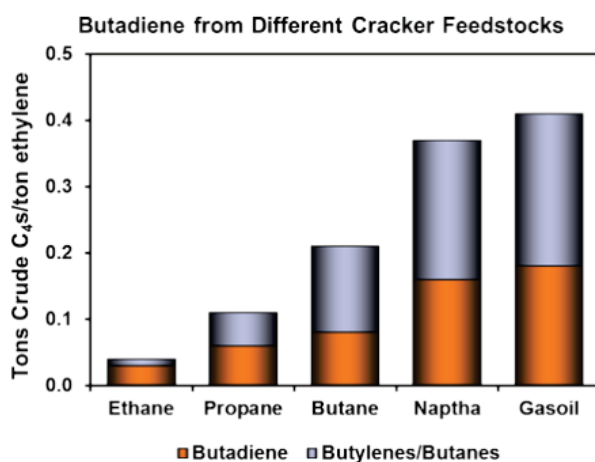


Figure 1.2- Butadiene produced from different cracker feedstock<sup>4</sup>

Until now the most established alternative route to produce BD has been via catalytic dehydrogenation of butanes obtained via petroleum based feedstock. This process is known to produce good yields of BD with selectivity up to 90% at competitive market prices. Though the process is already industrially viable, the high reaction temperatures (600°C-700°C) and issues relating to the catalyst stability leave much room for improvement. Also its inherent dependence on fossil based resources continues to be of concern.

In light of this growing environmental conscientiousness, both industry and academia are merging their competences in search of newer and more environmentally benign routes to produce BD<sup>1-3,7</sup>. In a comprehensive review, Sels et al.<sup>2</sup> summarize the routes to obtain BD from both fossil based and bio-based feedstocks. (Figure 1.3)

The most prominent amongst the new routes is the one from bio-ethanol. BD can be obtained from ethanol either by (i) one-step conversion of ethanol to BD employing mixed metal oxide catalysts (Lebedev Process) or by a (ii) two-step process involving dehydrogenation of ethanol to acetaldehyde in a separate step, followed by Butadiene production in the second stage by co-feeding acetaldehyde along with ethanol (Ostromyslensky process) Both these processes have been the pioneering approaches to BD production from the time of WWII.<sup>8,9</sup> Their proven industrial viability and easy and

cheap access to their starting material in form of bioethanol make them the most likely ‘green’ candidates for on-purpose BD production in near future.

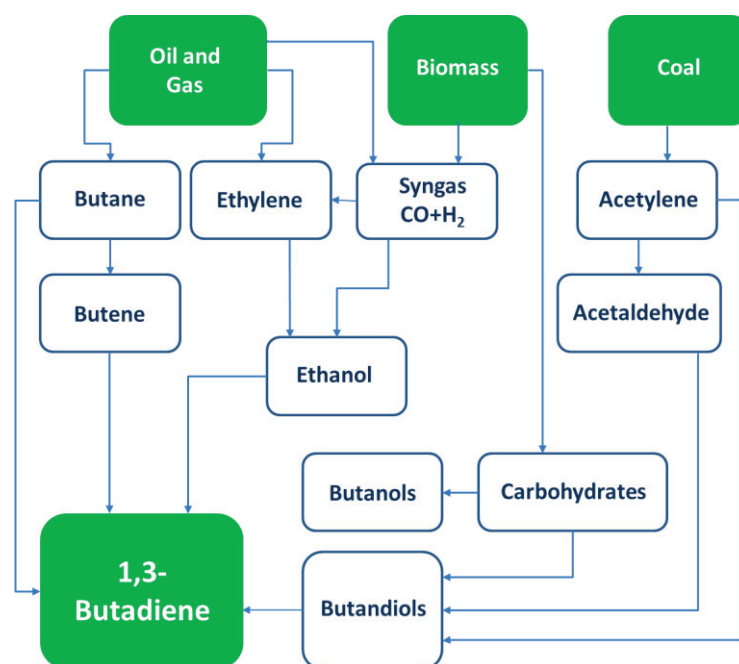


**Figure 1.3**-Possible synthesis routes for 1,3-butadiene from fossil based and bio derived feedstocks

Dehydration of monohydric and dihydric butanols (n-butanol, 2,3-butanediol, 1,4-butanediol, 1,3-butanediol) provides another attractive proposition<sup>10,11</sup>. Renewable C4 alcohols are increasingly available via fermentation of biomass or bio-derived syngas and their production is expected to rise in coming years. Two step acid catalyzed dehydration of monohydric alcohols and single step dehydration of dihydric alcohols are both being extensively studied. Special interest lies in the dehydration of 1,3 butanediol (1,3-BDO), whose conversion to BD is well known to the industry by Reppe’s process.<sup>12</sup>

The route from syngas (as waste gas from industries or biomass gasification) proceeds either via butanediols or via ethanol formation. Direct gas fermentation of CO to BD is also being studied.<sup>13-15</sup>

**Table 1.1** summarizes in detail the specific advantages and limitations of the processes discussed above.

**Table 1.1-** Advantages and limitations of the proposed bio-based routes to BD synthesis

Biomass	Advantages	Limitations
<b>Bio-Ethanol</b>	<ul style="list-style-type: none"> <li>-Industrial feasibility of the process is well proven with some functional plants in India and China</li> <li>-The price of bio-ethanol is expected to fall with its increased production</li> </ul>	<ul style="list-style-type: none"> <li>-To compete with fossil based existing technologies, major improvements are needed in terms of BD yield and selectivity</li> <li>-Issues exist related to catalyst lifetime and stability</li> </ul>
<b>Butanediols</b> (n-butanol, 2,3-butanediol, 1,4-butanediol)	<ul style="list-style-type: none"> <li>-There is a rise in the production of C4 alcohols produced via fermentation of biomass or syngas</li> <li>- Dehydration of 1,4-BDO is well known and gives good yields of BD at 280°C</li> </ul>	<ul style="list-style-type: none"> <li>-Dehydration of monohydric alcohols involves expensive, two-step dehydration and leads to production of mixture of butenes</li> <li>-Except for 1,4-BDO, the dehydration of diols requires higher temperatures (~400°C) and is less selective</li> </ul>
<b>Syngas</b>	<ul style="list-style-type: none"> <li>-Utilizes low quality biomass and eliminates biomass fractionation</li> </ul>	<ul style="list-style-type: none"> <li>- Research still in infancy</li> </ul>

#### A1.4. Emergence of bio-ethanol as a building block

With the renewed interest in butadiene production routes from Ethanol, Bio-ethanol, obtained from the fermentation of sugars, emerges to be the most relevant source of Bio-carbon. Today, Bioethanol is an important building block for synthesis of a variety of industrial chemicals.<sup>16,17</sup> Its annual production, which is an order of a magnitude higher than the global Butadiene demand, only corroborates its potential to be used as a raw material for Butadiene synthesis on an industrial scale in near future.<sup>2</sup>

The most commonly used plants to produce ethanol are sugar cane and sugar beet since the sucrose present in them is easily accessible for fermentation. Other plants used for fermentation are the corn, wheat potatoes or barley. The ethanol so produced is known as *first generation* ethanol and is presently the main route to bioethanol. However, there are two major concerns surrounding the first generation bioethanol and biofuels in general. The production of ethanol competes with the use of crops as food. Secondly, it excludes the use of most of the herbaceous biomass since the sugars in it are in the form of cellulose and hemicellulose which are more robust sugar polymers and thus less easily accessible. In fact, real success will lie in producing *second generation* bio-ethanol via efficient breakdown of cellulose to sugar monomers and its subsequent fermentation.

Nevertheless, efforts are being made in this area to obtain ethanol from several lignocellulosic sources such as straw, nut shells, bagasse and so on.<sup>16,17</sup>

Also the integration of algae (microalgae and macro-algae) as a sustainable feedstock for bioethanol is being evaluated. Though this approach can be useful considering food security and environmental impact, there are significant technological hurdles in its feasible commercialization.

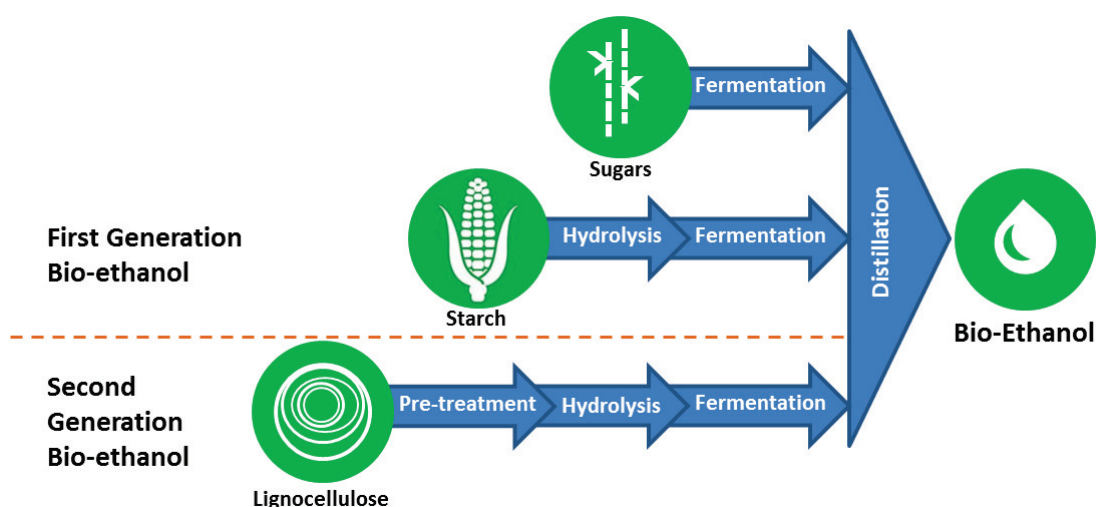
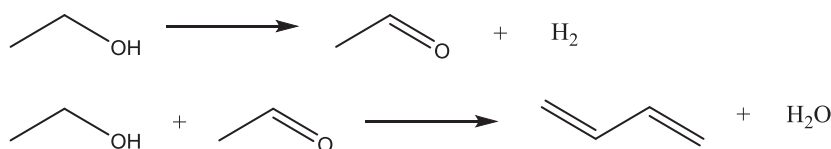


Figure 1.4- Schematic representation of first generation and second generation bioethanol synthesis

## A2. Towards on purpose butadiene production from bioethanol

### A2.1. Routes in consideration for on purpose butadiene production

Interestingly, the search for newer route has led to the rediscovery of synthesis routes from back in history, during the time of World War II. In the wartime effort, Ostromyslensky had proposed a catalytic route from a mixture of ethanol and acetaldehyde over alumina or clay catalysts at 440–460 °C, yielding 18% BD.<sup>18</sup> It was essentially a two-step process from ethanol to butadiene, involving dehydrogenation of ethanol to acetaldehyde in a separate step, followed by butadiene production in the second stage by co-feeding acetaldehyde along with ethanol. (See **scheme 1.1**)



**Scheme 1.1** - Two-step process to BD from ethanol by Ostromyslensky

Soon following this, in 1929, Sergei Lebedev proposed a process for direct conversion of ethanol to butadiene employing a mixture of zinc oxide and alumina catalyst at 400°C. He achieved a BD selectivity of 18%, directly from ethanol according to following reaction.<sup>19</sup>

**(Scheme 1.2)**



**Scheme 1.2-** One-step process to BD from ethanol by Lebedev

Both these process were later investigated by industries. In 1947, Union Carbide and Carbon Chemicals Corporation started performing the industrial manufacturing of BD from ethanol in the US over 2%Ta/SiO<sub>2</sub> using the two-step process.<sup>20</sup> After the war however, both these routes died out in the US and most of Europe, with the only surviving plants in India and China.

Though in the literature addition of acetaldehyde to ethanol has been reported to increase the overall BD yield by some authors, there is no evidence to support the preferentiality of one technological process over the other. However the following points are often cited in favor of the two-step process-

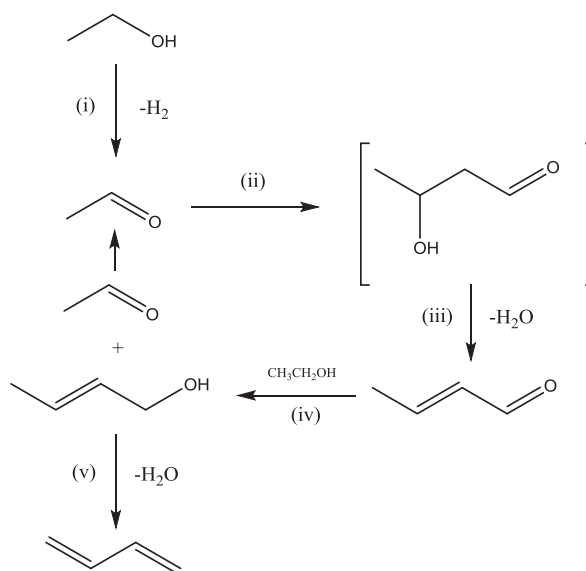
- The two-step process allows for an enhanced flexibility in the selection of appropriate reaction conditions for each reaction separately, thereby increasing the overall BD yield.<sup>8</sup> For example the ideal temperatures for conversion of ethanol to acetaldehyde over a copper oxide catalyst is considered to be 250°C whereas for the second step (conversion of ethanol and acetaldehyde to BD) 325-350°C are known to be thermodynamically favorable.
- Decoupling the dehydrogenation of ethanol from the steps of aldol condensation, MPV reduction and dehydration result in decreased catalyst complexity

- The ideal temperature range reported for the two-step process is around 325-350°C compared to 400-425°C reported for the one-step process
- The acetaldehyde which is produced in the first step of the transformation in a separate reactor can be treated as a value added product with its own market. This can in turn help in economizing the overall process.

## A2.2. Butadiene synthesis by Ostromyslensky's two-step process

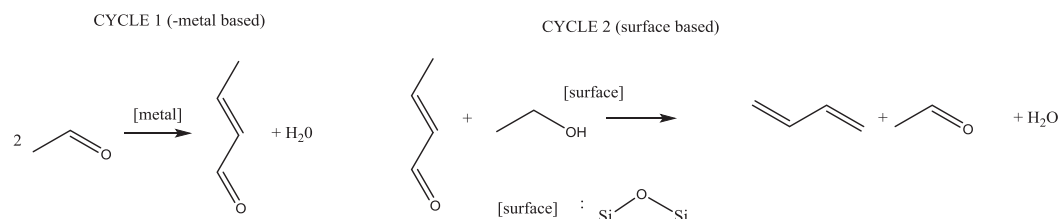
*Proposed mechanism*-Generally, the one-step and the two-step process for BD synthesis are only considered two technological options for BD production, essentially going through the same mechanisms<sup>21,22</sup>. However this has not yet been proven and pathway for this reaction remains a point of contention.

The Kagan mechanism, which was later validated by the thermodynamic studies by Bhattacharya et. al.<sup>23</sup> and Natta and Rigamonti, is the generally accepted mechanism. (Scheme 1.3) This mechanism proceeds via five preliminary steps- (i) acetaldehyde formation from Ethanol (ii) aldol condensation of acetaldehyde to acetaldol (iii) dehydration of acetaldol to crotonaldehyde (iv) Meerwein-Ponndorf-Verley reaction between crotonaldehyde and ethanol to obtain crotyl alcohol and acetaldehyde (v) dehydration of crotyl alcohol to butadiene.



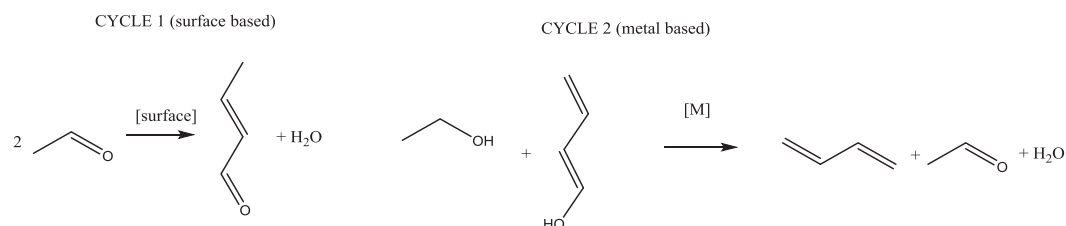
**Scheme 1.3**– Generally accepted reaction pathway for ETB conversion based on Kagan mechanism

Quattlebaum et al<sup>24</sup>. for the first time attempted a description of mechanism taking into account the role of catalyst and surface atoms of its support. The group suggested that the reactive siloxane bridges of silica-based catalyst participated in deoxygenation process by reacting with ethanol and enol, while oxide promoter (eg. Tantalum, zirconium, niobium oxides) perform aldol condensation



**Scheme 1.4** - Reaction mechanism for the two-step process suggested by Quattlebaum et al.

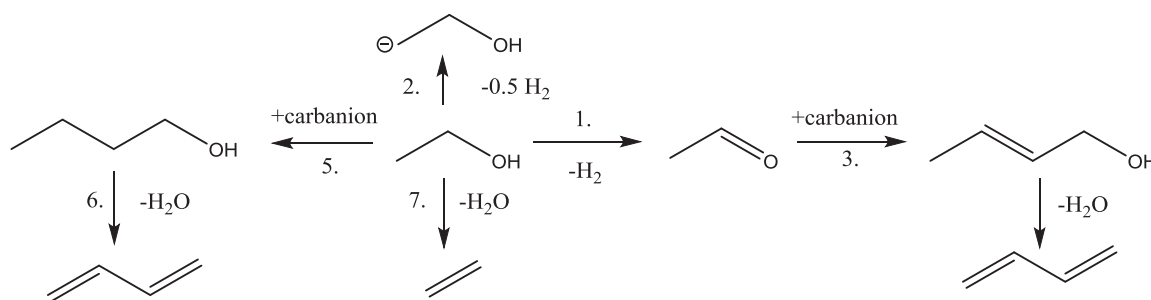
Later Jones et al. studying the reaction mechanism of the two step process over a 2%Ta<sub>2</sub>O<sub>5</sub>-SiO<sub>2</sub> catalyst suggested an opposite effect from catalyst components, the unmodified silica being more effective for acetaldehyde condensation and 2% Ta<sub>2</sub>O<sub>5</sub>-SiO<sub>2</sub> being more active for deoxygenation of the aldehyde.



**Scheme 1.5** - Reaction mechanism for the two-step process suggested by Jones et al.

Though the Kagan mechanism has been generally accepted, some issues have been identified with the proposed five step mechanism. The first issue concerns the assumption of acetaldol as an intermediate which has seldom been detected amongst the products of the reaction. The second issue is that the engineers at Union Carbide Corporation have reported that acetaldol was converted back to acetaldehyde when fed together with ethanol into a reactor packed with a 2% Ta/SiO<sub>2</sub> catalyst without producing butadiene. Together this might suggest that the reaction proceeds through a different pathway.

Based on this and their observation on purely basic MgO catalysts, Cavani *et al.*<sup>25,26</sup> have recently proposed a new, self-consistent mechanism featuring an intermediate carbanion species in the formation of C<sub>4</sub> molecules.



**Scheme 1.6** -Novel reaction pathway for the formation of butadiene from ethanol proposed by Cavani et al.<sup>26,27</sup>

Though these results are recent and need to be proven on catalytic systems other than MgO, they indicate the need to study the reaction pathway from ethanol to butadiene in further detail.

Though the mechanism of the reaction has not been unequivocally stated, several authors have described the thermodynamics for the conversion of ethanol to BD, mostly based on the Kagan mechanism.<sup>21</sup>  $\Delta G$  calculations for equilibrium conditions for both one step and two step processes indicate that there is no thermodynamic advantage when performing EtOH to BD in two steps. The increase in BD yield and selectivity of the two-stage process can therefore only be explained by kinetic factors, related to the catalyst properties.

### A2.3. Catalyst design

Due to the variety of elementary steps involved between conversion of ethanol and acetaldehyde to butadiene, it is certain that the catalyst responsible for this transformation must be multifunctional. It is widely accepted that the catalytic systems should possess a mixture of acidic, basic and redox properties. While the redox and basic sites can participate in dehydrogenation of ethanol to acetaldehyde, the acidic and basic sites can be thought to be active in the condensation and dehydration reactions. However, we know that transformation of ethanol and acetaldehyde to BD is marred by numerous side reactions which can be favoured or suppressed based on the kinetic and thermodynamic conditions. For example, excessive acidity in the catalytic system can lead to dehydration of ethanol to ethylene and diethyl ether.



and Bronsted acid sites were detected. While the Zr loading did not affect the Bronsted acidity, the Lewis acidity increased with increase in Zr%. Citing the amphoteric nature of Zirconium, the authors hypothesize that varying ZrO<sub>2</sub> loading can affect the acid/base properties of the catalysts. The optimal catalysts, recorded at 593 K for a WHSV of 1.8 h<sup>-1</sup> and EtOH/AA ratio of 3.5 had a butadiene yield of 31.6% for 3 hrs on stream.

Lee et al.<sup>33</sup>. Used ZrO<sub>2</sub>/SiO<sub>2</sub> catalysts synthesized from zirconium oxynitrate dispersed on mesocellular siliceous foam (MCF) by urea hydrolysis method. With optimization, butadiene selectivity of 73% for a WHSV of 3.7 h<sup>-1</sup> after 15 h was obtained. The deactivation of catalysts was attributed to coke formation. The activity is attributed to the high dispersion of the metal oxides, while the large pores of the support are thought of preventing mass transfer issues and coking.

Zhang et. al.<sup>34</sup>. Investigated ZnO promoted ZrO<sub>2</sub>-SiO<sub>2</sub> catalysts synthesized by a sol-gel method for the two-step ethanol transformation to butadiene. Surface acidity studies showed that the addition of ZnO into ZrO<sub>2</sub>-SiO<sub>2</sub> system decreased quantity of acidity yet did not change the strength of the acid sites on the catalysts. This is thought to lower the selectivity to dehydration products while boosting the BD selectivity. The best performance with ethanol/acetaldehyde conversion of 40.7% and BD selectivity of 83.3% was reached at 310°C, ethanol/acetaldehyde mole ratio of 3.5 and WHSV of 1.4 h<sup>-1</sup> using a 0.5 wt% ZnO doped ZrO<sub>2</sub>-SiO<sub>2</sub> catalyst.

### Tantalum based systems

Tantalum is considered to be amongst the most active catalyst in ETB transformation from the time of WWII. Corson et.al.<sup>8</sup> showed copper-doped silica-supported Tantalum oxide to be amongst the most active catalysts for the one-step conversion of ethanol.

A notable study is that by Chae et al.<sup>35</sup> who prepared a series of ordered mesoporous silica (OMS) supported Tantalum oxide samples by wetness impregnation technique followed by calcination at high temperature. The catalysts showed better catalytic performances towards butadiene production compared to the earlier systems, indicating need for better dispersed tantalum on silica catalysts. The study primarily focused on effect of surface morphology on catalytic activity while no conclusive comment was made on the surface active species.

A remarkable attempt to synthesize a well-defined active specie was recently made by Dzwigaj et al. who reported Ta incorporation into vacant T-atom sites of the SiBEA zeolites framework as mononuclear Ta(V) allowing for the preparation of highly selective catalysts for 1,3-butadiene synthesis. In the study higher Ta(V) content increased the formation of ethylene, which the authors relate to the formation of closed tantalum sites bound to four silicon atoms. Accordingly, these sites were said to be less active towards butadiene formation.

### Niobium based systems

Niobium oxide was found to be active for the two-step process by Toussaint et al.<sup>24</sup> in 1947. Ivanova et al.<sup>36</sup> reiterated this claim by adding niobium to the list of metals that could be used to produce butadiene from ethanol when appropriately promoted.

Kyriienko et al.<sup>37</sup> investigated niobium-modified zeolite BEA for the ETB reaction. The catalysts were synthesized by a two-step post-synthesis method similar to the Ta/SiBEA system mentioned above. The performance of the Nb/SiBEA system was reported to be poorer than the Ta/SiBEA system. At 350°C, with an EtOH/AA ratio of 2.7 and for a WHSV of 0.8 h<sup>-1</sup>, butadiene yield over 0.7% Nb/BEA was of 23.6, for a productivity of 0.11 gBD·g<sup>-1</sup>cat·h<sup>-1</sup>. Combining the observations from this study together with the observations made earlier by Toussaint et al.<sup>24</sup>, Niobium is an unlikely candidate for industrial application in two step synthesis of BD.

### Other systems

Palkovits et al.<sup>38</sup> tested a set of zeolite based catalysts, designed for variation of the concentration and relative ratio of acidic and basic sites for materials of comparable textural properties by varying the zeolite's module, adding magnesium oxide and exchanging the proton by alkaline and earth alkaline metals, respectively. MgO added zeolite material could facilitate the highest BD selectivity of 72%.

Tan et al.<sup>39</sup> Studied MgO–SiO<sub>2</sub> catalysts with different surface properties, synthesized by simple tuning of the calcination temperature. The best MgO–SiO<sub>2</sub> catalyst with a significant amount of amorphous magnesium silicates and few crystalline magnesium silicates, showed the highest BD selectivity of 80.7%.

### **A2.5. Towards better catalysis**

Whereas a series of catalyst compositions have been tested, most of the above studies are incomplete in their thorough physico-chemical characterization. The studies lack a molecular insight into the species populating the catalyst surface. As a result, definitive identification of the active sites on these catalytic systems remains an open question. Indeed the usual preparation of heterogeneous catalysts by wetness impregnation, sol-gel technique, wetness kneading, produces catalysts with a broad distribution of metal coordination environments<sup>40,41</sup>. This makes it difficult to characterize them at the molecular level.

In addition to insufficient understanding of the active sites, the inherent heterogeneous nature of the surface species mars the overall BD yield and catalyst productivity. This can be witnessed by a broad product distribution and to some extent catalyst deactivation due to formation of higher alkanes.

In this context Surface organometallic chemistry (SOMC) can provide invaluable tools in bridging the gap between homogeneous and heterogeneous catalysts by designing well-defined single site surface complexes. In the next section we discuss the principle and practicalities of the SOMC protocol to explore the possibility of designing well-defined catalysts for on-purpose synthesis of butadiene by Ostromyslensky's process.



**Part B:**  
**Surface Organometallic Chemistry**



## B. Surface Organometallic Chemistry

### B1. General Introduction

Catalysis represents an important driver for our chemical industries and thereby our economy. While heterogeneous catalysts are often thought to be more industrially viable due to their robust nature, easy recovery and regeneration, they barely possess the high degree of molecular uniformity inherent to their homogeneous counterparts.<sup>42-44</sup> As a result of their numerous, heterogeneous surface sites these catalysts lack selectivity towards a desired end product. Difficulty also lies in characterization of their active sites with molecular precision. This confines the development of new heterogeneous catalysts to an empirical approach rather than a rational one. To combine the advantages of both homogeneous and heterogeneous catalysis, efforts have been directed towards the generation of heterogeneous catalysts with well-defined active sites. In this respect, one of the powerful approaches is that of Surface Organometallic Chemistry (SOMC)<sup>45,46</sup>

Surface Organometallic Chemistry is a technique developed to tailor well-defined heterogeneous catalysts by grafting organometallic complexes on surface sites of a support in a controlled fashion.<sup>45</sup> This approach is based on controlling the concentration of grafting sites per unit area of the support, which in turn controls the final density of organometallics grafted on the surface. Due to its ability to perform molecularly controlled grafting, SOMC produces surface sites with a known co-ordination sphere. This attribute is essential in developing a structure activity relationship for a catalyst and in turn for rational design of ideal catalysts for a process.

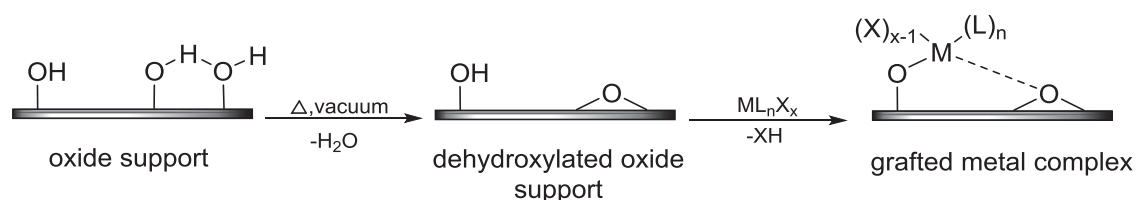


**Figure 1.6-** Schematic representation of preparation of a well-defined catalyst using SOMC

Keeping this in mind, the main requirements for applying SOMC approach would be the presence of a well-characterized support, and an organometallic complex - ML<sub>n</sub>X<sub>x</sub> (L= functional ligand, X= ancillary ligand).<sup>47,48</sup> Upon grafting the complex on the support, it can be used as a catalyst by itself or be subjected to post-treatments (calcination,

hydrogenation, sulfidation) to obtain a more stable structure or to attain a new functionality. Figure 1 schematically represents an ideal SOMC catalyst with its key components.

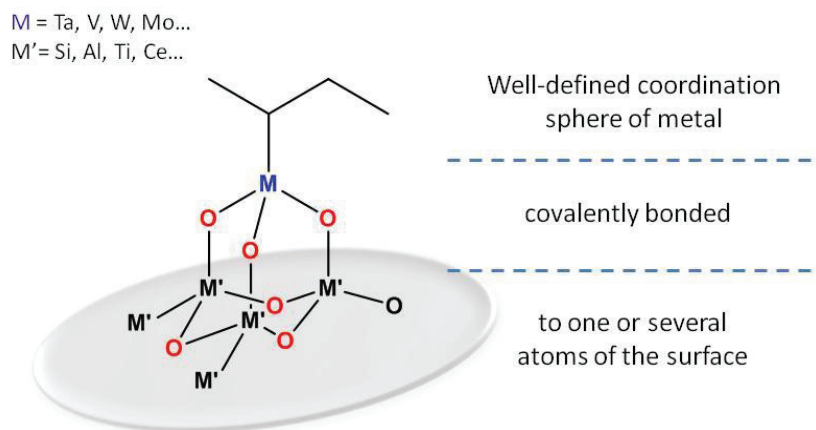


**Figure 1.7** Schematic representation of a well-defined catalyst using SOMC

### B1.1. Preparation and characterization of catalyst supports

Various supports such as silica<sup>49</sup>, alumina<sup>50</sup>, silica-alumina<sup>51</sup>, zeolites etc have been investigated for grafting organometallic moieties. Every support is unique in the grafting site it carries on its surface. Grafting sites for various SOMC supports have been listed in **Table 1.2**. Depending on the nature, density and homogeneity of these reactive sites, different behaviors are observed, many a times leading to completely different catalytic applications.

**Table 1.2-** Grafting sites present in some supports used for SOMC<sup>45</sup>

Support	Grafting site
• Silica	Hydroxyl groups called silanols ( $\equiv\text{Si-O(H)}$ )
• Silica-Alumina	Silanol groups; Si-O(H)-Al bridges
• Alumina	Hydroxyl groups (at least five different types); Al-O-Al bridges (where the bond is not covalent); Lewis acid sites

• Magnesia	Hydroxyl groups; lacunar magnesium sites
• Zeolites	Protons with different locations which can be more or less accessible; extra-framework aluminium sites; silanol groups on the external surface of the crystallites
• Carbon	All chemical functions can be found: alcohols, amines, ethers, thiols, ketones, aldehydes, carboxylic acid, etc

Silica represents one of the most studied supports. It is typically an amorphous solid with relatively high surface areas between 50 and 1000 m<sup>2</sup> g<sup>-1</sup>. Its texture and shape depends mostly upon the method of preparation. Flame pyrolysis of SiCl<sub>4</sub> and H<sub>2</sub>/O<sub>2</sub> above 1000 °C produces high purity, nonporous silica with surface areas between 50–380 m<sup>2</sup> g<sup>-1</sup>. Mesostructured materials such as MCM-41<sup>52</sup> and SBA-15<sup>40</sup> are prepared using sol-gel synthesis methods in the presence of a surfactant template to form ordered mesopores of desired shape and size. These are high surface area material with surface areas up to 1000 m<sup>2</sup> g<sup>-1</sup>.

Silica is made up of SiO<sub>4</sub> tetrahedra linked by siloxane (≡Si-O-Si≡) bridges and surface silanols (≡Si-OH). Heating under dynamic vacuum can affect the concentration and nature of these surface silanols. Under UHV, at 150°C the physisorbed water is removed from the surface of silica. Heating at higher temperatures leads to condensation of adjacent (≡Si-OH) groups and formation of (≡Si-O-Si≡) bridges with simultaneous evolution of water. Thus different dehydroxylation temperatures produce silica with varying topology. The transformation of silica surface can be monitored by IR spectroscopy where the stretching of isolated, vicinal and geminal silanols can be identified at 3747 cm<sup>-1</sup>, 3650 cm<sup>-1</sup> and 3750 cm<sup>-1</sup> respectively.

Quantitative estimation of these hydroxyl surface sites has also been performed by their chemical titration against metal alkyls (*n*-BuLi) or metal alkyl halides (MeMgBr). From this, the silanol density of SiO<sub>2-200</sub>, SiO<sub>2-500</sub> and SiO<sub>2-700</sub> has been calculated as 2.6, 1.4 and 0.7 OH/nm<sup>2</sup> respectively. These values were later verified by quantitative solid-state <sup>1</sup>H MAS NMR by Lefebvre et. al.<sup>53,54</sup>

### **B1.2. Grafting of organometallic complexes on catalyst support**

Grafting of a metal precursor onto the support is carried out under strict anhydrous and anaerobic conditions. This is due to the general sensitivity of organometallic complexes

to air and water along with the increased sensitivity of surface species supported on the surface of the oxides. A typical grafting reaction is carried out in a double-schlenk with a sintered glass filter between the two arms of the flask. (Figure)

A solution of the organometallic precursor is placed in one half of the double-schlenk while the support is added to the other half. The solution is then transferred by a freeze-pump-thaw cycle to the support through the filter. The resulting suspension is slowly stirred. After the reaction is complete, the supernatant is filtered into the other half of the double-Schlenk. To wash the reacted material, the solvent is transferred back into the other chamber of the double-Schlenk by vacuum distillation. The material is washed to remove the excess organometallic precursor adsorbed on its surface washing step 2-3 times.

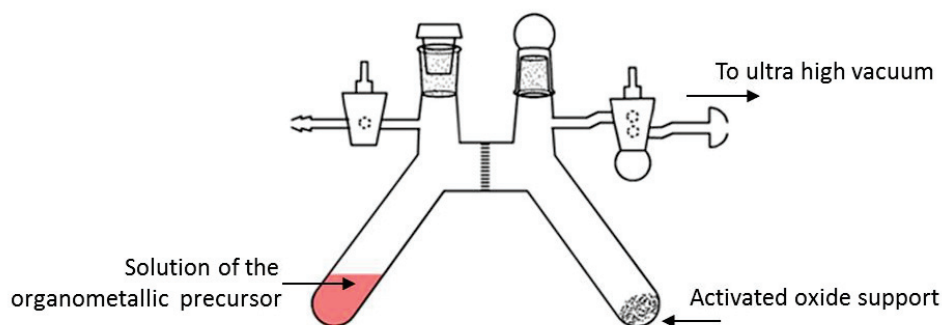


**Figure 1.8-** Schematic representation of grafting in a double-Schlenk flask by SOMC protocol

### **B1.3. Evolution of well-defined surface sites upon post-treatment**

In general terms, preparation of a solid industrial catalyst involves impregnation of a catalyst support with a solution containing a precursor of the active component, followed by post-treatments such as calcination, reduction, oxidation, or sulfidation.<sup>55</sup> The activity of the resulting catalyst depends upon the speciation of the active component along with its dispersion and distribution throughout the support. Though a homogeneous distribution of active sites is mostly thought to be desirable, the post-treatments often result in redistribution of the active species on the surface. (e.g. - forming agglomerates in case of calcination) Moreover, characterization studies dealing with the analysis of the metal speciation and distribution are scarce for traditional heterogeneous catalysts.

For the catalysts synthesized by SOMC techniques the evolution of surface species during various post-treatments has been monitored via various spectroscopic and analytical techniques.

**Calcination**, which can be defined as heat treatment (at temperatures typically above 400°C) performed under air, is a commonly applied treatment in both preparation and regeneration of SOMC catalysts. During catalyst preparation the aim is to remove the organic template and stabilization of the catalyst. The surface sites are largely reported to remain isolated (more so for early metals) when low surface loadings are used. However, calcination at very high temperatures can lead to incorporation of the metal into the support matrix and/or to sintering to form metal oxide clusters.

**Thermolysis under vacuum-** Supported organometallics with  $-\text{N}(\text{SiMe}_3)_2$ ,  $-\text{OSi}(\text{OtBu})_3$ ,  $-\text{OtBu}$ , or  $-\text{Cl}$  as ligands, readily lose their ligands when treated at high temperatures (>150–400°C) under vacuum, while remaining mostly isolated. Thermolysis involves reaction of the metal site with an adjacent siloxane bridges and generating more stable silicate species.

**Thermal treatment under H<sub>2</sub>-** The reaction of silica, alumina, and silica–alumina supported early transition metal alkyl complexes with dry hydrogen at 100–200 °C typically forms metal hydrides. The formation of supported metal hydrides is proposed to occur through hydrogenolysis of metal–carbon bonds to form highly reactive metal hydride species. For silica supported complexes, the hydride species further react with the adjacent siloxane bridges creating new metal oxygen bonds and transferring hydrides to the surface.

### B1.4. Characterization tools for studying the surface sites

One of the defining features of catalysts synthesized by SOMC technique is the detailed knowledge of the nature of species populating the surface of the catalyst. Such precise understanding of the surface is a result of advanced characterization techniques, which together provide the complete picture of the surface of the catalyst. **Table 1.3** enlists the commonly used characterization techniques and the information they provide

**Table 1.3-** Characterization techniques used for catalysts synthesized by SOMC protocol

Surface morphology and surface area	
• N <sub>2</sub> adsorption	surface area, porosity
• Transmission electron microscopy (TEM) and EDX	Morphology–aggregation state–composition and distribution of atoms of the solid matrix
• X-ray diffraction	Specific polymorph of the support and level of crystallinity
Metal co-ordination sphere	
• Elemental analysis	Metal and other elements loadings average composition of surface complexes establishing the stoichiometry of grafting
• Gas analysis	
• IR spectroscopy	Evidence for the disappearance and/or appearance of surface functionalities, e.g. consumption of surface OH groups and appearance of specific surface sites (C–H, N–H, C–C, M–H vibrations)
• Solid state NMR	Detailed molecular-level structure 61–76 types of ligands bound to the surface sites (usually via <sup>1</sup> H, <sup>13</sup> C, <sup>15</sup> N, <sup>31</sup> P NMR) reaction intermediates using labeled reactants measurement of acidity (phosphine oxide and pyridine adsorption) with <sup>15</sup> N and <sup>31</sup> P NMR
• Raman spectroscopy	Characterization of surface oxo and related species
• UV–vis spectroscopy	Evaluation of the isolation or agglomeration of surface species
• XANES	Metal oxidation state and geometry of surface complexes
• EXAFS	Coordination sphere of the metal: number, type and bond distance of atoms (ligands) bound to the metal sites
Complementary techniques	
• XPS	Metal oxidation state
• EPR	Characterization and titration of paramagnetic species

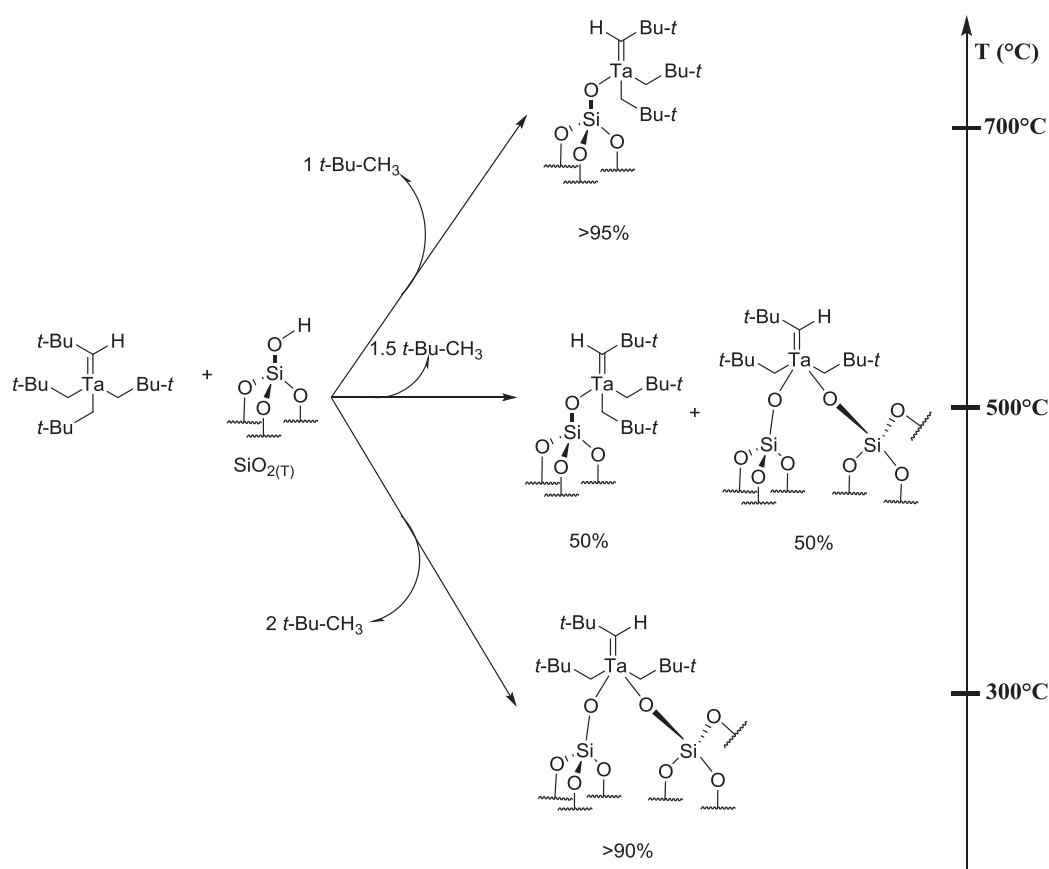
These spectroscopic and analytical techniques can also be accompanied by the preparation of soluble molecular analogues of the surface. These analogues can be more easily and precisely characterized by solution techniques. Such an approach is particularly powerful with silica-supported systems since numerous molecular analogues are already available. Quadrelli et. al. have published a comprehensive review on molecular models that mimic the surfaces of inorganic oxide supports and aid understanding their interaction with the grafted organometallic fragments. Additionally, crystallographic parameters of molecular complexes can be used for building models for the interpretation of XAS data of the supported species.

Computational chemistry is being increasingly employed as a complementary tool to obtain energy profiles that can relate to structural preferences and particular spectroscopic signatures of surface species. Computational methods can confirm or rule out possible structures and allow a deeper understanding of the relation between structure and reactivity. This understanding can be useful in thereby establishing the catalytic sites and mechanism of a reaction.

## **B2. Well defined silica supported Tantalum species**

### **B2.1. Grafting of Tantalum-alkyls on silica**

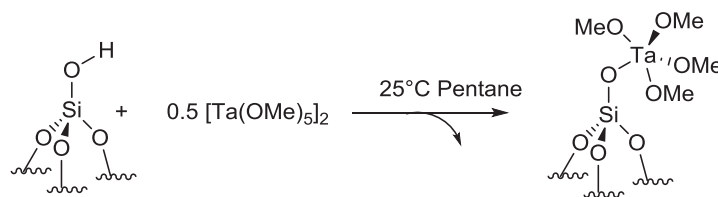
In 1995, Dufaud et al.<sup>56</sup> first succeeded in grafting tantalum onto silica by reacting  $\text{Ta}(\text{CH}^t\text{Bu})(\text{CH}_2^t\text{Bu})_3$  with the surface hydroxyls of a partially dehydroxylated silica. Based on IR spectroscopy, solid state NMR spectroscopies, elemental analyses, and quantitative chemical reactivity toward ethanol and  $\text{H}_2$ , it was shown that  $(\equiv\text{SiO})\text{Ta}(\text{CH}^t\text{Bu})(\text{CH}_2^t\text{Bu})_2$  is obtained as the sole surface species (> 95 %) when grafted on silica dehydroxylated at 700°C. This study was followed by other studies that showed that the nature and in the concentration of the surface silanol groups (by varying the temperature of dehydroxylation) can affect the nature of the resulting surface species. (**Scheme 1.7**) In 2001 Chabanas et al.<sup>57</sup> used high-resolution solid-state one-dimensional (1D) and two-dimensional (2D) NMR spectroscopy to study to define the structure of  $(\equiv\text{SiO})\text{Ta}(\text{CH}^t\text{Bu})(\text{CH}_2^t\text{Bu})_2$  at a molecular level and to investigate the reaction pathway leading to the grafted species.



**Scheme 1.7-** Formation of different well-defined Tantalum species depending on the dehydroxylation temperature of  $\text{SiO}_2$

## B2.2. Grafting of Tantalum-alkoxys on silica

Petroff et al.<sup>58</sup> demonstrated the grafting of tantalum alkoxy complex as shown in **scheme 1.8**. The appeal of grafting an alkoxy precursor compared to the organometallic  $\text{Ta}(\text{CH}^t\text{Bu})(\text{CH}_2^t\text{Bu})_3$  was its easy and comparatively cheap availability. Based on IR spectroscopy, elemental analysis and NMR studies it was found that by grafting tantalum methoxide  $\text{Ta}(\text{OMe})_5$  on  $\text{SiO}_{2-700}$  a monopodal ( $\equiv\text{SiO}$ ) $\text{Ta}(\text{OMe})_4$  surface specie was obtained. One of the primary concerns of the study was the inherent dimeric nature of tantalum alkoxy in solution. However upon EXAFS analysis, no Ta-Ta interaction was reported and the presence of an isolated monopodal tantalum methoxides supported on silica was confirmed.

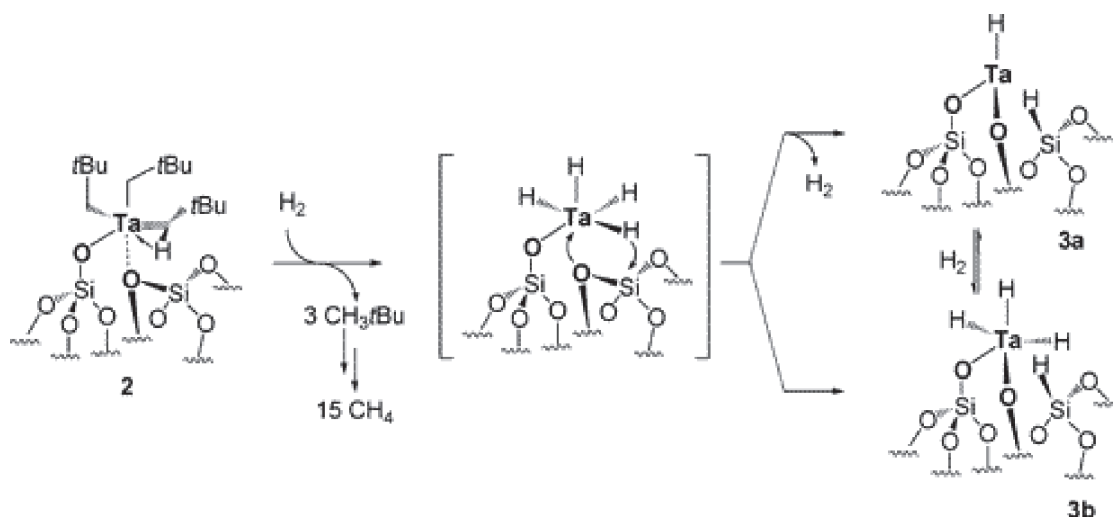


**Scheme 1.8-** Grafting of Ta(OMe)<sub>5</sub> onto SiO<sub>2</sub>-(700) according to Petroff et al.

### B2.3. Ta-H species supported on silica

Silica supported tantalum alkyls lead to a mixture of supported tantalum hydrides  $[(\equiv\text{SiO})_2\text{Ta}(\text{H})_x]_{(x=1,3)}$ , by treatment under hydrogen at 150 °C.<sup>59,60</sup> Soignier et al.<sup>44</sup> characterized these surface complexes by the combined use of several techniques such as IR and EXAFS spectroscopies as well as <sup>1</sup>H MAS, <sup>13</sup>C CP/MAS, 2D <sup>1</sup>H-<sup>13</sup>C HETCOR, and J-resolved solid-state NMR and mass balance analysis.

The proposed mechanism for the formation of supported tantalum hydrides involves a reaction of a siloxane bridge of silica with one hydrogen atom from the coordination sphere of tantalum generating tantalum hydrides and surface ( $\equiv\text{Si-H}$ ) species.



**Scheme 1.9-** Proposed mechanism for the formation of supported tantalum hydrides from tantalum alkyls upon treatment under hydrogen at 150 °C<sup>44</sup>

## C. Aim of the project

The most distinguishing advantage of surface organometallic chemistry is that, via a molecular approach, the coordination sphere of a grafted metal can be designed based on molecular considerations drawn from homogeneous organometallic chemistry. In this manner, catalysts with homogeneous and uniformly distributed active sites can be synthesized.

We have discussed both- (i) the current limitations in butadiene production from ethanol and acetaldehyde from the point of view of catalysis and (ii) the scope of SOMC in synthesizing novel catalysts with a molecular precision. Thus the aim of this work is to utilize the expertise of SOMC in developing to new tantalum-based catalysts for the transformation of ethanol/acetaldehyde to butadiene.

Towards this endeavor, the aim of this project is-

- To develop a family of well-defined  $\text{TaO}_x/\text{SiO}_2$  catalysts through SOMC protocol with varying Tantalum nuclearity
- To compare their performances to other classic  $\text{Ta(V)}/\text{SiO}_2$  heterogeneous catalysts discussed in literature for the conversion of ethanol and acetaldehyde to butadiene.

The study will provide new insights the structure activity relationship and study the role of support and metal oxide in the conversion of ethanol and acetaldehyde to butadiene. This understanding will be immensely useful in designing catalytic systems with better catalytic performances (Conversion, Selectivity and Catalyst Lifetime)

## D. References

1. Cavani, F., Albonetti, S., Basile, F. & Gandini, A. *Chemicals and fuels from bio-based building blocks*. (2016).
2. Makshina, E. V. *et al.* Review of old chemistry and new catalytic advances in the on-purpose synthesis of butadiene. *Chem. Soc. Rev.* **43**, 7917–7953 (2014).
3. Pomalaza, G., Capron, M., Ordonsky, V. & Dumeignil, F. Recent Breakthroughs in the Conversion of Ethanol to Butadiene. *Catalysts* **6**, 203 (2016).
4. Jeffery S. Plotkins. The Continuing Quest for Butadiene - American Chemical Society. Available at: <https://www.acs.org/content/acs/en/pressroom/cutting-edge-chemistry/the-continuing-quest-for-butadiene.html>.
5. Bruijninx, P. C. A. & Weckhuysen, B. M. Shale Gas Revolution: An Opportunity for the Production of Biobased Chemicals? *Angew. Chemie Int. Ed.* **52**, 11980–11987 (2013).
6. Middleton, R. S., Gupta, R., Hyman, J. D. & Viswanathan, H. S. The shale gas revolution: Barriers, sustainability, and emerging opportunities. *Appl. Energy* **199**, 88–95 (2017).
7. Ezinkwo, G. O., Tretyakov, V. P., Aliyu, A. & Ilolov, A. M. Fundamental Issues of Catalytic Conversion of Bio-Ethanol into Butadiene. *ChemBioEng Rev.* **1**, 194–203 (2014).
8. Corson, B. B., Jones, H. E., Welling, C. E., Hinckley, J. A. & Stahly, E. E. *Butadiene from Ethyl Alcohol. Catalysis in the One-and Two-Stop Processes. Industrial & Engineering Chemistry* **42**, (UTC, 1950).
9. W.J. Toussaint, J.T. Dunn, D. R. J. Production of Butadiene from Alcohol. (1947).
10. Duan, H., Yamada, Y. & Sato, S. Future Prospect of the Production of 1,3-Butadiene from Butanediols. *Chem. Lett* **45**, 1036–1047 (2016).
11. Langeveld, H., Meeusen, M. & Sanders, J. *The biobased economy: biofuels, materials and chemicals in the post-oil era*. (Earthscan, 2010).
12. Arpe, H.-J. & Weissermel, K. *Industrial organic chemistry*. (Wiley-VCH, 2010).
13. Griffin, D. W. & Schultz, M. A. Fuel and chemical products from biomass syngas: A comparison of gas fermentation to thermochemical conversion routes. *Environ. Prog. Sustain. Energy* **31**, 219–224 (2012).
14. Latif, H., Zeidan, A. A., Nielsen, A. T. & Zengler, K. Trash to treasure: production of biofuels and commodity chemicals via syngas fermenting microorganisms. *Curr. Opin. Biotechnol.* **27**, 79–87 (2014).
15. Henstra, A. M., Sipma, J., Rinzema, A. & Stams, A. J. Microbiology of synthesis

- gas fermentation for biofuel production. *Curr. Opin. Biotechnol.* **18**, 206 (2007).
16. Zabed, H., Sahu, J. N., Suely, A., Boyce, A. N. & Faruq, G. Bioethanol production from renewable sources: Current perspectives and technological progress. *Renew. Sustain. Energy Rev.* **71**, 475–501 (2017).
  17. Vohra, M., Manwar, J., Manmode, R., Padgilwar, S. & Patil, S. Bioethanol production: Feedstock and current technologies. *J. Environ. Chem. Eng.* **2**, 573–584 (2014).
  18. Ostromyslensky. *J. Russ. Phys.-Chem. Soc.* **47**, 1472–1506 (1915).
  19. Lebedev S. V. GB 331482. (1929).
  20. W.J. Toussaint and J.T. Dunn. US 2,421,361. (1947).
  21. Angelici, C., Weckhuysen, B. M. & Bruijninx, P. C. A. Chemocatalytic conversion of ethanol into butadiene and other bulk chemicals. *ChemSusChem* **6**, 1595–1614 (2013).
  22. Makshina, E. V., Janssens, W., Sels, B. F. & Jacobs, P. A. Catalytic study of the conversion of ethanol into 1,3-butadiene. *Catal. Today* **198**, 338–344 (2012).
  23. Bhattacharyya, S. K. & Sanyal, S. K. *Kinetic Study on the Mechanism of the Catalytic Conversion of Ethanol to Butadiene. Journal of Catalysis* **7**, (1967).
  24. Quattlebaum, W. M., Toussaint, W. J. & Dunn, J. T. Deoxygenation of Certain Aldehydes and Ketones: Preparation of Butadiene and Styrene. *J. Am. Chem. Soc.* **69**, 593–599 (1947).
  25. Chieragato, A. *et al.* On the Chemistry of Ethanol on Basic Oxides: Revising Mechanisms and Intermediates in the Lebedev and Guerbet reactions. *ChemSusChem* **8**, 377–388 (2015).
  26. Ochoa, J. V. *et al.* An analysis of the chemical, physical and reactivity features of MgO–SiO<sub>2</sub> catalysts for butadiene synthesis with the Lebedev process. *Green Chem.* **18**, 1653–1663 (2016).
  27. Chieragato, A. *et al.* On the chemistry of ethanol on basic oxides: Revising mechanisms and intermediates in the lebedev and guerbet reactions. *ChemSusChem* (2015).
  28. Sushkevich, V. L., Palagin, D. & Ivanova, I. I. With Open Arms: Open Sites of ZrBEA Zeolite Facilitate Selective Synthesis of Butadiene from Ethanol. *ACS Catal.* **5**, 4833–4836 (2015).
  29. Ordonsky, V. V, Sushkevich, V. L. & Ivanova, I. I. Study of acetaldehyde condensation chemistry over magnesia and zirconia supported on silica. *Journal Mol. Catal. A, Chem.* **333**, 85–93 (2010).
  30. Toussaint, W. J., Dunn, J. T. & Jackson, D. R. Production of Butadiene from Alcohol. *Ind. Eng. Chem.* **39**, 120–125 (1947).

31. Sushkevich, V. L., Ivanova, I. I., Ordonsky, V. V. & Taarning, E. Design of a Metal-Promoted Oxide Catalyst for the Selective Synthesis of Butadiene from Ethanol. *ChemSusChem* (2014). doi:10.1002/cssc.201402346
32. Han, Z., Li, X., Zhang, M., Liu, Z. & Gao, M. SI for Sol-gel synthesis of ZrO<sub>2</sub>-SiO<sub>2</sub> catalysts for the transformation of bioethanol and acetaldehyde into 1,3-butadiene. *RSC Adv.* 103982–103988 (2015).
33. Liang Cheong, J. *et al.* Highly Active and Selective Zr/MCF Catalyst for Production of 1,3-Butadiene from Ethanol in a Dual Fixed Bed Reactor System. (2016).
34. Xu, Y., Liu, Z., Han, Z. & Zhang, M. Ethanol/acetaldehyde conversion into butadiene over sol-gel ZrO<sub>2</sub>-SiO<sub>2</sub> catalysts doped with ZnO. *RSC Adv.* **7**, 7140–7149 (2017).
35. Chae, H.-J. *et al.* Butadiene production from bioethanol and acetaldehyde over tantalum oxide-supported ordered mesoporous silica catalysts. *Applied Catal. B, Environ.* **150–151**, 596–604 (2014).
36. Irina Igorevna Ivanova. US 8,921,635 B2 (2011).
37. Kyriienko, P. I. *et al.* Effect of the niobium state on the properties of NbSiBEA as bifunctional catalysts for gas- and liquid-phase tandem processes. *Journal Mol. Catal. A, Chem.* **424**, 27–36 (2016).
38. Klein, A., Keisers, K. & Palkovits, R. Formation of 1,3-butadiene from ethanol in a two-step process using modified zeolite catalysts. *Appl. Catal. A Gen.* **514**, 192–202 (2016).
39. Zhu, Q., Wang, B. & Tan, T. Conversion of Ethanol and Acetaldehyde to Butadiene over MgO-SiO<sub>2</sub> Catalysts: Effect of Reaction Parameters and Interaction between MgO and SiO<sub>2</sub> on Catalytic Performance. *ACS Sustain. Chem. Eng.* **5**, 722–733 (2017).
40. Pelletier, J. D. A. & Basset, J.-M. Catalysis by Design: Well-Defined Single-Site Heterogeneous Catalysts. *Acc. Chem. Res.* **49**, 664–677 (2016).
41. Copéret, C. *et al.* Surface Organometallic and Coordination Chemistry toward Single-Site Heterogeneous Catalysts: Strategies, Methods, Structures, and Activities. *Chemical Reviews* (2016).
42. Takehira, K., Hayakawa, T. & Ishikawa, T. Heterogeneous Catalysis in the Liquid-phase Oxidation of Olefins. IV. The Activity of a Supported Vanadium or Chromium Oxide Catalyst in the Decomposition of *t*-Butyl Hydroperoxide. *Bull. Chem. Soc. Jpn.* **53**, 2103–2110 (1980).
43. Dalton, J. C. S., Austin, J. M., Groenewald, T. & Spiro, M. Heterogeneous Catalysis in Solution. Part 18.1 The Catalysis by Carbons of Oxidation-Reduction Reactions. *J. Chem. Soc., Dalt. Trans.* **0**, 854–859 (1980).
44. Soignier, S. *et al.* Tantalum hydrides supported on MCM-41 mesoporous silica:

- Activation of methane and thermal evolution of the tantalum-methyl species. *Organometallics* **25**, 1569–1577 (2006).
45. Copéret, C. *et al.* Surface Organometallic and Coordination Chemistry toward Single-Site Heterogeneous Catalysts: Strategies, Methods, Structures, and Activities. *Chem. Rev.* **116**, 323–421 (2016).
  46. Candy, J.-P., Copéret, C. & Basset, J.-M. Analogy between Surface and Molecular Organometallic Chemistry. in *Surface and Interfacial Organometallic Chemistry and Catalysis* (ed. Copéret, C., Chaudret, B.) 151–210 (Springer-Verlag, 2005).
  47. McDaniel, M. P. & Welch, M. B. The activation of the phillips polymerization catalyst: I. Influence of the hydroxyl population. *J. Catal.* **82**, 98–109 (1983).
  48. Hoveyda, A. H. & Schrock, R. R. Catalytic Asymmetric Olefin Metathesis. *Chemistry (Easton)*. **7**, 945–950 (2001).
  49. Bilhou, J. L., Bilhou-Bougnol, V., Graydon, W. F., Basset, J. M. & Smith, A. K. Surface-linked metal cluster carbonyls: fixation, behaviour and reactivity of Rh<sub>6</sub>(CO)<sub>16</sub> bonded to a phosphinated silica. *J. Mol. Catal.* **8**, 411–429 (1980).
  50. Dufour, P., Houtman, C., Santini, C. C. & Basset, J.-M. Surface organometallic chemistry on oxides: Reaction of hydrogen with bis(allyl)rhodium grafted to silica, titania and alumina. *J. Mol. Catal.* **77**, 257–272 (1992).
  51. Le Roux, E. *et al.* Silica-Alumina-Supported, Tungsten-Based Heterogeneous Alkane Metathesis Catalyst: Is it Closer to a Silica- or an Alumina-Supported System? *Adv. Synth. Catal.* **349**, 231–237 (2007).
  52. Wang, X. X., Lefebvre, F., Patarin, J. & Basset, J.-M. Synthesis and characterization of zirconium containing mesoporous silicas: I. Hydrothermal synthesis of Zr-MCM-41-type materials. *Microporous Mesoporous Mater.* **42**, 269–276 (2001).
  53. Bartram, M. E., Michalske, T. A. & Rogers, J. W. A Reexamination of the Chemisorption of Trimethylaluminum on Silica. *J. Phys. Chem* **95**, 4453–4463 (1991).
  54. Millot, N., Santini, C. C., Lefebvre, F. & Basset, J.-M. Surface organometallic chemistry: a route to well-defined boron heterogeneous co-catalyst for olefin polymerisation. *Comptes Rendus Chim.* **7**, 725–736 (2004).
  55. A van de Water, L. G., Bergwerff, J. A., Leliveld, B. G., Weckhuysen, B. M. & de Jong, K. P. Insights into the Preparation of Supported Catalysts: A Spatially Resolved Raman and UV-Vis Spectroscopic Study into the Drying Process of CoMo/ $\gamma$ -Al<sub>2</sub>O<sub>3</sub> Catalyst Bodies. (2005).
  56. Dufaud, V., Niccolai, G. P., Thivolle-Cazat, J. & Basset, J. M. Surface Organometallic Chemistry of Inorganic Oxides: The Synthesis and Characterization of  $(\equiv\text{SiO})\text{Ta}(\text{=CHC}(\text{CH}_3)_3)(\text{CH}_2\text{C}(\text{CH}_3)_3)_2$  and  $(\equiv\text{SiO})_2\text{Ta}(\text{=CHC}(\text{CH}_3)_3)(\text{CH}_2\text{C}(\text{CH}_3)_3)$ . *J. Am. Chem. Soc.* **117**, 4288–4294 (1995).

57. Chabanas, M. *et al.* Molecular insight into surface organometallic chemistry through the combined use of 2D HETCOR solid-state NMR spectroscopy and silsesquioxane analogues. *Angew. Chemie - Int. Ed.* **40**, 4493–4496 (2001).
58. Petroff Saint-Arroman, R., Didillon, B., De Mallmann, A., Basset, J. M. & Lefebvre, F. Deperoxidation of cyclohexyl hydroperoxide by silica-supported alkoxo-tantalum complexes. *Appl. Catal. A* **337**, 78–85 (2008).
59. Vidal, V., Théolier, A., Thivolle-Cazat, J., Basset, J.-M. & Corker, J. Synthesis, Characterization, and Reactivity, in the C–H Bond Activation of Cycloalkanes, of a Silica-Supported Tantalum(III) Monohydride Complex:  $(\equiv\text{SiO})_2\text{TaIII-H}$ . *J. Am. Chem. Soc.* **118**, 4595 (1996).
60. Chow, C., Taoufik, M. & Quadrelli, E. A. Ammonia and dinitrogen activation by surface organometallic chemistry on silica-grafted tantalum hydrides. *Eur. J. Inorg. Chem.* 1349–1359 (2011).

# Chapter 2

## Tailoring 'single site' TaO<sub>x</sub> species on silica support via mild oxidation with N<sub>2</sub>O

*The aim of this chapter is to develop well-defined, 'single site' TaO<sub>x</sub> species on the surface of silica by reaction with N<sub>2</sub>O, a mild oxidant using the surface organometallic chemistry protocol.*



# Contents

<b>A. Introduction</b> .....	<b>42</b>
<b>B. Results and Discussions</b> .....	<b>44</b>
B1. New insights into silica-supported tantalum alkyl [ $\equiv\text{SiOTa}(\text{=CH}^t\text{Bu})(\text{CH}_2^t\text{Bu})_2$ ] and tantalum hydride [ $(\equiv\text{SiO})_2\text{Ta}(\text{H})_{x=1,3}$ ] systems via HR-STEM analysis.....	44
B2. Tailoring single site $\text{TaO}_x$ species on the surface of $\text{SiO}_{2-500}$ via mild oxidation with $\text{N}_2\text{O}$ .....	48
B3. Evolution of surface $\text{TaO}_x$ species with temperature .....	51
B4. Towards di-nuclear tantalum surface species supported on silica.....	53
<b>C. Conclusions</b> .....	<b>56</b>
<b>D. Experimental details</b> .....	<b>57</b>
D1. General procedure for the preparation of starting materials.....	57
D2. Synthesis and characterization of catalyst supports .....	57
D3. Synthesis and characterization of $[\text{Ta}(\text{=CH}^t\text{Bu})(\text{CH}_2^t\text{Bu})_3]$ .....	57
D4. Preparation of surface complexes by SOMC protocol.....	58
D5. Catalyst characterization by HRSTEM .....	59
D6. Catalyst characterization by EXAFS spectroscopy .....	59
<b>D. Experimental details</b> .....	<b>61</b>



## A. Introduction:

In our endeavor to prepare well-defined catalysts for butadiene synthesis from ethanol and acetaldehyde, our first strategy was to explore the possibility of designing ‘single site’ TaO<sub>x</sub>/SiO<sub>2</sub> catalysts for this transformation. The tools to tailor such catalysts were borrowed from surface organometallic chemistry (SOMC).

Synthesis of Group IV MO<sub>x</sub> species has been studied in the past. Petroff et al.<sup>1</sup> studied the synthesis  $(\equiv\text{SiO})_3\text{M}(\text{OH})$  by addition of O<sub>2</sub> to the corresponding metal hydrides,  $(\equiv\text{SiO})_3\text{MH}$  as “single site” heterogeneous catalysts for the selective deperoxidation of cyclohexyl hydro peroxide. It was found that the action of molecular oxygen at 25 °C onto supported metal hydrides is, however, not as clean.

In 2007, Rataboul *et al.*<sup>2,3</sup> first showed that isolated well-defined MO<sub>x</sub> species could indeed be tailored on the surface of silica via mild oxidation of corresponding metal hydrides  $(\equiv\text{SiO})_3\text{MH}$  by N<sub>2</sub>O. It was demonstrated that zirconium hydrides, which are a mixture of monohydride  $[(\equiv\text{SiO})_3\text{Zr}(\text{H})]$  (70%) and dihydride surface species  $[(\equiv\text{SiO})_2\text{Zr}(\text{H})_2]$  (30%) when treated with N<sub>2</sub>O produced the corresponding silica-supported zirconium mono- and di-hydroxide surface species  $[(\equiv\text{SiO})_3\text{Zr}(\text{OH})]$  (70%) and  $[(\equiv\text{SiO})_2\text{Zr}(\text{OH})_2]$  (30%).

Indeed gas phase interaction of both N<sub>2</sub>O and O<sub>2</sub> with metal atoms has been studied extensively using a variety of experimental and theoretical methods. Theoretical studies predominantly support end-on O-coordination of N<sub>2</sub>O to the metal atom ( $\eta^1\text{-O}$ ) with subsequent charge transfer (metal-to-N<sub>2</sub>O) and consequent M-O-NN bending occurring along the N-O bond scission pathway.<sup>4</sup> Whereas in the case of oxygen interaction with a metal, both end-on and side-on coordination is possible forming superoxo and peroxy type of complexes respectively. These complexes can further interact with other neighboring metal atoms.<sup>5</sup>

The predominance of linear M-O-NN binding in N<sub>2</sub>O complexes can then provide a cleaner pathway to oxidation of supported metal complexes. Building upon this, the reaction of  $[(\equiv\text{SiO})_2\text{Ta}(\text{H})_{x=1,3}]$  with N<sub>2</sub>O is a novel attempt to generate well defined ‘single site’ Group V MO<sub>x</sub> moiety on the surface of silica.



## B. Results and Discussions:

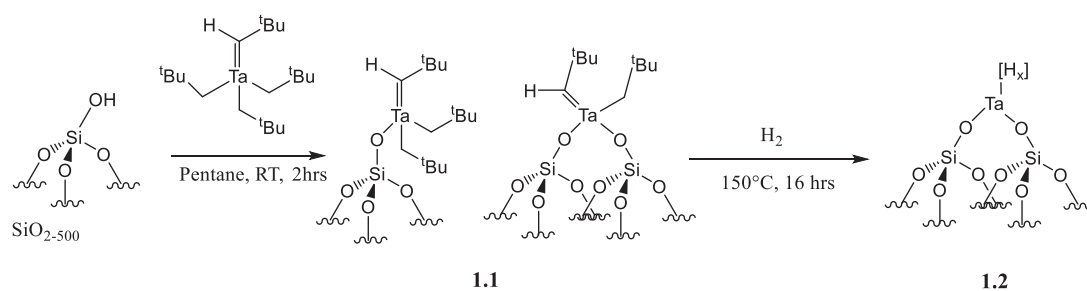
### B1. Synthesis of known silica-supported tantalum alkyl $[\equiv\text{SiOTa}(=\text{CH}^t\text{Bu})(\text{CH}_2^t\text{Bu})_2]$ and tantalum hydride $[(\equiv\text{SiO})_2\text{Ta}(\text{H})_{x=1,3}]$ species and their novel HR-STEM analysis

Tailoring well-defined tantalum alkyl  $[\equiv\text{SiOTa}(=\text{CH}^t\text{Bu})(\text{CH}_2^t\text{Bu})_2]$  and tantalum hydride  $[(\equiv\text{SiO})_2\text{Ta}(\text{H})_{x=1,3}]$  species on the surface of partially dehydroxylated silica has been a model study in multi-technique surface organometallic chemistry.<sup>6-9</sup> Extensive characterization and mechanistic investigations by the combined use of IR and EXAFS spectroscopies as well as <sup>1</sup>H MAS, <sup>13</sup>C CP/MAS, 2D <sup>1</sup>H-<sup>13</sup>C HETCOR<sup>9</sup>, and solid-state NMR and mass balance analysis have allowed for a detailed molecular description of these silica-grafted complexes.

The first step of this strategy was to synthesize  $[\equiv\text{SiOTa}(=\text{CH}^t\text{Bu})(\text{CH}_2^t\text{Bu})_2]$  species. For this the grafting procedure from the literature was reproduced.<sup>6</sup> A known quantity of the silica dehydroxylated at 500°C was reacted with a pentane solution of molecular  $[\text{Ta}(=\text{CH}^t\text{Bu})(\text{CH}_2^t\text{Bu})_3]$ , containing a stoichiometric amount of tantalum with respect to the full coverage of the starting silanols. This complex was named **complex 1.1**. Analysis of the lightly orange solid by <sup>1</sup>H NMR, <sup>13</sup>C NMR, DRIFT, quantitative titration of evolved neopentane and elemental analysis of the final solids confirmed that the expected species were obtained with full coverage of the surface silanols. In IR spectroscopy, the  $\nu(\text{O-H})$  band at 3747 cm<sup>-1</sup> assigned to isolated silanol groups disappears, indicating complete consumption of hydroxyl groups. In addition to the sample, with full coverage of surface silanols, another sample with 2 wt% Ta loading was prepared by the same procedure with the purpose of catalytic testing.

The next step was synthesis of their corresponding hydrides  $[(\equiv\text{SiO})_2\text{Ta}(\text{H})_{x=1,3}]$ . Their formation has already been reported in the literature by reaction of  $[(\text{SiO})\text{Ta}(=\text{CH}^t\text{Bu})(\text{CH}_2^t\text{Bu})_2]$  species with H<sub>2</sub>.<sup>6,10</sup> The reaction yields light brown powder. These tantalum hydride species supported on silica have been extensively characterized by IR and EXAFS spectroscopies, by chemical reactivity and by quantification of the evolved gases during its formation.

Consistent with the literature, when  $[(\equiv\text{SiO})\text{Ta}(=\text{CH}^t\text{Bu})(\text{CH}_2^t\text{Bu})_2]$  was treated with hydrogen at  $150^\circ\text{C}$  for 16hrs, the IR bands in the range  $2700\text{-}3000\text{ cm}^{-1}$   $\nu(\text{C-H})$  and  $1300\text{-}1500\text{ cm}^{-1}$   $\delta(\text{C-H})$  disappeared and a new set of bands appeared in the  $1800\text{ cm}^{-1}$  region corresponding to the Ta-H stretching modes with two shoulders at  $1815$  and  $1855\text{ cm}^{-1}$ . Also the  $\nu(\text{Si-H})$  bands increase in intensity. This can be explained by the fact that the proposed mechanism for the formation of the supported hydride species involves a reaction of an adjacent siloxane bridge of silica with an hydrogen from the coordination sphere of tantalum, giving rise to new Si-H species on the surface. The  $^1\text{H}$  solid state MAS NMR (500MHz) spectrum displays a signals at  $0.9\text{ ppm}$  ( $\text{Si-C}(\text{CH}_3)_3$ ),  $2.0\text{ ppm}$  ( $\text{Si-OH}$ ), and  $4.5\text{ ppm}$  ( $\text{Si-H}$  and  $\text{Si-H}_2$ ) respectively. The presence of Ta-H bond can be attributed to a weak signal observed at  $15.3\text{ ppm}$ . A sample prepared in this manner was coded **complex-1.2**



Scheme 2.1

Table 2.1- Grafting of  $[\text{Ta}(=\text{CH}^t\text{Bu})(\text{CH}_2^t\text{Bu})_3]$  on  $\text{SiO}_2\text{-500}$  by impregnation in pentane at  $25^\circ\text{C}$ 

Complex	Metal Loading	Neopentane release/Ta	DRIFT
<b>complex-1.1</b>	5.56%	1.5	$2900\text{-}3000\text{ cm}^{-1}$ $\nu$ (CH) $1500\text{-}1300\text{ cm}^{-1}$ $\delta$ (C-H)
<b>complex-1.2</b>	5.56%	-	$1800\text{ cm}^{-1}$ $\nu$ (Ta-H) $2900\text{-}3000\text{ cm}^{-1}$ $\nu$ (CH) $1500\text{-}1300\text{ cm}^{-1}$ $\delta$ (C-H)

In recent years newer characterization possibilities for these complexes have emerged due to advances in transmission electron microscopy (TEM) techniques.<sup>11</sup> These techniques can be useful in the visualization of isolated metal atoms anchored on supports and thus in direct observation of singly dispersed catalytic sites on the substrate material, necessary to understand its catalytic performance and reaction mechanism.

High-resolution scanning transmission electron microscopy (HRSTEM) represents a new avenue in characterization for the study of immobilized inorganic or organometallic centers. This technique was never before used in the characterization of well-defined surface organometallic species. We herein report the first attempt to directly visualize silica-supported tantalum alkyls  $[\equiv\text{SiOTa}(=\text{CH}^t\text{Bu})(\text{CH}_2^t\text{Bu})_2]$  and tantalum hydrides  $[(\equiv\text{SiO})_2\text{Ta}(\text{H})_{x=1,3}]$  species by HRSTEM. Micrographs of the two samples can be seen in **Figure 2.1-a** and **2.2-a** respectively. For both the samples homogeneously distributed tantalum atoms are visible without appearance of larger clusters. Software assisted counting of the tantalum atoms showed that for  $[\equiv\text{SiOTa}(=\text{CH}^t\text{Bu})(\text{CH}_2^t\text{Bu})_2]$  more than 90% of the tantalum atoms were isolated whereas for  $[(\equiv\text{SiO})_2\text{Ta}(\text{H})_{x=1,3}]$  around 82% of tantalum centers are isolated with a few examples di-nuclear and tri-nuclear moieties.

For both the samples software assisted analysis of the images afforded a statistical distribution of the sizes of the tantalum centers as shown in Figure 1b and 2b as a histogram. For  $[\equiv\text{SiOTa}(=\text{CH}^t\text{Bu})(\text{CH}_2^t\text{Bu})_2]$  the FWHM (Full width at half maximum) of the Lorentzian fit of the histogram is considerably narrow with an average size of the tantalum center around 0.251 nm. For  $[(\equiv\text{SiO})_2\text{Ta}(\text{H})_{x=1,3}]$ , which has been heated to 150°C during hydrogenation, the fit is slightly less narrow.

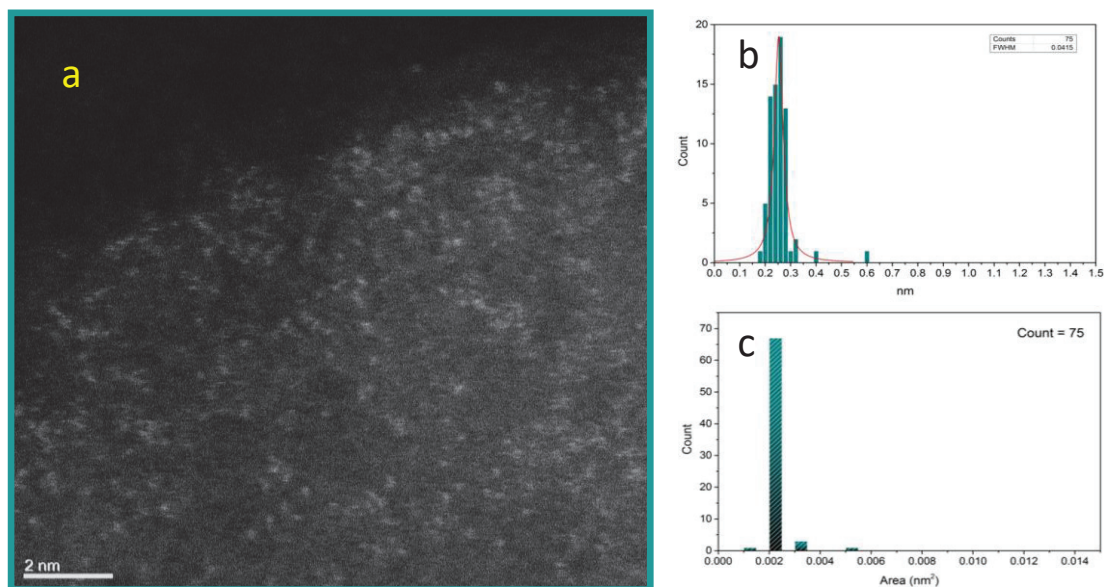


**Figure 2.1-** Representative HR-STEM micrographs of (a)  $[\equiv\text{SiOTa}(=\text{CH}^t\text{Bu})(\text{CH}_2^t\text{Bu})_2]$  and statistical evaluation of the STEM micrographs in the form of (b) size distribution histogram of the Ta centres (c) area distribution histogram of the Ta centres

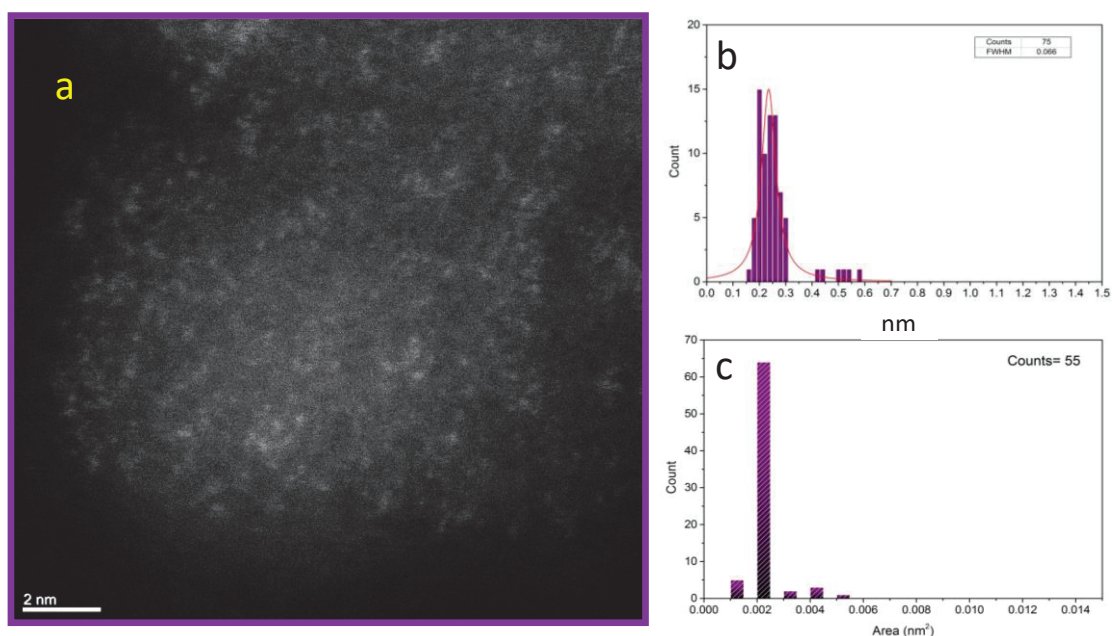


**Figure 2.2-** Representative HR-STEM micrographs of (a)  $[(\equiv\text{SiO})_2\text{Ta}(\text{H})_{x=1,3}]$  and statistical evaluation of the STEM micrographs in the form of (b) size distribution histogram of the Ta centres (c) area distribution histogram of the Ta centres

## B2. Tailoring single site TaO<sub>x</sub> species on the surface of silica

The reaction of **complex 1.2** with N<sub>2</sub>O is a novel attempt to generate well-defined Ta-OH species supported on silica. Upon treating **complex 1.2** with dried nitrous oxide at room temperature for 2 hrs, a pale white powder was obtained. This material was named **SOMC-I<sub>FC</sub>**. The DRIFT spectroscopy shows complete disappearance of the peak at 1815 and 1830 cm<sup>-1</sup> ( $\nu$  Ta-H). At the same time a new band appears at 3721cm<sup>-1</sup>. This band can be assigned to the  $\nu$  Ta-OH. The same was confirmed by <sup>1</sup>H solid state MAS NMR (500MHz) spectroscopy. Resonances were observed at 1.1 ppm (Si-C(CH<sub>3</sub>)<sub>3</sub>), 2.0 ppm (Si-OH). The signals at 4.33 ppm and 6.9 ppm could be attributed to the new hydroxyl groups formed on tantalum.

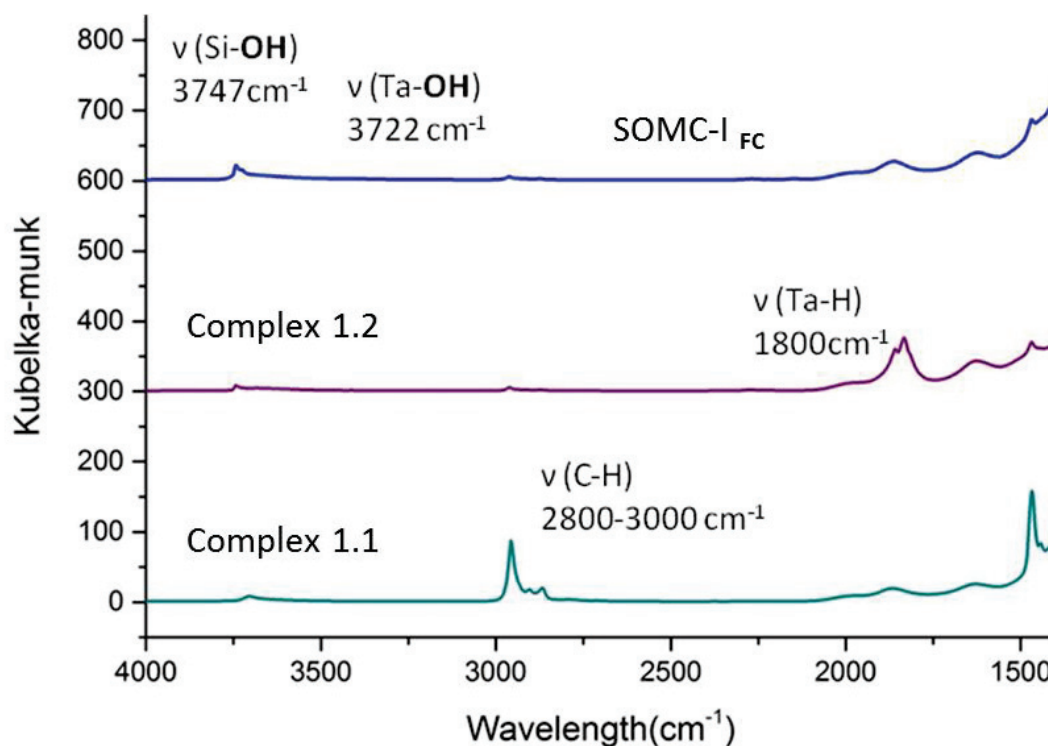


**Figure 2.3-** IR spectra for the preparation of SOMC-I<sub>FC</sub> under inert conditions.

The sample prepared by the same procedure with 2 wt% Ta loading was prepared by the same procedure for the purpose of catalytic testing was coded **SOMC-I**

## EXAFS analysis of SOMC-IFC:

The resulting white powder, **SOMC-IFC** was analyzed by Ta LIII-edge EXAFS to get an insight into the molecular structure of the surface species. Reported below is the fit performed by Dr. Aimery de Mallmann.

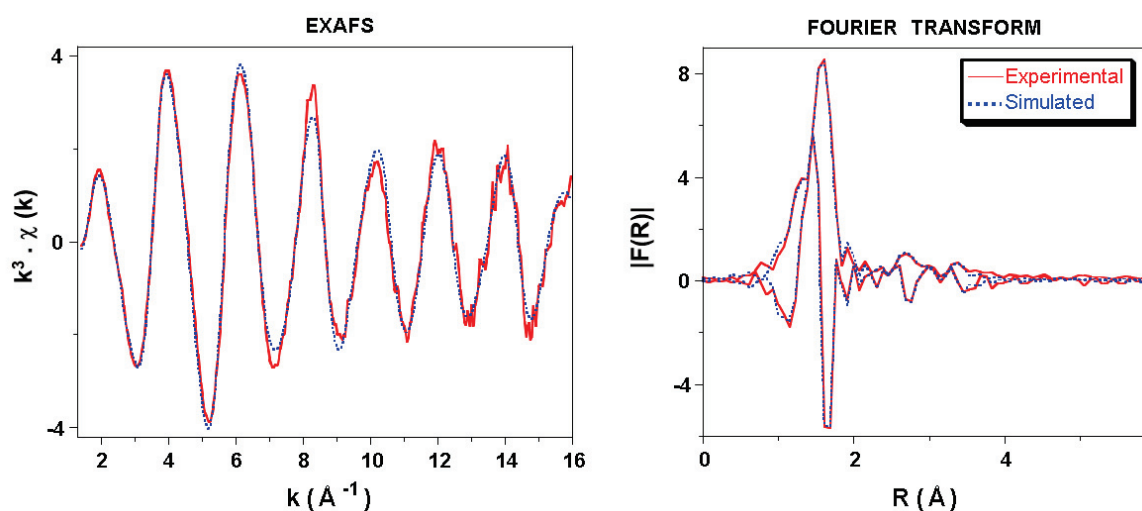


**Figure 2.4**-TantalumLIII-edge  $k^3$ -weighted EXAFS (left) and corresponding Fourier transform (right, modulus and imaginary part; R uncorrected from phase shift) with comparison to simulated curves for SOMC-I

**Table 2.2**- EXAFS parameters <sup>(a)</sup> The errors generated by the EXAFS fitting program “RoundMidnight” are indicated between parentheses.

Type of Neighbor	Number of neighbors (or paths)	Distance (Å)	$\sigma^2$ (Å <sup>2</sup> )
<i>Ta-O<sub>a</sub></i>	1.1(5)	1.76(3)	0.0055(38)
<i>Ta-O<sub>a</sub></i>	3.0(4)	1.91(1)	0.0025(6)
<i>Ta-O</i>	0.6(3)	3.00(4)	0.001(3)
<i>Ta-Si</i>	2.4(9)	3.28(7)	0.018(8)
<i>MS 3l &amp; 4l O'-Ta-O<sup>(b)</sup></i>	2 x 2.0(12)	3.80(12)	0.042(25)

<sup>(a)</sup> $\Delta k$ : [1.4 - 16 Å<sup>-1</sup>] -  $\Delta R$ : [0.5 - 4.0 Å] ([0.5 - 2.3 Å], when considering only the first coordination sphere);  $S_0^2 = 0.86$ ;  $\Delta E_0 = 6.2 \pm 1.0$  eV (the same for all shells); Fit residue:  $\rho = 2.1$  %; Quality factor:  $(\Delta\chi)^2/\nu = 1.04$  ( $\nu = 21/34$ ) ( $\rho_1 = 3.9$  % and  $[(\Delta\chi)^2/\nu]_1 = 1.86$  with  $\nu = 11/18$ , considering only the first coordination sphere of Ta).

The presence of an oxygen atom at a distance of 1.75 Å from tantalum indicates the presence of a Ta=O bond. The distance of 1.91 Å for the other three oxygen atoms as the

first shell around tantalum is in good agreement with the values found in the literature.<sup>12</sup> In the second coordination sphere, the presence of two silicon atoms at 3.26 Å from tantalum indicates the presence of bi-podal specie on the surface of silica. It is to be noted that no Ta-Ta interactions were found.

From the previous results from IR spectroscopy and <sup>1</sup>H solid state MAS NMR, we expect the presence of a Ta-OH bond. This can be explained by the proposition that of the three oxygen neighbors in the first co-ordination sphere of Ta, two oxygens correspond to the Si-O-Ta bonds, while the remaining oxygen corresponds to the Ta-OH bond as witnessed by the spectroscopies.

#### HRSTEM analysis:

After analyzing the molecular structure of the TaO<sub>x</sub> species with EXAFS spectroscopy, an attempt was made to visualize the spatial arrangement of the same on the surface of the precatalyst with HR-STEM.

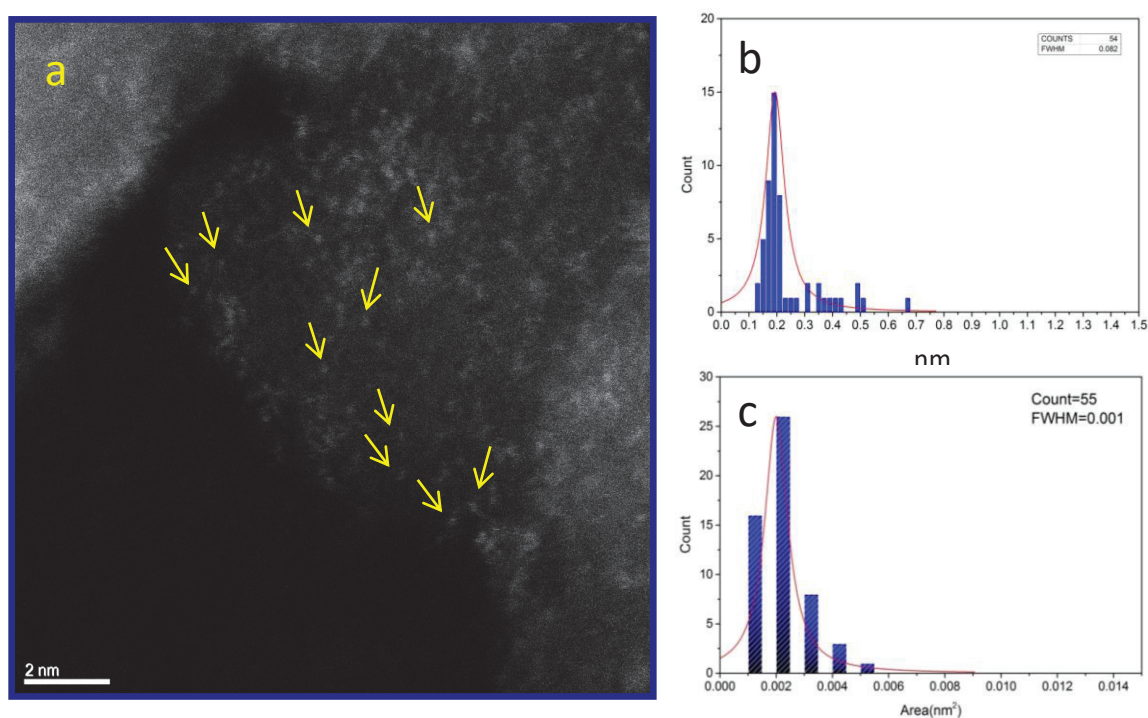
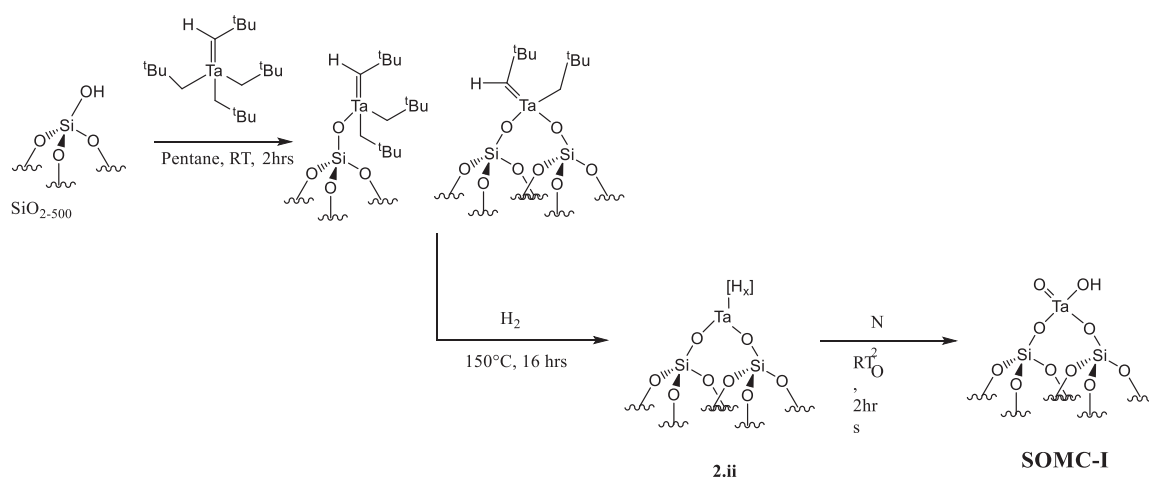


**Figure 2.5-** Representative HR-STEM micrographs of (a)  $[(\equiv\text{SiO})_2\text{Ta}(=\text{O})(\text{OH})]$  and statistical evaluation of the STEM micrographs in the form of (b) size distribution histogram of the Ta centres (c) area distribution histogram of the Ta centres

**Figure 2.5** shows the HR-STEM micrograph of the surface of **SOMC-I**. Isolated tantalum centers can be seen homogeneously distributed throughout the surface. However when compared to **complex 1.1** and **complex 1.2**, a small degree of agglomeration is witnessed. Upon measuring the diameters of the individual tantalum centers using the software ImageJ, a histogram for the size distribution of the tantalum centers was plotted. The distribution was fitted by a lorentzian function, for which the FWHM was still narrow but now greater than that of the distribution for  $[(\equiv\text{SiO})_2\text{Ta}(\text{H})_{x=1,3}]$ .



Scheme 2.2

### B3. Evolution of surface $\text{TaO}_x$ species with temperature

The above spectroscopic and microscopic analyses inform us of the molecular structure and spatial arrangement of surface species as evolved at room temperature. However, since the ultimate aim of this study is to evaluate the performance of these catalysts in synthesis of butadiene from ethanol and acetaldehyde by Ostromyslensky process, the evolution of these surface species at the target reaction temperature of  $325^\circ\text{C}$  was studied.

**SOMC-I** was heated to  $325^\circ\text{C}$  under UHV for 6hrs. The material was labeled **SOMC-I ( $\Delta 325^\circ\text{C}$ )**. A DRIFT spectrum for the same was then collected under argon (Figure 6). It was observed that upon heating, the peak at  $3721\text{cm}^{-1}$  attributed to  $\text{Ta-OH}$  stretching vibration disappears and while only the  $\text{Si-OH}$  stretching persists.



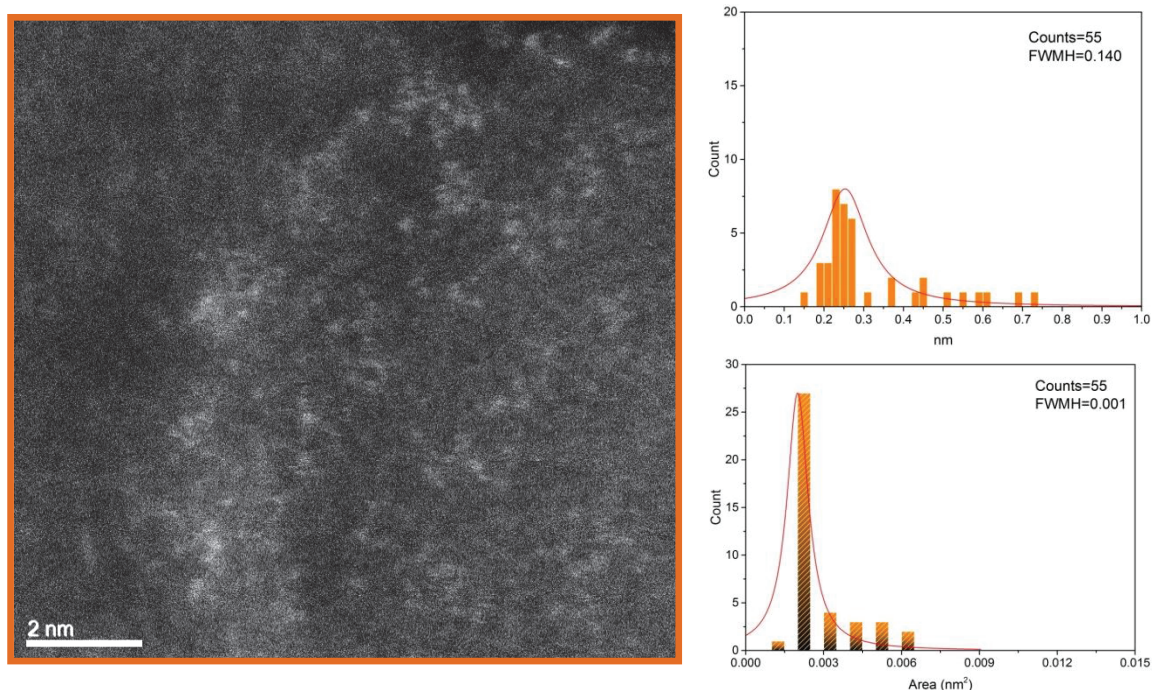


**Figure 2.7**—Representative HR-STEM micrographs of (a) SOMC-I ( $\Delta 325^\circ\text{C}$ ) and statistical evaluation of the STEM micrographs in the form of (b) size distribution histogram of the Ta centres (c) area distribution histogram of the Ta centres

#### **B4. Towards di-nuclear tantalum surface species (Ta-O-Ta) supported on silica**

In an attempt to synthesize well-defined di-nuclear tantalum species on silica, a second  $[\text{Ta}(=\text{CH}^t\text{Bu})(\text{CH}_2^t\text{Bu})_3]$  molecule was grafted on **SOMC-I**<sub>FC</sub>

Upon the second grafting, the white powder turned light orange. In the DRIFT spectroscopy, the  $\nu(\text{O-H})$  band at  $3721\text{ cm}^{-1}$  assigned to Ta-OH stretching frequencies as well as Si-OH stretching frequency at  $3747\text{ cm}^{-1}$  disappeared, indicating consumption of hydroxyl groups. New bands appeared at  $2900\text{-}3000\text{ cm}^{-1}$  and  $1500\text{-}1300\text{ cm}^{-1}$  region, which could be assigned to  $\nu(\text{C-H})$  and  $\delta(\text{C-H})$  vibrations of the neopentyl ligands bonded to the second tantalum.

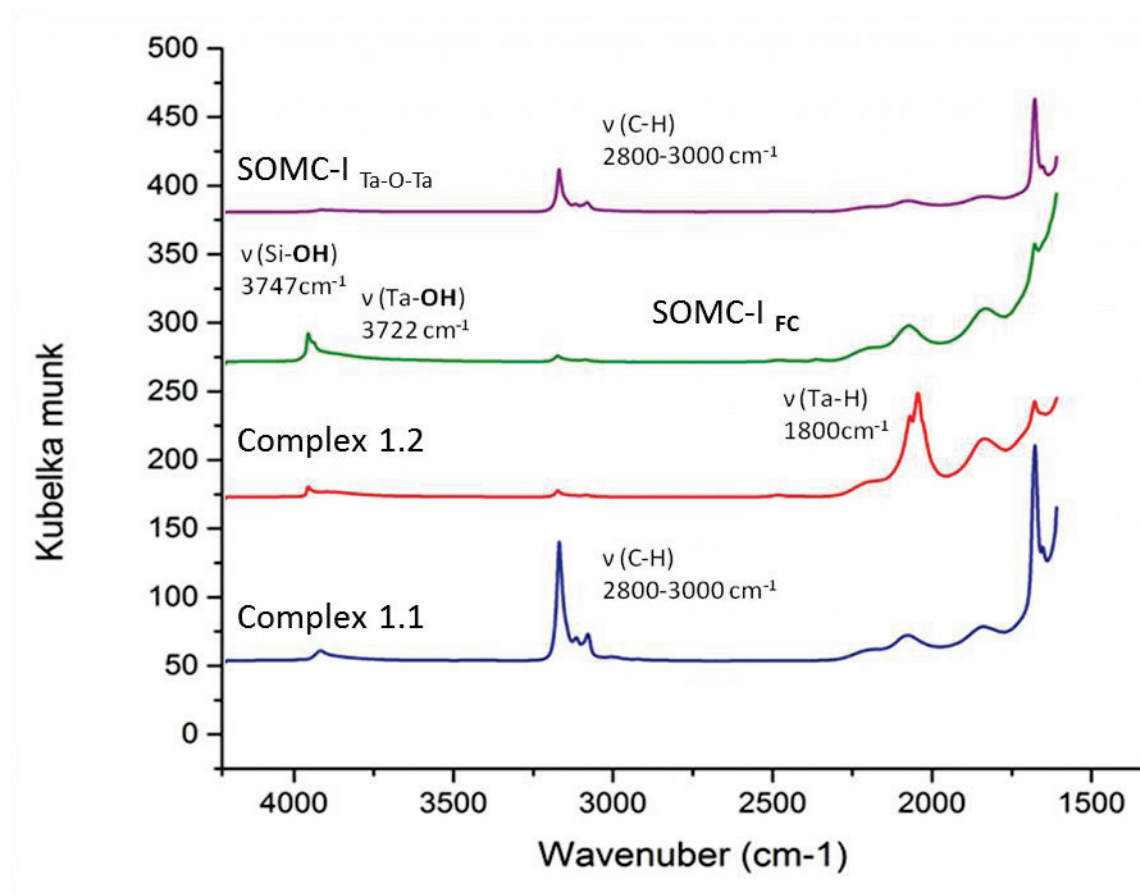


**Figure 2.8**-IR spectra for the formation of SOMC-I<sub>Ta-O-Ta</sub> under inert conditions

After grafting the material was given three washing cycles to remove the excess physisorbed molecular complex. Post washing, the volatiles were condensed into a reactor of known volume in order to quantify the neopentane released during the reaction. The released gas was quantified by gas chromatography. Analysis of the gas phase during this grafting indicates the release of 1.6 equiv. of neopentane per grafted Ta atom. Elemental analysis on the resulting solid shows a 8.59 wt% Ta and 3.13 wt% C. Firstly, considering that the Ta wt% of SOMC-I<sub>FC</sub> was 5.6%, it can be said that about 54% grafting was achieved in this step. Also the ratio of carbon to the second Tantalum can be calculated as 15C/Ta. However, formation of 54% dimeric Ta-O-Ta species on the surface cannot be assumed as we know from the DRIFT that the tantalum alkyl precursor also reacted with the surface Si-OH functionality.

This suggests that the grafting of second molecule on the surface of SOMC-I<sub>FC</sub> is not as straightforward. A monopodal grafting of second tantalum grafting (as hypothesized) should have resulted in release of 1 equivalent of neopentane ligand per grafted tantalum.

## Chapter 2

Release of approximately 1.5 equiv. of ligand, suggests a mixture of monopodal and bipodal grafting of second Ta.

Thorough characterization of the material by EXAFS and other spectroscopic techniques will give better insight into the grafting. However, we can propose this as a potential strategy to selectively tailor Ta-O-Ta dimeric species on silica surface. The sample was tested for catalytic activity under the code **SOMC-I<sub>Ta-O-Ta</sub>**.

## C. Conclusion

Upon oxidative treatment of  $[(\equiv\text{SiO})_2\text{Ta}(\text{H})_{x=1,3}]$  with  $\text{N}_2\text{O}$  at room temperature, the material (**SOMC-I<sub>FC</sub>**) was characterized by IR, NMR spectroscopies, as well as elemental analysis. Formation of well-defined isolated mono-tantalate specie  $[(\equiv\text{SiO})_2\text{Ta}(=\text{O})(\text{OH})]$  was established via EXAFS analysis. HRSTEM analysis of **SOMC-I** found largely isolated dispersion of Ta (V) centre, with some degree of agglomeration.

Evolution of these species at high temperature was studied via DRIFT and HRSTEM analysis. Upon heat treatment under vacuum, these isolated tantalum species were observed to aggregate into string-like and cluster formations.

An attempt to yield well-defined di-nuclear tantalum species was performed by reacting the  $[(\equiv\text{SiO})_2\text{Ta}(=\text{O})(\text{OH})]$  species with another molecule of  $[\text{Ta}(=\text{CH}^t\text{Bu})(\text{CH}_2^t\text{Bu})_3]$ . Preliminary results from DRIFT, elemental analysis and gas analysis suggest a mixture of monopodal and bi-podal tantalum species formed on the surface of **SOMC-I<sub>FC</sub>**.

## D. Experimental Details:

### D1. General procedure for preparation of starting material

All experiments were carried out under controlled atmosphere, using schlenk and glovebox techniques. For the synthesis and treatment of the surface species, reactions were carried out using high-vacuum lines ( $1.34 \times 10^{-5}$  torr) and glovebox techniques.

Pentane and diethyl ether were distilled on NaK alloy and benzophenone/Na, respectively, followed by degassing by freeze-pump-thaw cycles. Hydrogen was dried over freshly regenerated molecular sieves (3 Å) and deoxo traps; N<sub>2</sub>O was purchased from Linde and used as received (purity of N<sub>2</sub>O: 5.0)

### D2. Synthesis and characterization of catalyst support

Typically SiO<sub>2</sub> (Aerosil® Degussa, 200 m<sup>2</sup>.g<sup>-1</sup>) was compacted with distilled water calcined at 200 °C in air for 1 h and partially dehydroxylated at 500°C and 700°C under high vacuum ( $10^{-5}$  torr) for 16 h at 3°C/min to give SiO<sub>2-500</sub> and SiO<sub>2-700</sub> respectively.<sup>13</sup>

### D3. Synthesis and characterization of molecular precursor

Synthesis of Neopentylmagnesiumchloride, NpMgCl. 7.4 g of magnesium (300 mmol, 1.3 equiv) with 30 ml of distilled ether, 30 ml of distilled THF, 25 g of neopentyl chloride (235 mmol) and 0.4 ml of 1,2-dichloroethane ( $4.6 \times 10^{-3}$  mmol) were introduced, under argon, in a 250 ml glass two neck reactor equipped with a cooler. The mixture was then refluxing at 60°C for 15 h. After filtration and dilution with 60 ml of distilled ether, a pale yellow solution was stored under argon. The titration was done following the literature procedure.<sup>14</sup>

Synthesis of [Ta(=CH<sup>t</sup>Bu)(CH<sub>2</sub><sup>t</sup>Bu)<sub>3</sub>] The molecular precursor was prepared following the literature procedure with 4 g of TaCl<sub>4</sub> (18.65 mmol) and 34 ml of <sup>t</sup>BuCH<sub>2</sub>MgCl at 1.46 M. Reddish orange crystals were obtained by sublimation : 2.8 g, 54% yield. <sup>1</sup>H NMR (C<sub>6</sub>D<sub>6</sub>) δ ppm : (8, [CH<sub>2</sub>C(CH<sub>3</sub>)<sub>3</sub>]), 1.15 (12, [CH<sub>2</sub>C(CH<sub>3</sub>)<sub>3</sub>]).

#### D4. Preparation of surface complexes by SOMC protocol

**Complex 1.1:** A solution of  $[\text{Ta}(=\text{CH}^t\text{Bu})(\text{CH}_2^t\text{Bu})_3]$  (0.43 g, 0.9 mmol) in pentane (15 mL) and  $\text{SiO}_2-(500)$  (2 g, 0.9 mmol OH/g) was stirred at 25 °C for 2 h. After filtration, the solid was washed three times with pentane. The solvent was then removed, and the light orange solid was dried under dynamic vacuum at 25 °C.  $^1\text{H}$  MAS solid-state NMR (300 MHz, 25 °C):  $\delta$  (ppm) 1 (s,  $\text{CH}_2, \text{CH}_3$ ).  $^{13}\text{C}$  CP-MAS solid-state NMR (300 MHz, 25 °C):  $\delta$  (ppm) 34 (s,  $\text{C}(\underline{\text{C}}\text{H}_3)_3$ ), 95 (s,  $\underline{\text{C}}\text{H}_2\text{-}^t\text{Bu}$ ). Infrared ( $\text{cm}^{-1}$ ): 1450-1500 s,  $\delta(\text{C-H})$ ), 2800-3000 (s,  $\nu(\text{C-H})$ ). Gas-phase analysis: 1.5 equiv/Ta of  $\text{CH}_3\text{-}^t\text{Bu}$  evolved. Elemental analysis: % wt Ta 5.56% C 5.52%

**Complex 1.2:** In a 500 mL reactor, 1.68 g of *Complex 1.1* (0.94 mmol of Ta) was treated with 700m Bar of  $\text{H}_2$ . The temperature was increased to 150 °C (3 °C/min) and was maintained at this temperature for 16 h. The color of the solid turned from light orange to brown within first hour of the reaction. A second treatment under  $\text{H}_2$  was carried out to ensure a complete hydrogenolysis of the ligands and to yield  $[\text{Ta-H}]$ .  $^1\text{H}$  MAS solid-state NMR (500 MHz, 25 °C):  $\delta$  (ppm) 0.9 (s, Si-R), 2.0 (s, SiO-H), 4.5 (s, Si-H and  $\text{SiH}_2$ ), 15.3 (w, Ta-H). Infrared ( $\text{cm}^{-1}$ ): 1850 (broad,  $\nu$  (Ta-H) and  $\nu$  ( $\text{TaH}_3$ )), 2200, 2260 (m,  $\nu(\text{Si-H})$  and  $\nu(\text{SiH}_2)$ ), 2800-3000 (w,  $\nu(\text{C-H})$ ). Gas-phase analysis: Methane was detected but could not be quantified. Elemental analysis: %wt Ta 5.56% C 0.48%.

**SOMC I<sub>FC</sub>:** In a 500 mL reactor, 1.15 g of *Complex 1.2* (0.31 mmol of Ta) was treated with  $\text{N}_2\text{O}$  (800 mBar, in the absence of light). The color turned immediately from beige to white. After 2 h at 25 °C, the gas phase was evacuated under dynamic-vacuum at 25 °C for 2 h. A second treatment under  $\text{N}_2\text{O}$  was carried out to ensure a complete consumption of the hydride.  $^1\text{H}$  MAS solid-state NMR (500 MHz, 25 °C):  $\delta$  (ppm) 1.0 (s, Si-R), 2.0 (s, SiO-H), 4.3 (s, Ta ( $\text{OH}$ )<sub>2</sub>), 6.9 (s, TaO-H). Infrared ( $\text{cm}^{-1}$ ): 3710 (m,  $\nu$  (Ta O-H)), 2900 (w,  $\nu(\text{C-H})$ ). Elemental analysis: %wt Ta 5.56% C 0.42%

**SOMC-I<sub>Ta-O-Ta</sub>** - A solution of  $[\text{Ta}(=\text{CH}^t\text{Bu})(\text{CH}_2^t\text{Bu})_3]$  (0.12 g) in pentane (10 mL) and *SOMC I<sub>FC</sub>* (0.550 g) was stirred at 25 °C for 2 h. After filtration, the solid was washed three times with pentane. The solvent was then removed, and the white solid was dried under dynamic vacuum at 25 °C. Infrared ( $\text{cm}^{-1}$ ): 1450-1500 s,  $\delta(\text{CH}_2, \text{CH}_3)$ ), 2800-3000 (s,  $\nu(\text{C-H})$ ). Gas-phase analysis: 1.6 equiv/Ta of  $\text{CH}_3\text{-}^t\text{Bu}$  evolved. Elemental analysis: %wt Ta 8.59% C 3.13%

### D5. Catalyst characterization by HRSTEM

HR-STEM experiments were performed at IRCELYON on TITAN ETEM from. The microscope has a STEM mode allowing guaranteed atomic imaging at 0.136 nm in HAADF, ADF and bright field mode. The aberration of sphericity is adjustable thanks to a "Cs" corrector of "objective" type (for high resolution imaging).

All the analysis was performed using an electron beam of 300kV, with a dose of  $83.2e/A^2 s$  at a magnification of 5.1Mx.

### D6. Catalyst characterization by EXAFS spectroscopy

X-ray absorption spectra were acquired at ESRF on BM23 beam-line (experiment code IN-986), at room temperature at the tantalum  $L_{III}$  edge, with a double crystal Si (111) monochromator detuned 70% to reduce the higher harmonics of the beam. The spectra were recorded in the transmission mode between 9.65 and 10.9 keV. The supported Ta samples were packaged within an argon filled dry box in a double air-tight sample holder equipped with kapton windows.

The program FEFF8 was used to calculate theoretical files for phases and amplitudes based on model clusters of atoms. (Ankudinov, A. L.; Ravel, B.; Rehr, J. J.; Conradson, S. D. *Phys. Rev. B*:**1998**, 58, 7565-7576.) The value of the scale factor was determined from the  $k^2$  and  $k^3 \cdot \chi(k)$  spectra of a reference compound, a sample of  $LiTaO_3$  diluted in BN and carefully mixed and pressed as a pellet.

The refinements were performed by fitting the structural parameters  $N_i$ ,  $R_i$ ,  $\sigma_i$  and the energy shift,  $\Delta E_0$  (the same for all shells). The fit residue,  $\rho$  (%), was calculated by the following formula:

$$\rho = \frac{\sum_k [k^3 \chi_{exp}(k) - k^3 \chi_{cal}(k)]^2}{\sum_k [k^3 \chi_{exp}(k)]^2} * 100$$

As recommended by the Standards and Criteria Committee of the International XAFS Society, (Reports of the Standards and Criteria Committee of the International XAFS Society **2000**: [http://ixs.iit.edu/subcommittee\\_reports/sc/](http://ixs.iit.edu/subcommittee_reports/sc/)) the quality factor,  $(\Delta\chi)^2/v$ ,

where  $v$  is the number of degrees of freedom in the signal, was calculated and its minimization considered in order to control the number of variable parameters in the fits.

## E. References

1. Petroff Saint-Arroman, R. Catalyse hétérogène Composés cycliques Hafnium -- Composés organiques Peroxydation Tantale -- Composés organiques Zirconium -- Composés organiques. (2002).
2. Rataboul, F. *et al.* Molecular Understanding of the Formation of Surface Zirconium Hydrides upon Thermal Treatment under Hydrogen of  $[(\text{tSiO})\text{Zr}(\text{CH}_2\text{tBu})_3]$  by Using Advanced Solid-State NMR Techniques. *J. Am. Chem. Soc.* **126**, 12541–12550 (2004).
3. Rataboul, F. *et al.* Synthesis, characterization and propane metathesis activity of a tantalum-hydride prepared on high surface area ‘silica supported zirconium hydroxide’. *Dalt. Trans* 923–927 (2007).
4. Tolman, W. B. Binding and Activation of  $\text{N}_2\text{O}$  at Transition Metal Centers: Recent Mechanistic Insights. *Angew Chem Int Ed Engl.* **49**, 1018–1024 (2010).
5. Holland, P. L. Metal-Dioxygen and Metal-Dinitrogen Complexes: Where Are The Electrons. *Dalt. Trans.* **39**, 5415–5425 (2010).
6. Vidal, V., Théolier, A., Thivolle-Cazat, J., Basset, J.-M. & Corker, J. Synthesis, Characterization, and Reactivity, in the C–H Bond Activation of Cycloalkanes, of a Silica-Supported Tantalum(III) Monohydride Complex:  $(\equiv\text{SiO})_2\text{TaIII-H}$ . *J. Am. Chem. Soc.* **118**, 4595 (1996).
7. Soignier, S. *et al.* Tantalum hydrides supported on MCM-41 mesoporous silica: Activation of methane and thermal evolution of the tantalum-methyl species. *Organometallics* **25**, 1569–1577 (2006).
8. Le Roux, E. *et al.* Detailed structural investigation of the grafting of  $[\text{Ta}(\text{=CHtBu})(\text{CH}_2\text{tBu})_3]$  and  $[\text{Cp}^*\text{TaMe}_4]$  on silica partially dehydroxylated at 700 °C and the activity of the grafted complexes toward alkane metathesis. *J. Am. Chem. Soc.* **126**, 13391–13399 (2004).
9. Chabanas, M. *et al.* Molecular insight into surface organometallic chemistry through the combined use of 2D HETCOR solid-state NMR spectroscopy and silsesquioxane analogues. *Angew. Chemie - Int. Ed.* **40**, 4493–4496 (2001).
10. Chow, C., Taoufik, M. & Quadrelli, E. A. Ammonia and dinitrogen activation by surface organometallic chemistry on silica-grafted tantalum hydrides. *Eur. J. Inorg. Chem.* 1349–1359 (2011).
11. Zwaschka, G. *et al.* Supported sub-nanometer Ta oxide clusters as model catalysts for the selective epoxidation of cyclooctene. *New J. Chem.* **42**, 3035–3041 (2018).
12. Merle, N. *et al.* Well-defined silica supported bipodal molybdenum oxo alkyl complexes: a model of the active sites of industrial olefin metathesis catalysts.

- Chem. Commun. Chem. Commun* **53**, 11338–11341 (1133).
13. Copéret, C. *et al.* Surface Organometallic and Coordination Chemistry toward Single-Site Heterogeneous Catalysts: Strategies, Methods, Structures, and Activities. *Chemical Reviews* (2016).
  14. Schrock, R. R., Messerle, L. W., Clayton Wood, D. & Guggenberger, L. J. *Multiple Metal-Carbon Bonds- Preparation and Characterization of Several Alkylidene Complexes.* (1978).

# Chapter 3

TaO<sub>x</sub> species supported on silica with O<sub>2</sub> as oxidant

*The aim of this chapter is to better understand the reactivity of molecular oxygen towards silica supported tantalum organometallic complexes and thereby synthesize a family of well-defined TaO<sub>x</sub>/SiO<sub>2</sub> pre-catalysts for the Ostromyslensky reaction.*



# Contents

<b>A. Introduction</b> .....	<b>67</b>
<b>B. Results and discussions</b> .....	<b>71</b>
B1. Synthesis of TaO <sub>x</sub> /SiO <sub>2</sub> catalysts via oxidation of known silica-supported tantalum alkyl species with molecular O <sub>2</sub> .....	71
B2. Characterization of surface species for TaO <sub>x</sub> /SiO <sub>2</sub> catalysts .....	74
B3. Synthesis and characterization of TaO <sub>x</sub> /SiO <sub>2</sub> catalysts via oxidation of silica-supported alkoxo tantalum species with molecular O <sub>2</sub> .....	77
<b>C. Conclusions</b> .....	<b>81</b>
<b>D. Experimental details</b> .....	<b>82</b>
D1. General procedure for the preparation of starting materials.....	83
D2. Preparation of surface complexes by SOMC protocol .....	83
D3. <i>In operando</i> FTIR spectroscopy experiments .....	84
D4. Catalyst characterization by EXAFS spectroscopy .....	84
<b>E. References</b> .....	<b>85</b>







## A. Introduction

One of the common approaches employed in the synthesis of state-of-the-art Ta/SiO<sub>2</sub> catalysts for Ostromyslensky process has been via impregnation of a tantalum precursor (TaCl<sub>5</sub><sup>1,2</sup>, Ta(OEt)<sub>5</sub><sup>3</sup>) on the surface of the oxide support followed by calcination under dynamic flow of air at high temperatures. Catalysts synthesized in this way have been most prominently characterized by Wachs et al.<sup>4-6</sup>

Interaction of molecular with silica-supported tantalum alkyls synthesized by SOMC has been studied in the past. It is known that the peralkyl tantalum complexes are highly sensitive towards oxygenated molecules like alcohol, water or molecular oxygen. The reactivity of molecular oxygen with supported peralkyl tantalum complex ( $\equiv\text{SiO}$ )Ta(CH<sup>t</sup>Bu)(CH<sub>2</sub><sup>t</sup>Bu)<sub>2</sub> was first studied by Petroff. *et. al.*<sup>7</sup> in 2002. The volumetric titration of oxygen consumed per supported tantalum species gave 1.8 molecules of O<sub>2</sub> per ( $\equiv\text{SiO}$ )Ta(CH<sup>t</sup>Bu)(CH<sub>2</sub><sup>t</sup>Bu)<sub>2</sub>. The reaction was exothermic with the solid changing its colour from light orange to white.

**Figure 3.1** presents the *in situ* IR spectroscopy of the reaction of molecular oxygen onto ( $\equiv\text{SiO}$ )Ta(CH<sup>t</sup>Bu)(CH<sub>2</sub><sup>t</sup>Bu)<sub>2</sub>. The study indicated the presence of both carboxylate and alkoxo ligands in the coordination sphere of organometallic complex.

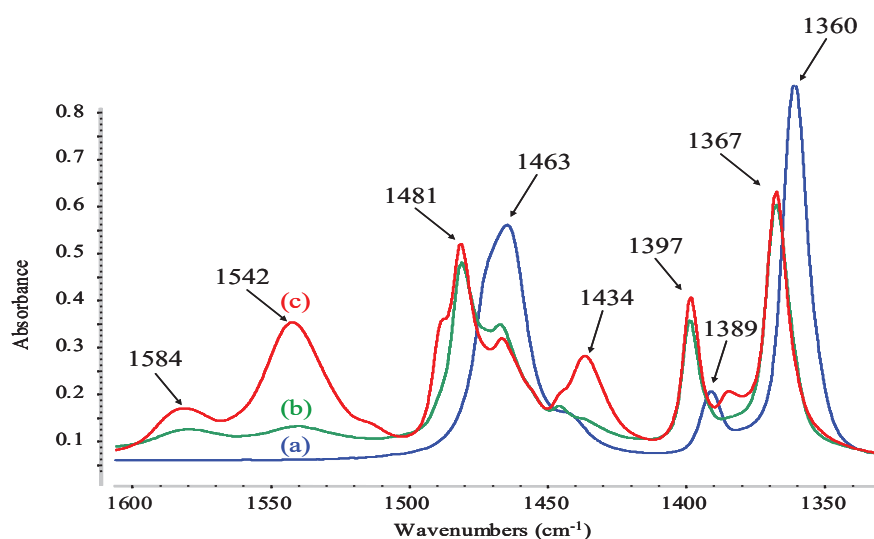


**Figure 3.1-** IR studies of the action of O<sub>2</sub> on  $\equiv\text{SiOTa}(\text{CH}^t\text{Bu})(\text{CH}_2^t\text{Bu})_2$

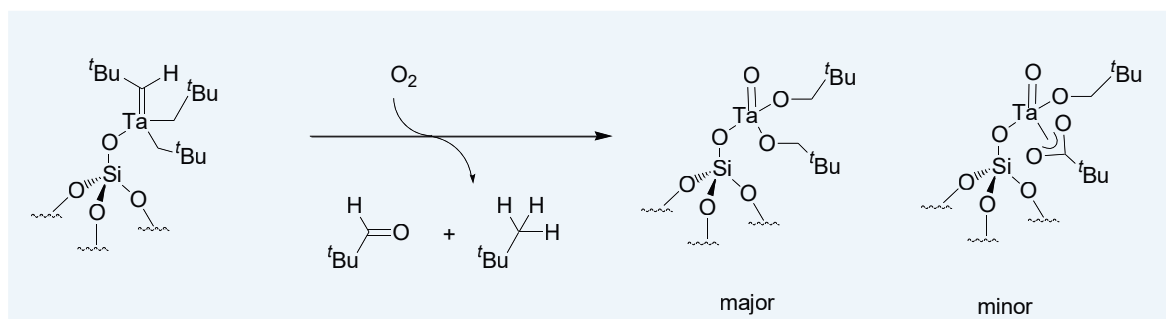
(a) :  $\equiv\text{SiOTa}(\text{CH}^t\text{Bu})(\text{CH}_2^t\text{Bu})_2$

(b) :  $\equiv\text{SiOTa}(\text{CH}^t\text{Bu})(\text{CH}_2^t\text{Bu})_2 + \text{O}_2$ , 2 hours at 25 °C.

(c) :  $\equiv\text{SiOTa}(\text{CH}^t\text{Bu})(\text{CH}_2^t\text{Bu})_2 + \text{O}_2$ , 24 hours at 70 °C

The  $^{13}\text{C}$  CP MAS NMR of the partially labeled  $^{13}\text{C}$  complex confirmed the transformation of the alkyl and alkylidene ligands and the formation of alkoxo species on the surface. The spectra also confirmed presence of carboxylates on the surface.

Based on the IR and NMR studies, a mechanism was proposed that suggested that the addition of molecular oxygen onto  $(\equiv\text{SiO})\text{Ta}(\text{CH}^t\text{Bu})(\text{CH}_2^t\text{Bu})_2$  produces different supported tantalum complexes with alkoxo, oxo and carboxylate ligands in their coordination sphere, the major product being probably  $(\equiv\text{SiO})\text{Ta}(\text{O})(\text{OCH}_2^t\text{Bu})_2$ . **Scheme 3.1** summarises the proposed reactivity of  $(\equiv\text{SiO})\text{Ta}(\text{CH}^t\text{Bu})(\text{CH}_2^t\text{Bu})_2$  towards molecular oxygen.



**Scheme 3.1:** Proposed reactivity of  $(\equiv\text{SiO})\text{Ta}(\text{CH}^t\text{Bu})(\text{CH}_2^t\text{Bu})_2$  towards molecular oxygen

The reactivity of grafted tantalum organometallic complex with oxygen at room temperature was further studied at an electronic level by Jacinto et. al.<sup>8,9</sup> The changes in the local Ta electronic structure were followed by in situ high-energy resolution off-resonant spectroscopy (HEROS). The study revealed that the reaction of  $\equiv\text{SiOTa}(\text{CH}^t\text{Bu})(\text{CH}_2^t\text{Bu})_2$ , with molecular oxygen results predominantly in formation of Ta dimers, in contrast with the isolated tantalum oxo alkoxo complexes proposed earlier.

Indeed it is difficult to elucidate the exact structure of the oxidized complex considering the tantalum atom can be present on the surface in different coordination environments, as isolated or oligomeric species. In this scenario, even X-ray absorption spectroscopies, like HEROS, only allow access to the information on heavy nuclei, namely metal centers, indicating the nature and number of ligands surrounding the metal within its first (and, with lesser accuracy, second) coordination sphere. Also, Raman spectroscopy which is highly powerful in probing the presence of specific groups in a given material, and is

highly sensitive to detect subtle changes at the molecular level cannot not be adapted to these systems since at such low surface loadings, the weak Raman scattering of the dehydrated surface  $\text{TaO}_x$  species do not give rise to any distinct vibrations against the stronger  $\text{SiO}_2$  support vibrations.<sup>10</sup>

With this in mind, our primary aim was to synthesize and study the surface species generated upon dynamic oxidation of tantalum alkyls grafted on the surface of silica by SOMC protocol.

In addition to the family of catalysts synthesized from  $[\text{Ta}(=\text{CH}^t\text{Bu})(\text{CH}_2^t\text{Bu})_3]$  another set of catalysts were synthesized by grafting commercially available tantalum ethoxide on the surface of partially dehydroxylated silica. The advantage of synthesizing supported alkoxo tantalum species starting from alkoxo tantalum complexes, in comparison to the starting complex  $\text{Ta}(\text{CH}^t\text{Bu})(\text{CH}_2^t\text{Bu})_3$ , is the important reduction of the number of synthesis steps. Indeed alkoxo tantalum are commercially available complexes in the contrary to the alkyl tantalum species. But a disadvantage of grafting molecular alkoxo tantalum onto silica comes from thermodynamics. Indeed, the enthalpy of this reaction is almost equal to zero. The grafting reaction may then not be as clean as when the starting material is tantalum alkyl.<sup>11</sup>

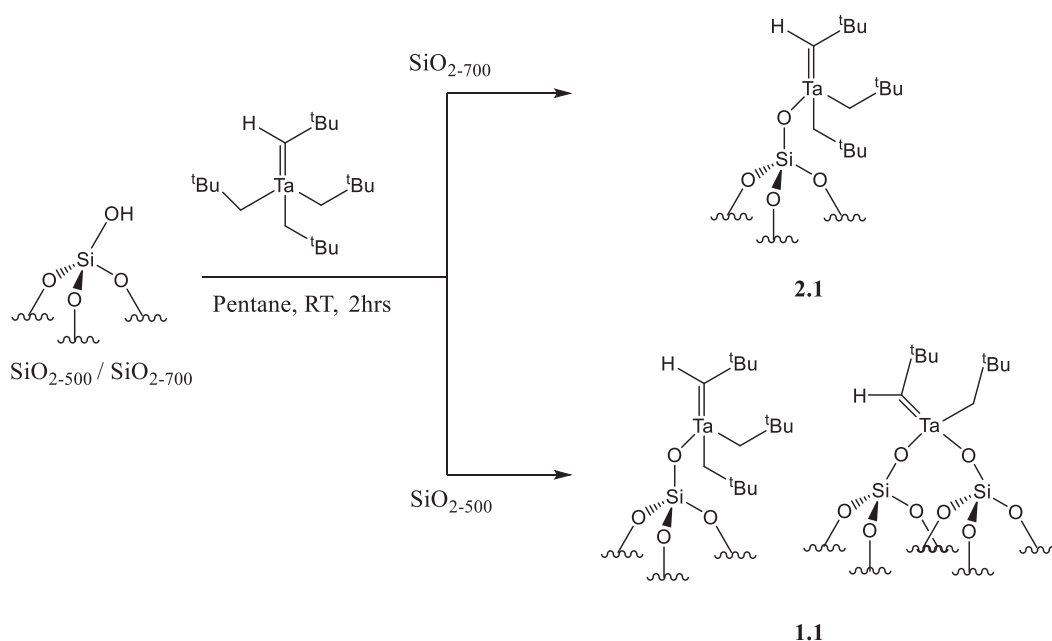


## B. Results and discussions

### B1.1. Synthesis of TaO<sub>x</sub>/SiO<sub>2</sub> catalysts via oxidation of known silica-supported tantalum alkyl species with molecular O<sub>2</sub>

Silica (Aerosil-200) dehydroxylated at 700°C (SiO<sub>2-700</sub>) and 500°C (SiO<sub>2-500</sub>) was prepared and characterized for grafting [Ta(=CH<sup>t</sup>Bu)(CH<sub>2</sub><sup>t</sup>Bu)<sub>3</sub>]. The organometallic complex was prepared as described in literature<sup>12</sup>. The impregnation technique typically consisted of stirring at 25°C a mixture of activated silica and Ta complex in pentane with 1 equivalent of [Ta(=CH<sup>t</sup>Bu)(CH<sub>2</sub><sup>t</sup>Bu)<sub>3</sub>] per 1 equivalent of surface silanol.

After three washing cycles, the volatiles were condensed into a reactor of known volume in order to quantify the neopentane (NpH) released during the reaction. The released gas was quantified by gas chromatography. The resultant solid was dried under UHV for an hour to obtain a light orange powder which was characterized by DRIFT, SSNMR and elemental analysis.



The grafting was done for different loadings of tantalum. Further another grafting was performed to obtain a pre-catalyst with tantalum loading of 2 wt% on SiO<sub>2-700</sub>. This sample was prepared from the point of view of catalytic testing in transformation of

EtOH/AA to BD, to ensure compatibility while comparing with the state-of-the-art catalysts, which are reported at 2 wt% Ta loading. The same grafting, to ensure 2 wt% of tantalum was repeated on SBA-15 dehydroxylated at 700°C, to study the effect of catalyst surface area on catalytic activity (later discussed in chapter 4). **Table 3.2** reports the results from elemental analysis, gas analysis and DRIFT experiments for the samples mentioned above.

**Table 3.1** - Grafting of  $[Ta(=CH^tBu)(CH_2^tBu)_3]$  on  $SiO_{2-700}$  by impregnation in pentane at 25°C

Sample	Metal Loading	Neopentane Release/Ta	DRIFT
<b>Complex 2.1</b>	5.1%	1NpH/Ta	2900-3000 $cm^{-1}$ $\nu$ (CH) 1500-1300 $cm^{-1}$ $\delta$ (C-H)
<b>Complex 1.1</b>	5,6%	1.5NpH/Ta	2900-3000 $cm^{-1}$ $\nu$ (CH) 1500-1300 $cm^{-1}$ $\delta$ (C-H)

The materials obtained by the above procedure were calcined under the flow of dry oxygen at 500°C for 10 hrs under the experimental conditions earlier reported by Wachs et al.<sup>5</sup> Upon contacting with oxygen, the light orange colour of the samples immediately turned white. DRIFT spectroscopy showed disappearance of IR bands attributed to  $\nu$  (C-H) and  $\delta$ (C-H) at 2800-3000 $cm^{-1}$  and 1500-1300  $cm^{-1}$  respectively which are diagnostic to the neopentyl ligands. However a concomitant appearance of  $\nu$  (O-H) band at 3747  $cm^{-1}$  was also observed.

It is to be noted that detailed spectroscopic characterizations were carried out only for the material based on  $SiO_{2-700}$ . The material obtained after calcination of sample obtained by 1:1 grafting of  $[Ta(=CH^tBu)(CH_2^tBu)_3]$  to surface silanols was named **SOMC-II<sub>FC</sub>** (to signify full coverage of silanols). Whereas the material obtained from tantalum loading of 2 wt% was named **SOMC-II**.

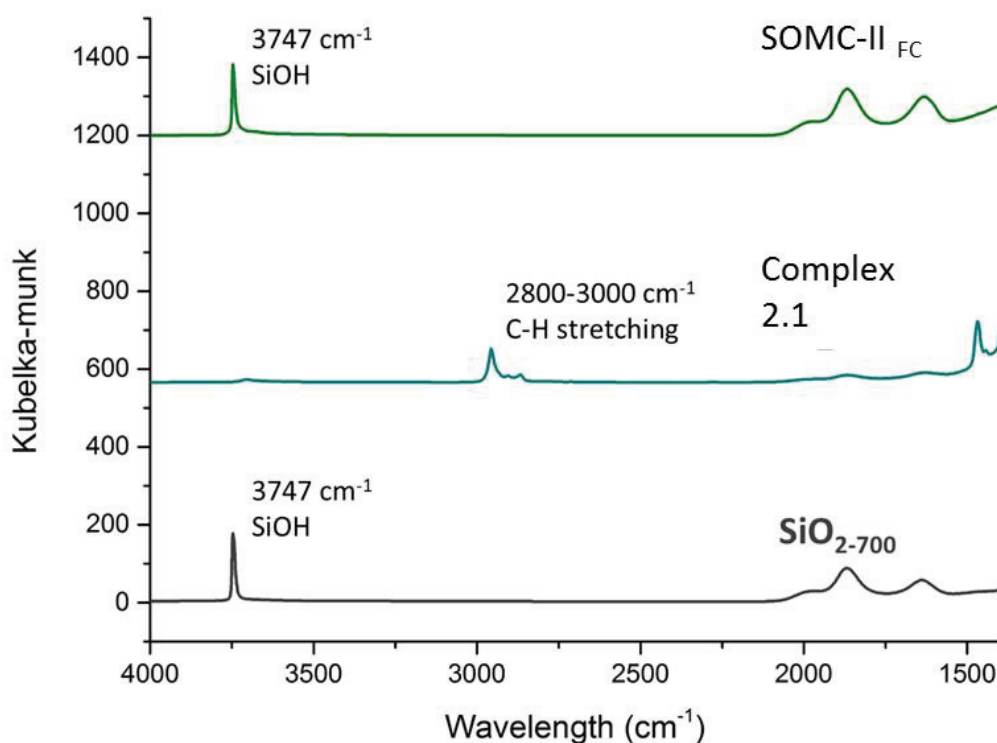
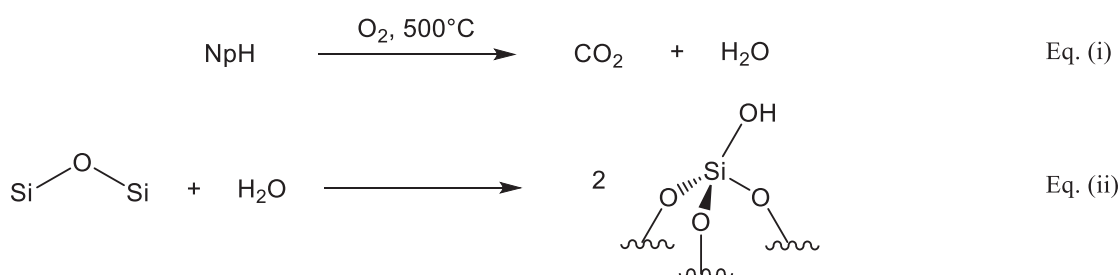


**Figure 3.2-** DRIFT spectroscopy of  $\text{SiO}_2\text{-700}$ , Complex 2.1 and SOMC II<sub>FC</sub>

It was expected that the reappearance of the  $\nu$  (O-H) band at  $3747\text{ cm}^{-1}$  was due to the water produced during the combustion of neopentyl groups. (Eq. ii) To investigate this, in operando FTIR study was carried out during dynamic oxidation of  $[\text{Ta}(=\text{CH}^t\text{Bu})(\text{CH}_2^t\text{Bu})_3]$  grafted silica disk under continuous flow of oxygen upto  $500^\circ\text{C}$  as shown in **Figure 3.6**. The study showed that the appearance of  $\nu$  (O-H) band at  $3747\text{ cm}^{-1}$  coincided with the consumption of  $\nu$  (C-H) bands at  $2800\text{-}3000\text{ cm}^{-1}$ . Such evidence suggests that the water is formed in-situ during the combustion of neopentyl and neopentylidene groups re-hydroxylate the surface of silica (**Eq.i**)



**Scheme 3.3**

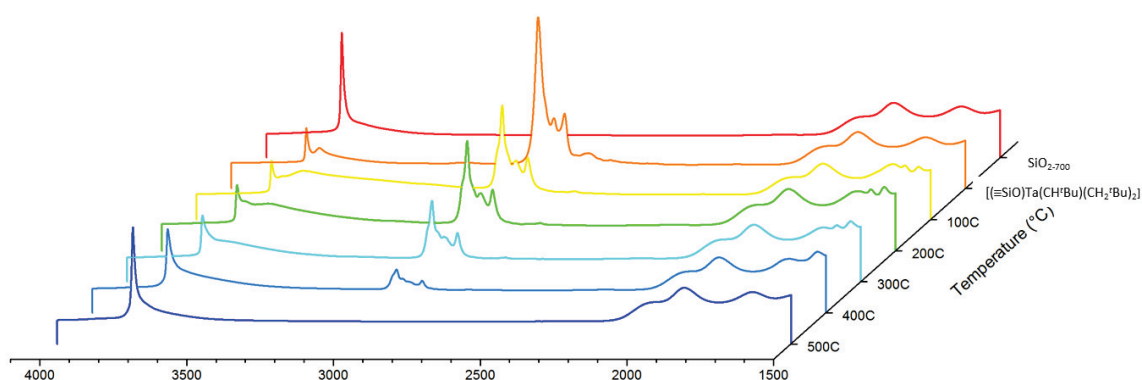


**Figure 3.3** - In-situ FTIR study of calcination carried on a Tantalum Shrock grafted Silica-700 disk at temperatures from 100°C to 500°C.

## B2. Characterization of surface species for TaO<sub>x</sub>/SiO<sub>2</sub> catalysts

The material SOMC-II<sub>FC</sub> was further completely characterized by UV-vis-Diffused reflectance spectroscopy, XRD, and EXAFS spectroscopy.

The in situ UV-vis DRS of the sample is shown in Figure 3.7. The spectra revealed a single, LMCT band at 233 nm corresponding to an  $E_g$  value of 5.2-5.3 eV. This can indicate the presence surface tetrahedral TaO<sub>x</sub> species on silica.<sup>4-6</sup> Concurrently the absence of the 265 nm LMCT band of crystalline Ta<sub>2</sub>O<sub>5</sub> indicates that the crystalline Ta<sub>2</sub>O<sub>5</sub> phase was absent.<sup>6</sup>

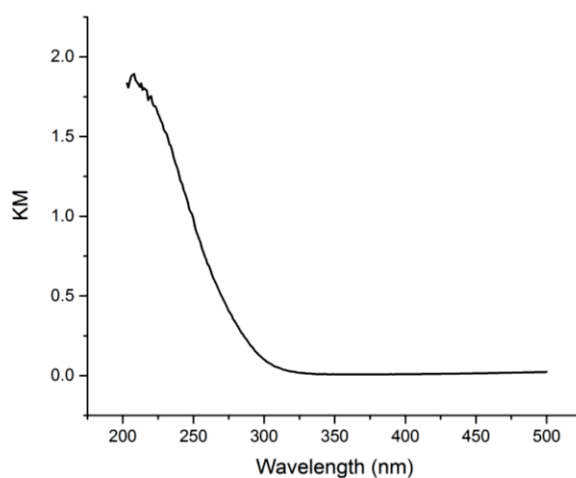


**Figure 3.4**- UV-vis spectroscopy of SOMC II-A<sub>FC</sub>

The data was in agreement with XRD characterization of **SOMC-II**<sub>FC</sub> where crystalline Ta<sub>2</sub>O<sub>5</sub> phase could not be observed.

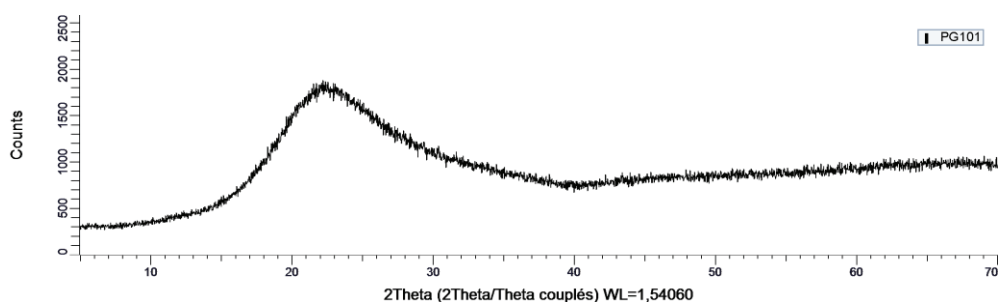


**Figure 3.5-** XRD spectrum of **SOMC-II**<sub>FC</sub>

### HRSTEM Analysis-

In an attempt to visualize the silica supported species on the surface of **SOMC-II** by HRSTEM. Microgram of the sample can be seen in **Figure 3.6**.

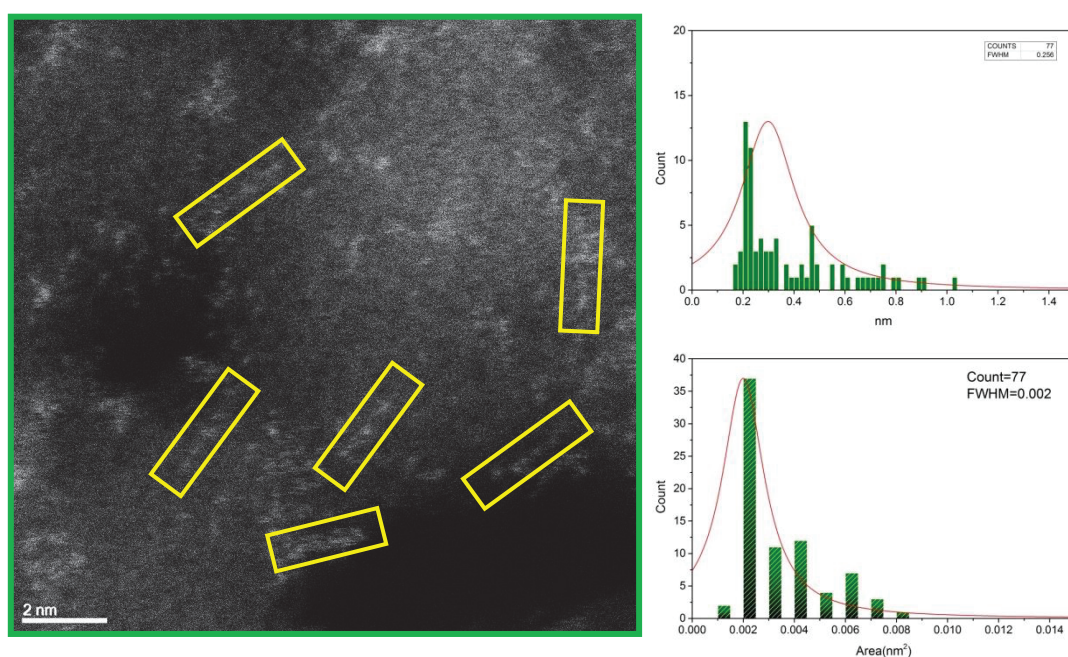


**Figure 3.6-** Representative HR-STEM micrographs of (a) **SOMC-II** and statistical evaluation of the STEM micrographs in the form of (b) size distribution histogram of the Ta centres (c) area distribution histogram of the Ta centres

Unlike the homogeneously distributed isolated TaO<sub>x</sub> species witnessed on the surface of **SOMC-I** in the previous chapter, for the calcinated **SOMC-II**, co-existence of isolated

Ta (V) centers along with Ta species in a string like arrangement was observed. A few small clusters were also evidenced. Software assisted analysis of the images afforded a statistical distribution of the sizes of the tantalum centers as shown in the histogram. The FWHM of the Lorentzian fit of the histogram was found to be considerably broad in comparison with **SOMC-I**.

### EXAFS Analysis-

Reported below is the Ta L<sub>III</sub>-edge EXAFS fit of **SOMC-II<sub>FC</sub>** performed by Dr. Aimery DeMalmann. The spectrum agrees with the following first coordination sphere around Ta: ca. five sigma-bonded oxygen atoms, (i) ca. two at 1.83(2) Å and (ii) ca. three at 1.913(4) Å. Of which the later can be assigned to the siloxide (Si-O-Ta) ligands.<sup>13</sup>

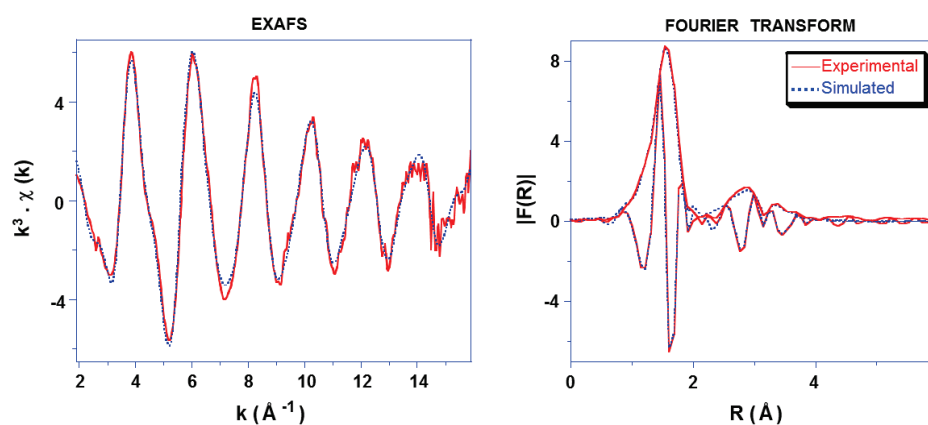
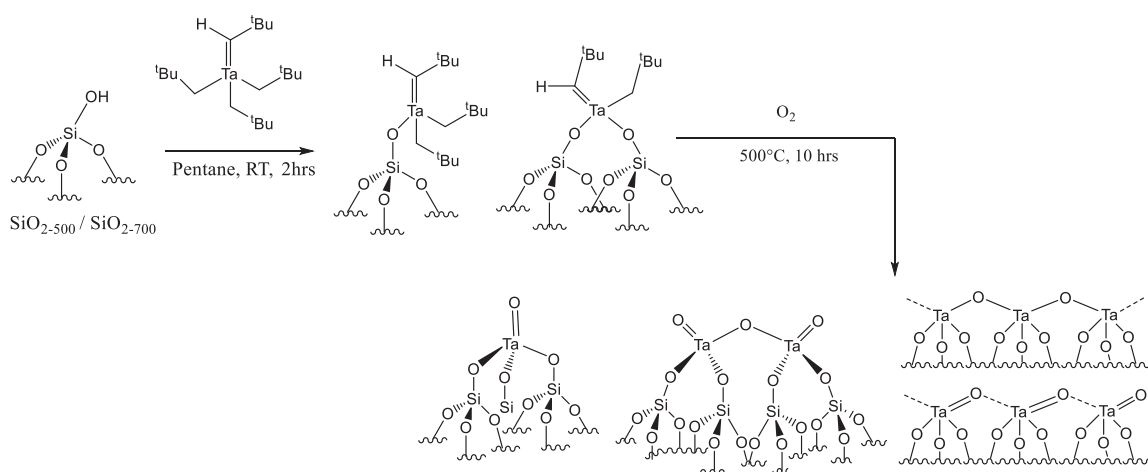


**Figure 3.7:** Tantalum L<sub>III</sub>-edge  $k^3$ -weighted EXAFS (left) and corresponding Fourier transform (right, modulus and imaginary part; R uncorrected from phase shift) with comparison to simulated curves for a Ta-Schrock complex grafted onto SiO<sub>2-500</sub> and then calcined by O<sub>2</sub> at 500°C. Solid lines: experimental; dashed lines: spherical wave theory.

**Table 3.1** - EXAFS parameters. (a) The errors generated by the EXAFS fitting program “RoundMidnight” are indicated between parentheses

Type of neighbour	Number of neighbours	Distance (Å)	$\sigma^2$ (Å <sup>2</sup> )
<i>Ta-O<sub>a</sub></i>	4.9(4)	1.905(5)	0.0040(5)
<i>Ta-O</i>	1.2(9)	2.98(4)	0.0076(54)
<i>Ta-Si</i>	2.2(11)	3.29(3)	0.0059(31)
<i>MS 3l &amp; 4l O'-Ta-O<sup>(b)</sup></i>	2 x 1.9(10)	3.88(4)	0.007(5)
( <i>Ta-Ta</i> )	0.1(3)	3.44(5)	0.002(7) )

Furthermore, the fit was improved when considering further layers of back-scatterers, one to two O atoms at 3.00(3) Å, assigned to surface oxygens, ca. three Si atoms at 3.54(3) Å and multiple scattering pathways for Ta-O-Si and O-Ta-O' corresponding to a quasi linear arrangement of both groups of three atoms in the supported species (a O-Ta-O' alignment would indicate a bi-pyramidal geometry for the Ta sites). The results from EXAFS study concur with the absence of Ta<sub>2</sub>O<sub>5</sub> phase on the surface of. The presence of two Tantalum neighbours indicates a possibility of **SOMC II<sub>FC</sub>** being a mixture of mononuclear, di-nuclear and oligomer like species.



Scheme 3.3

### B3.Synthesis of TaO<sub>x</sub>/SiO<sub>2</sub> catalysts via oxidation with molecular O<sub>2</sub>

With the view of synthesizing pre-catalysts with a tantalum precursor which is more industrially viable and economically favorable compared to the organometallic [Ta(=CH<sup>t</sup>Bu)(CH<sub>2</sub><sup>t</sup>Bu)<sub>3</sub>], silica dehydroxylated at 700°C (SiO<sub>2-700</sub>) and 500°C (SiO<sub>2-500</sub>) was grafted with commercially available tantalum ethoxide. The impregnation technique typically consisted of stirring at 25°C a mixture of SiO<sub>2-700</sub> and tantalum ethoxide in toluene. The calculations were made to graft 1 equivalent of Ta per equivalent of surface silanol. The material obtained from grafting performed on SiO<sub>2-700</sub> was coded **Complex-2.1'** while that obtained via grafting on SiO<sub>2-500</sub> was coded **Complex-2.2'**.

Another grafting was performed to obtain a pre-catalyst with 2 wt% of tantalum. This sample was prepared from the point of view of catalytic testing in transformation of EtOH/AA to BD, to ensure compatibility while comparing with the state-of-the-art catalysts, which are reported at 2 wt% Ta loading. (later discussed in chapter 4).

After washings the resultant solid was dried under UHV for an hour to obtain a white powder which was characterized by DRIFT, SSNMR and elemental analysis. To the best of our knowledge, the grafting of tantalum ethoxide on dehydroxylated silica by SOMC protocol has not been reported in the literature. **Table 3.4** shows the preliminary results obtained from the DRIFT and SSNMR characterization of the resulting solid.

Sample	%Metal Loading	DRIFT
<b>Complex 2.1'</b>	5.3%	2900-3000cm <sup>-1</sup> $\nu$ (CH) 1500-1300 cm <sup>-1</sup> $\delta$ (C-H)
<b>Complex 2.2'</b>	5.8%	3747 cm <sup>-1</sup> , $\nu$ (O-H) 2900-3000cm <sup>-1</sup> $\nu$ (CH) 1500-1300 cm <sup>-1</sup> $\delta$ (C-H)

<sup>13</sup>C MAS solid-state NMR spectra of the material obtained showed two main signals at 17 ppm and 68 ppm. The attribution of these signals can be done based on the signals from molecular [Ta(OEt)<sub>5</sub>]<sub>2</sub> reported in literature. The signal at 16 ppm is characteristic of the methyl group of the ethoxy ligands O-CH<sub>2</sub>-CH<sub>3</sub>, bonded either to silicium ( $\equiv$ Si-OEt) or tantalum (Ta-OEt). The resonance at 68 ppm can be attributed to the carbon of methylene O-CH<sub>2</sub>-CH<sub>3</sub> in the ethoxy group coordinated to tantalum.

Commercial [Ta(OEt)<sub>5</sub>]<sub>2</sub> is available in the form of a dimer. Therefore a critical point when grafting [Ta(OMe)<sub>5</sub>]<sub>2</sub> on a silica surface is to know whether the surface tantalum complex is mono- or di-nuclear. No clear conclusion could be drawn based on SS NMR and UV-vis-DRS spectroscopy. Further spectroscopic investigation will be needed to confirm the exact nature of the supported species.

Nonetheless, the materials obtained by the above procedure were calcined under the flow of dry oxygen at 500°C for 10 hrs. The material obtained after calcination of **SOMC-2.1'** was named **SOMC-II'**<sub>FC</sub>. Whereas the material obtained from tantalum loading of 2 wt% was named **SOMC-II'**.

**Figure 3.8** shows the DRIFT spectra for the formation of **SOMC-II'**<sub>FC</sub> by calcination of Complex 2.1'. Similar to the samples grafted with tantalum alkyls, upon calcination the IR bands attributed to  $\nu$  (C-H) and  $\delta$ (C-H) at 2800-3000 $\text{cm}^{-1}$  and 1500-1300  $\text{cm}^{-1}$  respectively, disappeared and appearance of a band at 3747  $\text{cm}^{-1}$  was also observed.

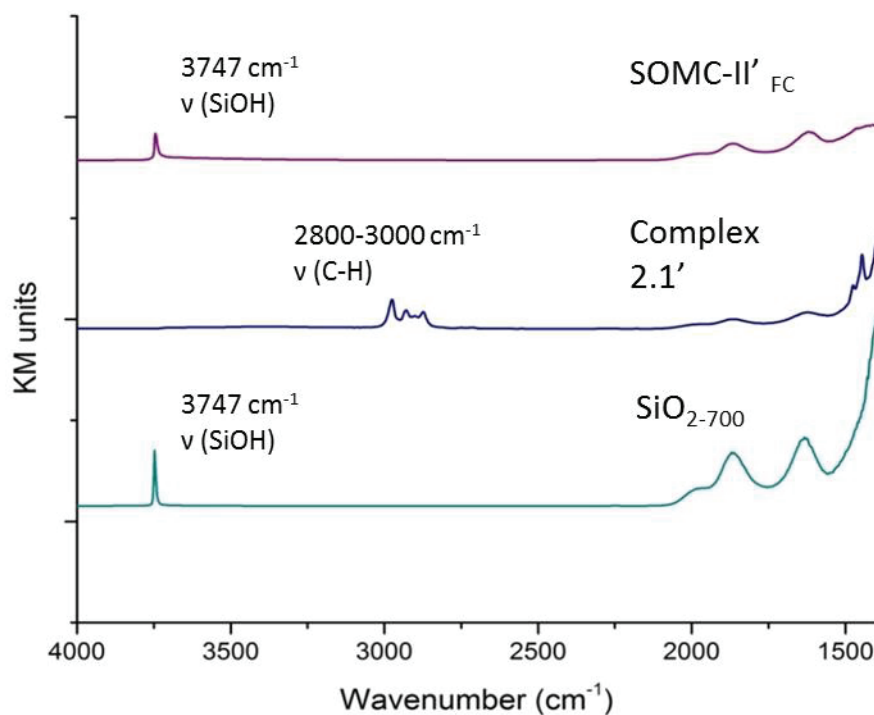


**Figure 1.8-** DRIFT spectroscopy of  $\text{SiO}_{2-700}$ , Complex 2.1' and SOMC II'<sub>FC</sub>

The material was analyzed by XRD. Figure 3.9 shows the XRD spectrum of **SOMC-II'**<sub>FC</sub>.

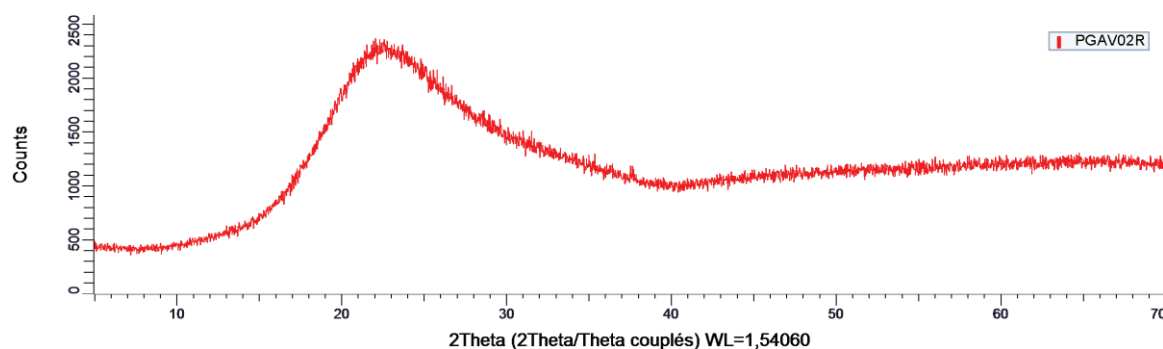


**Figure 3.9-** XRD spectrum of **SOMC-II'**<sub>FC</sub>

Tanaka et al. reported formation  $Ta_2O_5$  micro-crystallites upon calcination of tantalum ethoxide grafted silica, after the attainment of monolayer of tantalum species on the surface of silica. No peak corresponding to crystalline  $Ta_2O_5$  phase was observed in the XRD spectra of **SOMC-II'**<sub>FC</sub>.

Further characterization by EXAFS and HRSTEM would give better insight into the structure and nature of surface species on these materials. Nevertheless, all the pre-catalysts were tested in the catalytic conversion of EtOH/AA to BD. (discussed in chapter 4 and 5)

## C. Conclusions:

The reactivity of previously known  $[\equiv\text{SiOTa}(\text{=CH}^t\text{Bu})(\text{CH}_2^t\text{Bu})_2]$  species with oxygen was investigated under continuous flow conditions at 500°C for 10 hrs. The resulting material was completely characterized by IR and NMR spectroscopy, UV-DRS spectroscopy and XRD. The latter two analysis confirmed absence of  $\text{Ta}_2\text{O}_5$  microcrystals on the surface. EXAFS analysis corroborated the absence of  $\text{Ta}_2\text{O}_5$  phase while indicating the possibility of some Ta-Ta interaction. The HRSTEM microscopy evidenced co-existence of isolated Ta (V) centers along with Ta species in a string like arrangement. This data together with the information from literature suggested the presence of a mixture of mononuclear, di-nuclear and oligomer like species on the surface of the material.

An attempt was made to reproduce the above synthesis strategy with cheaper and commercially available  $[\text{Ta}(\text{OEt})_5]_2$ . The formation of these catalysts was monitored by DRIFT, SSNMR and XRD.

## D. Experimental Details:

### D1. General procedure for preparation of starting material

All experiments were carried out under controlled atmosphere, using schlenk and glovebox techniques for the organometallic synthesis. For the synthesis and treatments of the surface species, reactions were carried out using high-vacuum lines ( $1.34 \times 10^{-3}$  kPa) and glovebox techniques.

Pentane and diethyl ether were distilled on NaK alloy and benzophenone/Na, respectively, followed by degassing by freeze-pump-thaw cycles.

### D2. Synthesis of catalyst supports

SiO<sub>2</sub> (Aerosil Degussa, 200 m<sup>2</sup> g<sup>-1</sup>) was compacted with distilled water and partially dehydroxylated at 500 °C and 700 °C under vacuum (10-5 torr) for 12 h.

SBA-15 was synthesized according to the procedure reported in literature.<sup>14</sup> The BET surface area calculated by N<sub>2</sub> adsorption experiments was 981.42 m<sup>2</sup>/g.

### D3. Preparation of surface complexes by SOMC protocol

**Complex 1.1:** A solution of [Ta(=CH<sup>t</sup>Bu)(CH<sub>2</sub><sup>t</sup>Bu)<sub>3</sub>] (0.43 g, 0.9 mmol) in pentane (15 mL) and SiO<sub>2-(500)</sub> (2 g, 0.9 mmol OH/g) was stirred at 25 °C for 2 h. After filtration, the solid was washed three times with pentane. The solvent was then removed, and the light orange solid was dried under dynamic vacuum at 25 °C. <sup>1</sup>H MAS solid-state NMR (300 MHz, 25 °C): δ (ppm) 1 (s, CH<sub>2</sub>, CH<sub>3</sub>). <sup>13</sup>C CP-MAS solid-state NMR (300 MHz, 25 °C): δ (ppm) 34 (s, C(CH<sub>3</sub>)<sub>3</sub>), 95 (s, CH<sub>2</sub>-<sup>t</sup>Bu). Infrared (cm<sup>-1</sup>): 1450-1500 s, δ(C-H), 2800-3000 (s, ν(C-H)). Gas-phase analysis: 1.5 equiv/Ta of CH<sub>3</sub>-<sup>t</sup>Bu evolved. Elemental analysis: % wt Ta 5.56% C 5.52%

**Complex 2.1-** A solution of [Ta(=CH<sup>t</sup>Bu)(CH<sub>2</sub><sup>t</sup>Bu)<sub>3</sub>] (0.12 g) in pentane (15 mL) and SiO<sub>2-(700)</sub> (1 g) was stirred at 25 °C for 2 h. After filtration, the solid was washed three times with pentane. The solvent was then removed, and the white solid was dried under dynamic vacuum at 25 °C. <sup>1</sup>H MAS solid-state NMR (300 MHz, 25 °C): δ (ppm) 0.8 (s, CH<sub>2</sub>, CH<sub>3</sub>). <sup>13</sup>C CP-MAS solid-state NMR (300 MHz, 25 °C): δ (ppm) 35 (s, C(CH<sub>3</sub>)<sub>3</sub>), 90 (s, CH<sub>2</sub>-<sup>t</sup>Bu). Infrared

( $\text{cm}^{-1}$ ): 1300-1500 s,  $\delta(\text{CH}_2, \text{CH}_3)$ , 2800-3000 (s,  $\nu(\text{C-H})$ ). Gas-phase analysis: 1 equiv/Ta of  $\text{CH}_3\text{-}^1\text{Bu}$  evolved. Elemental analysis: % wt Ta 5.1% C 4.86%

**Complex 2.1'**- A solution of  $[\text{Ta}(\text{OEt})_5]_2$  (0.11 mL) in Toluene (20 mL) and  $\text{SiO}_2\text{-}(500)$  (1 g) was stirred at 25 °C for 2 h. After filtration, the solid was washed three times with Toluene. The solvent was then removed, and the white solid was dried under dynamic vacuum at 25 °C.  $^1\text{H}$  MAS solid-state NMR (300 MHz, 25 °C):  $\delta$  (ppm) 0.8 (s,  $\text{CH}_2, \text{CH}_3$ )  $^{13}\text{C}$  MAS solid-state NMR (300 MHz, 25 °C):  $\delta$  (ppm) 17 ppm(s,  $\text{CH}_2, \underline{\text{C}}\text{H}_3$ ), 67.91 ppm (s,  $\underline{\text{C}}\text{H}_2, \text{CH}_3$ ). Infrared ( $\text{cm}^{-1}$ ): 1300- 1500 s,  $\delta(\text{CH}_2, \text{CH}_3)$ , 2600-2900 (s,  $\nu(\text{C-H})$ )

**Complex 2.2'**-A solution of  $[\text{Ta}(\text{OEt})_5]_2$  (0.06 mL) in toluene (20 mL) and  $\text{SiO}_2\text{-}(700)$  (1 g) was stirred at 25 °C for 2 h. After filtration, the solid was washed three times with Toluene. The solvent was then removed, and the white solid was dried under dynamic vacuum at 25 °C.  $^1\text{H}$  MAS solid-state NMR (300 MHz, 25 °C):  $\delta$  (ppm) 0.8 (s,  $\text{CH}_2, \text{CH}_3$ ).  $^{13}\text{C}$  MAS solid-state NMR (300 MHz, 25 °C):  $\delta$  (ppm) 17 ppm(s,  $\text{CH}_2, \underline{\text{C}}\text{H}_3$ ), 68 ppm (s,  $\underline{\text{C}}\text{H}_2, \text{CH}_3$ ). Infrared ( $\text{cm}^{-1}$ ): 1300- 1500 s,  $\delta(\text{CH}_2, \text{CH}_3)$ , 2600-2900 (s,  $\nu(\text{C-H})$ ).

#### D4. In operando FTIR spectroscopy experiments

A self-supporting disk of silica of known weight was dehydroxylated at 700°C for 12hrs under UHV.  $[\text{Ta}(=\text{CH}^1\text{Bu})(\text{CH}_2^1\text{Bu})_3]$  was sublimed on this disk at 80 °C,  $10^{-5}$  torr. This was followed by a reverse sublimation to remove the excess of the organometallic precursor. During this process, the pellet turned from white to orange. Following this the pellet was calcinated under flow of dry  $\text{O}_2$ . Transmission FTIR spectroscopy was used to study pellet at every 100°C from 50 to 500°C.

#### D5. X-ray diffraction

The crystallographic information of all samples was investigated at CDHL, University of Lyon (Villeurbanne) by powder X-ray diffraction (XRD, Bruker D8 Advance, Cu,  $\text{K}\alpha$  radiation,  $\lambda = 1.5406 \text{ \AA}$ , 40 kV, 40 mA). The samples were prepared in the form of fine homogeneous powder. A thin smooth layer of the samples mounted on a non-crystalline substrate such as PMMA (Poly (methylmethacrylate)) was held in the path of X-rays. The diffracted X-rays correspond to all sets of planes in the crystal powder which could be

orientated in every possible direction relative to the X-ray beam. The XRD patterns with diffraction intensity versus  $2\theta$  were recorded, usually from  $10^\circ$  to  $70^\circ$  at a scanning speed of  $2^\circ$  per min. A LYNXEYE XE detector with an opening of  $3^\circ$  was used to detect the diffracted beam.

### D5. Catalyst characterization by EXAFS spectroscopy

X-ray absorption spectra were acquired at ESRF on BM23 beam-line (experiment code IN-986), at room temperature at the tantalum  $L_{III}$  edge, with a double crystal Si(111) monochromator detuned 70% to reduce the higher harmonics of the beam. The spectra were recorded in the transmission mode between 9.65 and 10.9 keV. The supported Ta samples were packaged within an argon filled dry box in a double air-tight sample holder equipped with kapton windows.

The program FEFF8 was used to calculate theoretical files for phases and amplitudes based on model clusters of atoms. (Ankudinov, A. L.; Ravel, B.; Rehr, J. J.; Conradson, S. D. *Phys. Rev. B*:1998, 58, 7565-7576.) The value of the scale factor was determined from the  $k^2$  and  $k^3 \cdot \chi(k)$  spectra of a reference compound, a sample of  $LiTaO_3$  diluted in BN and carefully mixed and pressed as a pellet.

The refinements were performed by fitting the structural parameters  $N_i$ ,  $R_i$ ,  $\sigma_i$  and the energy shift,  $\Delta E_0$  (the same for all shells). The fit residue,  $\rho$  (%), was calculated by the following formula:

$$\rho = \frac{\sum_k [k^3 \chi_{\text{exp}}(k) - k^3 \chi_{\text{cal}}(k)]^2}{\sum_k [k^3 \chi_{\text{exp}}(k)]^2} * 100$$

As recommended by the Standards and Criteria Committee of the International XAFS Society, (Reports of the Standards and Criteria Committee of the International XAFS Society 2000: [http://ixs.iit.edu/subcommittee\\_reports/sc/](http://ixs.iit.edu/subcommittee_reports/sc/)) the quality factor,  $(\Delta\chi)^2/\nu$ , where  $\nu$  is the number of degrees of freedom in the signal, was calculated and its minimization considered in order to control the number of variable parameters in the fits.

## E. References

1. Chae, H.-J. *et al.* Butadiene production from bioethanol and acetaldehyde over tantalum oxide-supported ordered mesoporous silica catalysts. *Applied Catal. B, Environ.* **150–151**, 596–604 (2014).
2. Kim, T. W. *et al.* Butadiene production from bioethanol and acetaldehyde over tantalum oxide-supported spherical silica catalysts for circulating fluidized bed. *Chem. Eng. J.* **278**, 217–223 (2015).
3. Kyriienko, P. I., Larina, O. V., Soloviev, S. O., Orlyk, S. M. & Dzwigaj, S. High selectivity of TaSiBEA zeolite catalysts in 1,3-butadiene production from ethanol and acetaldehyde mixture. *Catal. Commun.* **77**, 123–126 (2016).
4. Lee, E. L. & Wachs, I. E. In Situ Spectroscopic Investigation of the Molecular and Electronic Structures of SiO<sub>2</sub> Supported Surface Metal Oxides. *J. Phys. Chem. C* **111**, 14410–14425 (2007).
5. Chen, Y., Fierro, J. L. G., Tanaka, T. & Wachs, I. E. Supported Tantalum Oxide Catalysts: Synthesis, Physical Characterization, and Methanol Oxidation Chemical Probe Reaction. *J. Phys. Chem. B* **107**, 5243–5250 (2003).
6. Baltes, M. *et al.* Supported Tantalum Oxide and Supported Vanadia-tantala Mixed Oxides : Structural Characterization and Surface Properties. *J. Phys. Chem. B.* **105**, 6211–6220 (2001).
7. Petroff Saint-Arroman, R. Catalyse hétérogène Composés cycliques Hafnium -- Composés organiques Peroxydation Tantale -- Composés organiques Zirconium -- Composés organiques. (2002).
8. Błachucki, W. *et al.* Study of the reactivity of silica supported tantalum catalysts with oxygen followed by in situ HEROS. *Phys. Chem. Chem. Phys.* **17**, 18262–18264 (2015).
9. Błachucki, W. *et al.* In situ high energy resolution off-resonant spectroscopy applied to a time-resolved study of single site Ta catalyst during oxidation. *Nucl. Instruments Methods Phys. Res. Sect. B Beam Interact. with Mater. Atoms* **411**, 63–67 (2017).
10. Weckhuysen, B. M., Jehng, J.-M. & Wachs, I. E. In Situ Raman Spectroscopy of Supported Transition Metal Oxide Catalysts: 18 O<sub>2</sub> – 16 O<sub>2</sub> Isotopic Labeling Studies. *J. Phys. Chem. B* **104**, 7382–7387 (2000).
11. Petroff Saint-Arroman, R., Didillon, B., De Mallmann, A., Basset, J. M. & Lefebvre, F. Deperoxidation of cyclohexyl hydroperoxide by silica-supported alkoxo-tantalum complexes. *Appl. Catal. A* **337** (2008), 78–85 (2008).
12. Schrock, R. R. Alkylidene complexes of niobium and tantalum. *Acc. Chem. Res.* **12**, 98–104 (1979).

13. Merle, N. *et al.* Well-defined silica supported bipodal molybdenum oxo alkyl complexes: a model of the active sites of industrial olefin metathesis catalysts. *Chem. Commun. Chem. Commun* **53**, 11338–11341 (1133).
14. Choi, M., Heo, W., Kleitz, F. & Ryoo, R. Facile synthesis of high quality mesoporous SBA-15 with enhanced control of the porous network connectivity and wall thickness. *Chem. Commun.* **0**, 1340–1341 (2003).

# Chapter 4

Catalytic performance of SOMC catalysts compared to state of the art

*The aim of this chapter is to evaluate the catalytic activity of the family of well-defined catalysts synthesized by the SOMC in Chapters 2 and 3 and to mark their performance against the state-of-the-art catalysts reported in literature.*



# Contents

<b>A. Introduction.....</b>	<b>89</b>
<b>B. Results and discussion .....</b>	<b>93</b>
B1. General description of catalytic tests and analytical methods.....	93
B2. Catalytic activity of catalysts synthesized by SOMC protocol .....	94
B2.1. Comparison of the [Ta(=CH <sup>t</sup> Bu)(CH <sub>2</sub> <sup>t</sup> Bu) <sub>3</sub> ] based catalysts .....	96
B2.1. Comparison of the [Ta(=CH <sup>t</sup> Bu)(CH <sub>2</sub> <sup>t</sup> Bu) <sub>3</sub> ] based catalysts with Ta(OEt <sub>5</sub> ) based catalysts .....	98
B3. Butadiene selectivity and product distribution.....	100
B4. Post-catalysis analysis .....	102
<b>C. Conclusions.....</b>	<b>103</b>
<b>D. Experimental details .....</b>	<b>104</b>
D1. General description of the catalytic reactor .....	105
D2. Analysis of coke formation by Thermo-gravimetric Analysis (TGA).....	106
<b>E. References .....</b>	<b>108</b>



## A. Introduction:

The transformation of ethanol and acetaldehyde to butadiene is a complex process involving a network of reactions such as dehydration, dehydrogenation and aldol condensation.<sup>1</sup> Such process demands for a multifunctional catalyst, with an appropriate balance in number, strength and ideal proximity of acidic, basic and redox sites in order to maximise the productivity of the reaction.<sup>2,3</sup>

In recent years there has been a growing upsurge in the study of catalytic systems for the two step process. Though these studies are helpful in pointing towards the usefulness of certain metals or supports in a catalyst to improve the overall BD yield, there is no clear evidence on the nature of the species populating the surface of the catalyst. In the absence of this understanding, it is difficult to generate or balance the acid/base or redox sites on the catalyst surface in a way that provides for the ideal reaction kinetics.<sup>4</sup>

To this end we synthesized two families of TaO<sub>x</sub>/SiO<sub>2</sub> pre-catalysts with well-defined surface species (as reported in Chapter 2 and 3). Upon extensive characterization it could be concluded that these pre-catalysts differ in their dominant surface species in terms of tantalum nuclearity and the tantalum co-ordination sphere. In this chapter, we evaluate the activity of these catalysts in the transformation of ethanol and acetaldehyde to BD. With the reliable knowledge of the chemical and structural identity of this catalyst we would like to better appreciate its correlation to the catalyst performance (detailed discussion in Chapter 5)

Furthermore, the aim of this chapter is to compare the catalytic performances of these two families of SOMC pre-catalysts with the state of the art catalysts studied in literature.

Following the original catalyst developed by Ostromyslensky, ample study on Ta/SiO<sub>2</sub> systems as catalysts for two step ETB transformations is available. Of these, a notable study is that by Jeon *et al.*<sup>5</sup> who prepared a series of ordered mesoporous silica (OMS) supported Tantalum oxide samples. The catalysts showed better catalytic performances towards butadiene production compared to the earlier systems, indicating need for better dispersed tantalum on silica catalysts. (We refer to this catalytic system as **WI-i**). Another remarkable attempt to synthesize a well-defined catalyst was recently made by Dzwigaj *et*

*al.*<sup>6</sup>, who tailored isolated mononuclear Tantalum (V) centers in the zeolite framework. (**Zeo-i**) Resulting catalysts were highly selective in the transformation of ethanol and acetaldehyde to butadiene. Both these systems represent two of the best performing catalysts in the second step of Ostromyslensky process (i.e. transformation of ethanol and acetaldehyde to BD).

**Table 4.1**-Reported catalysts and reaction conditions for the two step ETB process <sup>4</sup>

Catalyst	Metal loading	Catalyst Preparation	Reaction Temperature	WHSV (gEtOH+gC <sub>2</sub> H <sub>4</sub> O)·gcat·h <sup>-1</sup>	EtOH/AA	Conversion	Selectivity	BD
Ta <sub>2</sub> O <sub>5</sub> /SiO <sub>2</sub>	2%	Solv impr.	325°C-350°C	LHSV = 1 h <sup>-1</sup>	2.5	31,5%	72%	22,7
Ta <sub>2</sub> O <sub>5</sub> /SiO <sub>2</sub> SBA-15	2%	Solv impr.	350°C	LHSV = 1 h <sup>-1</sup>	2.5	37%	80%	29,6
ZrO <sub>2</sub> /SiO <sub>2</sub>	2%	Sol-gel	320°C	1.8 h <sup>-1</sup>	3.5	45,4%	69,7%	31,6
ZrO <sub>2</sub> /SiO <sub>2</sub>	5,5%	Sol-gel	350°C	1.8 h <sup>-1</sup>	2,5	n.a	36%	
ZrO <sub>2</sub> /SiO <sub>2</sub>	1,6%	Sol-gel	310°C	1.8 h <sup>-1</sup>	3.5	40,7%	83,3%	33,9
MgO/SiO <sub>2</sub>	-	Solv impr.	350°C	0,35 h <sup>-1</sup>	3.0	29,7%	80,7%	24,0
Ta-SiBEA zeolite	3%		350°C	-	2.2	42,9%	87,5%	37,5

It is worthy to note that there is a limitation in comparing the catalytic activity of the catalysts mentioned in literature. This is due to the differences in both, the catalytic systems as well as the conditions of catalytic testing. Even while comparing only the silica supported tantalum oxide systems, the catalysts may differ in metal loadings, surface areas and surface morphologies. Also the testing conditions vary slightly in reaction temperatures, flow rates, molar ratios (EtOH/AA) and time on stream. **Table 4.1** provides the summary of these details for the catalysts in comparison. We have tried to maintain as much uniformity possible in terms of reaction conditions while drawing these comparisons.

## B. Results and Discussions:

### B1. General description of catalytic tests-

The catalytic tests for production of butadiene from ethanol and acetaldehyde were performed in a lab scale continuous flow reactor under atmospheric pressure. A catalyst amount of 0.25 g was loaded in the reactor in the form of powder. Inlet feed molar ratios were always constant and were set at 2 mol% ethanol and acetaldehyde mixture with 98% nitrogen. Downstream products were fed to an automatic sampling system for gas-chromatography. **Figure 4.1** shows the schematic diagram for the lab scale reactor used in the catalytic testing.

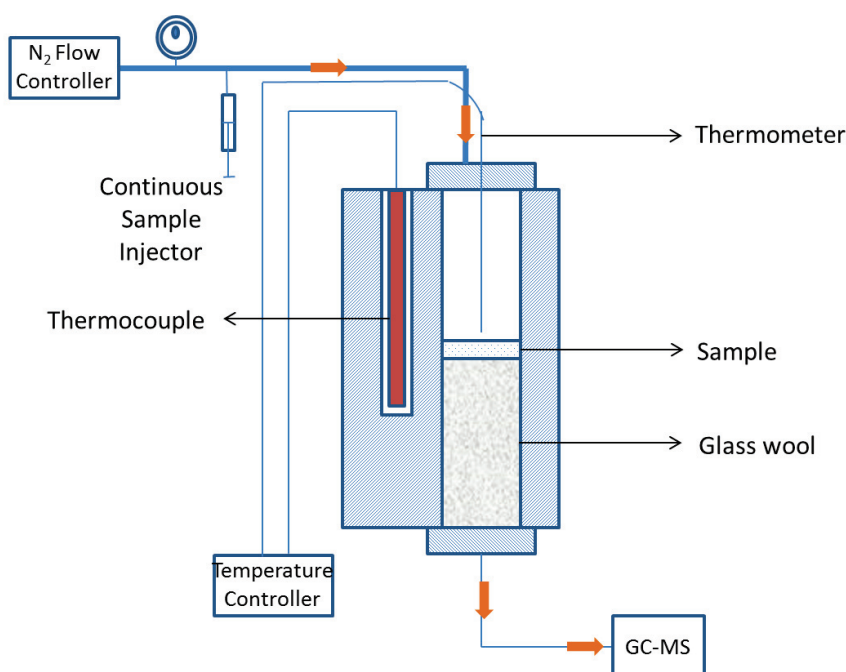


**Figure 4.1-** Reaction apparatus for synthesis of Butadiene from Ethanol and Aldehyde

From the thermodynamic study, it is known that, reaction temperatures between 325 and 430°C are preferred for this transformation, since lower temperatures restrict acetaldehyde formation, whereas higher temperatures limit the aldol condensation.<sup>7,8</sup> Toussaint et al.<sup>9</sup> investigated the influence of the reaction temperature, the molar ratio of EtOH to AA and the space velocity on the catalyst activity of a 2 wt% Ta<sub>2</sub>O<sub>5</sub> on silica. Highest BD selectivity was obtained for reaction temperatures 325-350°C for a feed mixture with a EtOH: AA ratio of 2-2.5.

Keeping this in mind, the catalysts were tested at a reaction temperature of 325°C with the molar ratio of the feed being maintained at EtOH: AA=2.5. The weight hour space velocity (WHSV) of the feed was maintained at  $0.5 g_{\text{EtOH/AA}} \cdot g^{-1}_{\text{cat}} \cdot h^{-1}$ . Independent study of the effect of these parameters (contact times and EtOH: AA ratio) on the catalytic activity will be discussed separately in chapter 5, with focus on mechanistic study.

The percentage values of conversion, selectivity and yield were determined from the gas chromatograms, using the **Eq. (i)-(iii)**-

$$\text{Conversion} = \frac{(\text{Total C moles} - (\text{C mole unreacted EtOH} + \text{C mole unreacted AA}))}{\text{Total C moles}} \times 100 \quad \text{Eq. (i)}$$

$$\text{Selectivity} = \frac{\text{C moles BD in product}}{\text{Total C moles in product except EtOH and AA}} \times 100 \quad \text{Eq. (ii)}$$

$$\text{BD Yield} = \frac{\text{Total conversion} \times \text{BD Selectivity}}{100} \quad \text{Eq. (iii)}$$

## B2. Catalytic activity of SOMC catalysts

**Table 4.2** shows the total conversion of ethanol (EtOH) and acetaldehyde (AA) and the BD selectivity of all the TaO<sub>x</sub>/SiO<sub>2</sub> pre-catalysts synthesized via the aforementioned two routes by the SOMC protocol. However, detailed discussion on the catalytic behavior has been made only for the pre-catalysts with tantalum loading  $\approx 2$  wt%. Catalytic activity results for the pre-catalysts with tantalum loading  $> 2$  wt% can be seen in **Table 4.2** from **(5)-(10)**. (The reported data has been normalized in order to be comparable with the catalytic results reported in literature. In general a carbon loss of  $\approx 25\%$  has been reported for each of the catalyst)

**Table 4.2-** Catalytic activity of SOMC based catalysts in conversion of EtOH/AA to BD

Catalyst code	% Metal loading	Surface area m <sup>2</sup> /g	% Conversion	BD Selectivity	Selectivity				BD Yield
					Ethylene	Diethyl ether	Ethyl acetate	others	
1. SOMC-I	1.9	171	55.5	86.9	3.8	2.2	2.2	4.8	48.2
2. SOMC-II	2.5	160	37.2	85.9	3.1	1.9	3.0	5.1	31.9
3. SOMC-II-SBA	2.25	971	41.5	85.6	2.7	1.6	3.1	6.0	35.5
4. SOMC-II'	2.0	163	52.0	85.8	3.6	2.2	3.2	4.8	44.7
<b>Reaction conditions-</b> Reaction Temperature 325°C, WHSV = 0.5 g <sub>EtOH/AA</sub> ·g <sub>cat</sub> <sup>-1</sup> ·h <sup>-1</sup> Time on Stream=8hrs, EtOH/AA=2.5:1									
5. SOMC-I <sub>FC</sub>	5.6	163	40.5	69.8	14	13.3	2.1	0.8	28.3
6. SOMC-I <sub>Ta-O-Ta</sub>	8.6	157	67.3	70.5	17	9.8	2	0.7	47.4
7. SOMC-II- <sub>500-FC</sub>	5.6	151	47.9	51.2	15.4	17.6	2	0.7	24.5
8. SOMC-II <sub>FC</sub>	5.1	159	66	63.8	18.9	15.3	1.3	0.8	42.1
9. SOMC-II' <sub>500-FC</sub>	5.8	161	26.8	65.3	14.3	18.3	2	-	17.5
10. SOMC-II' <sub>FC</sub>	5.3	157	42.3	55.5	22.4	19.9	1.5	0.6	23.4
<b>Reaction conditions-</b> Reaction Temperature 325°C, WHSV = 0.5 g <sub>EtOH/AA</sub> ·g <sub>cat</sub> <sup>-1</sup> ·h <sup>-1</sup> Time on Stream=8hrs, EtOH/AA=3.5:1									

*Note-* **Complex 1.2** and **Complex 2.2'** were calcined at 500°C for 10 hrs to give SOMC-II-<sub>500-FC</sub> and SOMC-II'<sub>500-FC</sub> for the purpose of catalytic testing

### B2.1. Comparison of the $[\text{Ta}(=\text{CH}^t\text{Bu})(\text{CH}_2^t\text{Bu})_3]$ based catalysts

**Figure 4.2** shows the total conversion of EtOH/AA for  $[\text{Ta}(=\text{CH}^t\text{Bu})(\text{CH}_2^t\text{Bu})_3]$  based SOMC catalysts over 8hrs time on stream.

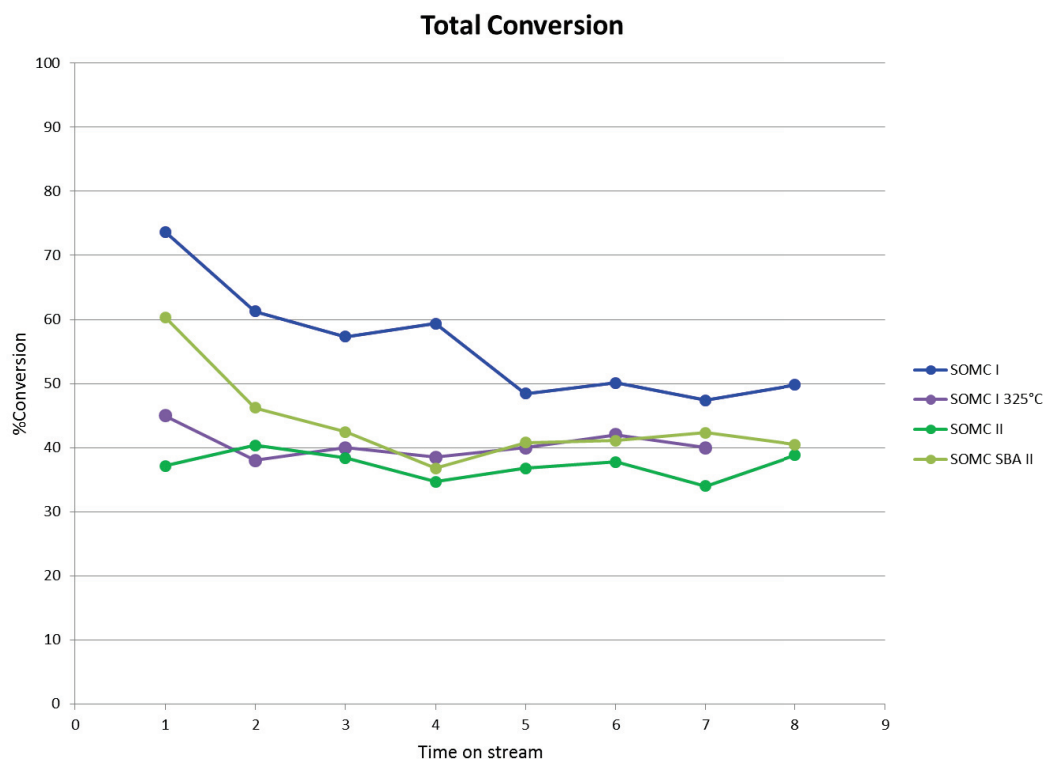


**Figure 4.2-** Total conversion of EtOH/AA for  $[\text{Ta}(=\text{CH}^t\text{Bu})(\text{CH}_2^t\text{Bu})_3]$  based SOMC catalysts over 8hrs time on stream

The largest difference in activity can be observed between the  $\text{N}_2\text{O}$ -oxidized SOMC-I and  $\text{O}_2$ -oxidized SOMC-II.

According to the above figure, for **SOMC-I**, the highest conversions are observed at the start of the catalysis. The values of conversion keep dropping until they become stable after TOS=5hrs. For **SOMC-II** however the conversion values are stable throughout the run of the reaction. As shown in Chapter 2 and 3, the major difference between these two pre-catalysts lies in the presence of mostly isolated  $[(\equiv\text{SiO})_2\text{Ta}(=\text{O})(\text{OH})]$  species in **SOMC-I** versus mostly string like species in **SOMC-II**. This analysis might suggest that the isolated sites on the **SOMC-I** are the active species in conversion of EtOH/AA, which over time tend to evolve into string like species similar to **SOMC-II**.

This evolution of surface species can be better visualized through HRSTEM. **Figure 4.3** shows the representative HRSTEM micrographs of **SOMC-I** before catalysis and after 8 hrs time on stream. Post-catalysis the isolated Ta(V) sites were seen to align in a string like arrangement, similar to the organization witnessed on the surface of **SOMC-II**. For **SOMC-II**, which has been subjected to calcination at 500°C during its synthesis, the surface species remain mostly consistent during the entire run of the reaction. (**Figure 4.4**).

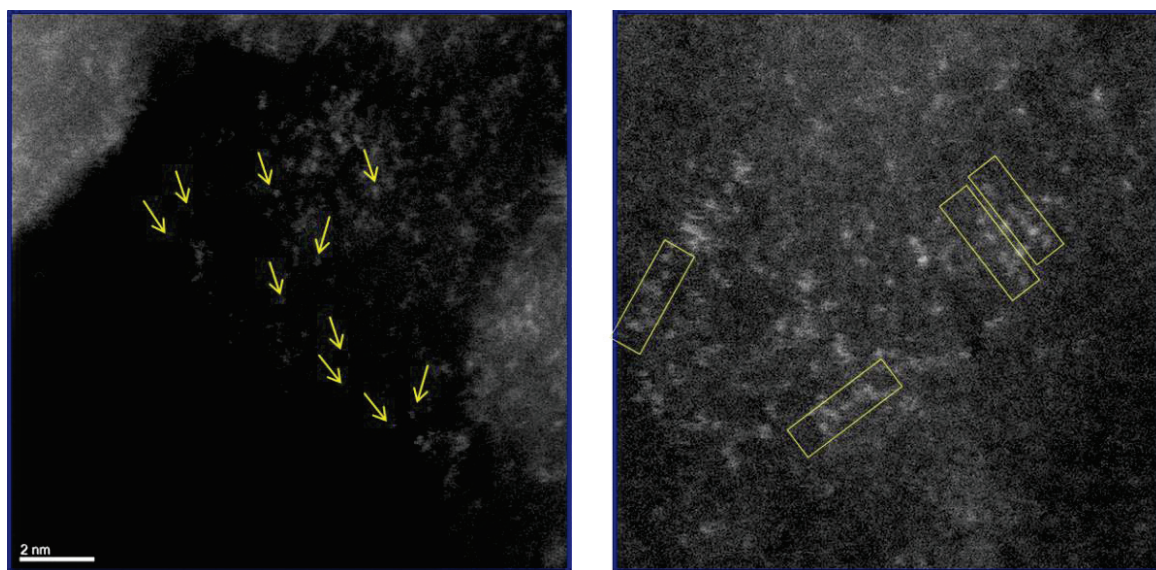


**Figure 4.3-** Representative HRSTEM micrographs of SOMC-I before catalysis and post 8 hrs time on stream

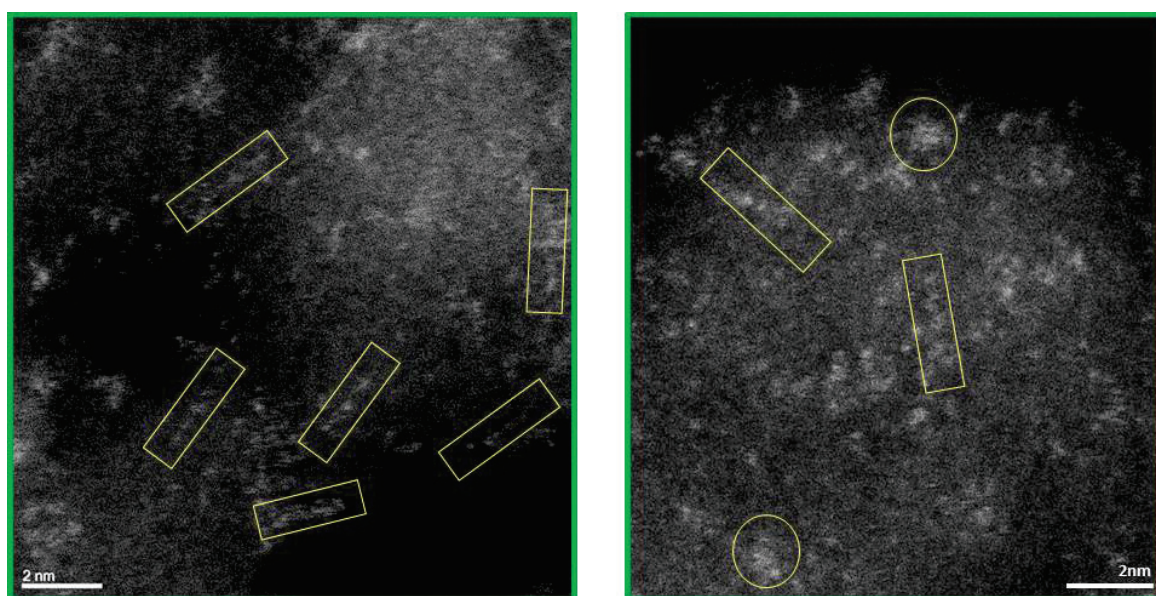


**Figure 4.4-** Representative HRSTEM micrographs of SOMC-II before catalysis and post 8 hr time on stream

To test this hypothesis, we tested the catalytic activity of **SOMC-I** ( $\Delta 325^\circ\text{C}$ ). (See chapter 2). This catalyst, (which is SOMC-I heated at  $325^\circ\text{C}$  for 6hrs) showed catalysis extremely similar to SOMC-II. It is to be noted that HRSTEM micrographs of **SOMC-I** ( $\Delta 325^\circ\text{C}$ ) evidenced aggregation of isolated species into string like and cluster like formations. These results lie in line with the above finding.

Catalytic performance of **SOMC-II-SBA** was also investigated. **SOMC-II-SBA** synthesized by the same strategy as that of **SOMC-II**, represents a catalytic system with better dispersed tantalum active sites by the virtue of larger surface area of SBA-15. The catalyst showed slightly better BD yield of 35.5% as compared to **SOMC-II**. However notably, the catalytic activity was seen to be maximum at the start of the reaction while progressively dropping and reaching a stable value after TOS=5hrs. From preliminary evidence such a drop in activity could be attributed to coalescence of isolated Ta active sites.

### B2.2. Comparison of the $[\text{Ta}(\text{=CH}^t\text{Bu})(\text{CH}_2^t\text{Bu})_3]$ based catalysts with $\text{Ta}(\text{OEt})_5$ based catalysts

**SOMC-II'** was synthesized by grafting tantalum ethoxide as precursor on silica dehydroxylated at  $700^\circ\text{C}$  instead of the organometallic precursor  $[\text{Ta}(\text{=CH}^t\text{Bu})(\text{CH}_2^t\text{Bu})_3]$ . This was followed by calcination under dry  $\text{O}_2$  at  $500^\circ\text{C}$  for 10hrs.

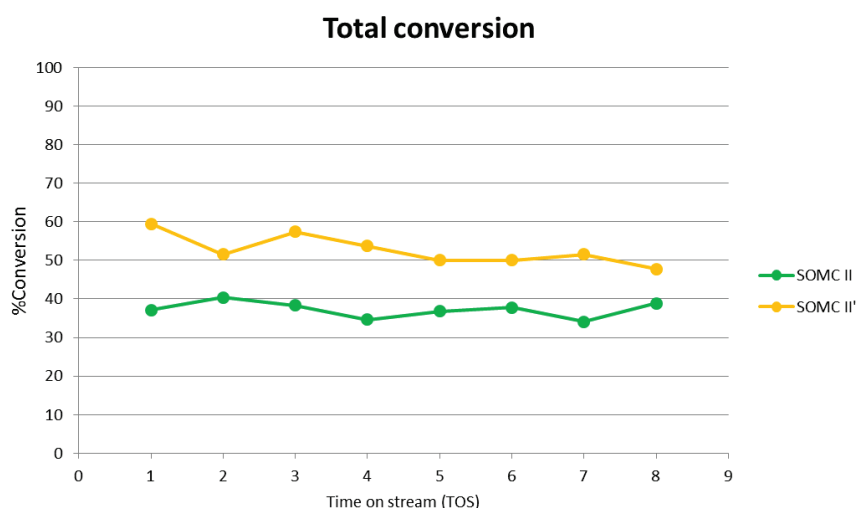


**Figure 4.5-** Total conversion of EtOH/AA for SOMC-II and SOMC-II' 8hrs time on stream

**Figure 4.5** shows the conversion of EtOH/AA over SOMC-II and SOMC-II'. Since the EXAFS analysis of the catalysts (discussed in Chapter 3) did not point towards markedly different surface species, SOMC-II' showed significant improvement in the total conversion. However it is notable that similar to SOMC-II, the conversions remain stable throughout the time on stream for SOMC-II'.

**Figure 4.6** summarizes the catalytic activity of the SOMC catalysts in comparison with the best performing state-of-the-art TaO<sub>x</sub> systems.

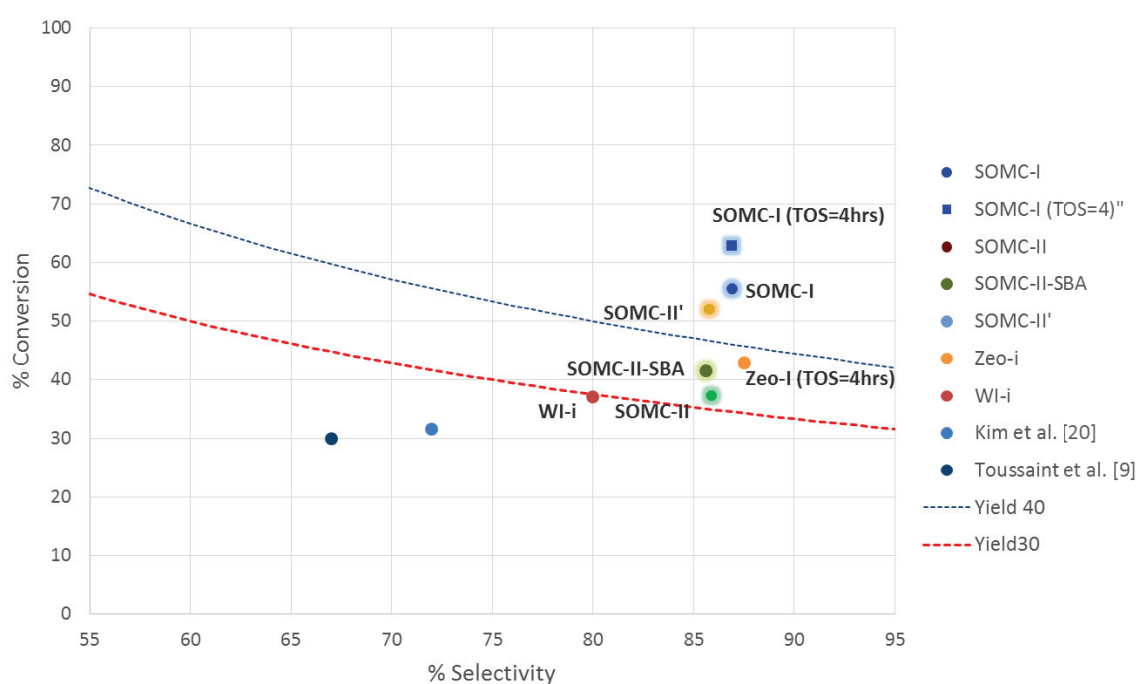
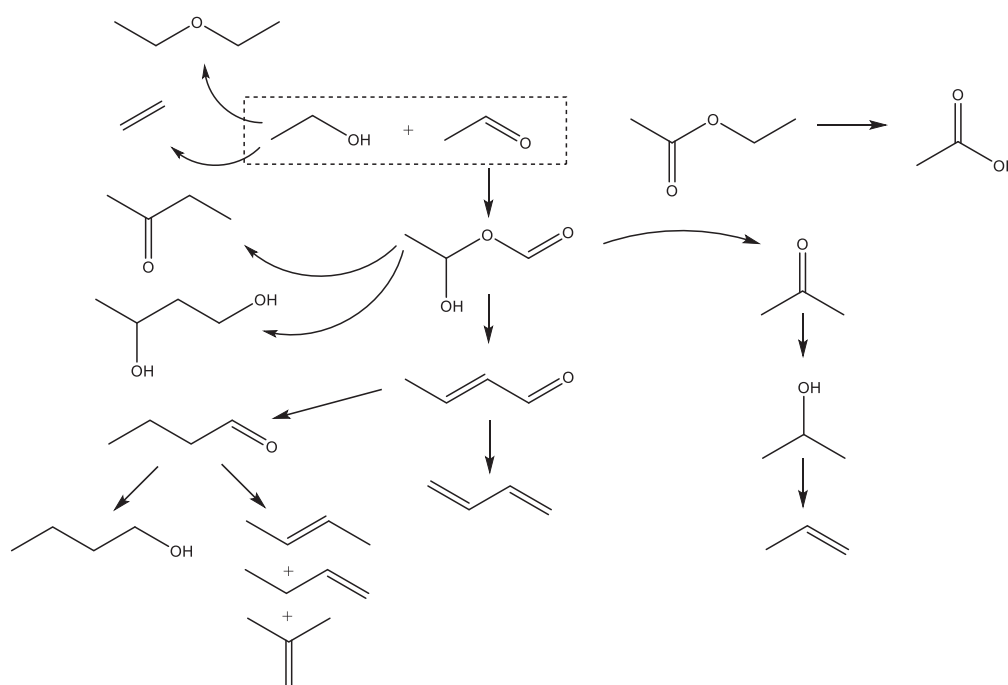


**Figure 4.6-** Catalytic activity of SOMC based catalysts compared to state-of-the-art tantalum based catalysts in conversion of EtOH/AA to BD

### B3. Butadiene selectivity and product distribution

As mentioned earlier, the reaction from ethanol to BD generates several by-products. The product distribution is affected by several factors such as the reaction conditions and the catalytic system. A difference in temperature alters the thermodynamics and kinetics of the process, possibly favoring the formation of byproducts.<sup>4,10,11</sup> (**Scheme 4.1**) However taking into consideration the overall thermodynamics of ETB process, in the temperature range of 325-430°C, BD yield and selectivity are kinetically determined.<sup>12,13</sup> Thus, it is the choice of catalyst that plays a major role in determining the product distribution and BD selectivity.



**Scheme 4.1** -Reaction by-products for EtOH/AA to BD as presented by Quattlebaum et. al<sup>14</sup>

**Figure 4.7** shows the selectivity of **SOMC-I** and **SOMC-II** towards BD monitored over 8hrs time on stream. As it has been discussed before, the two catalysts have different distribution of surface species- **SOMC-I** has predominantly isolated  $[(\equiv\text{SiO})_2\text{Ta}(=\text{O})(\text{H})]$  species whereas **SOMC-II** has a co-existing isolated Ta(V) species along with oligomer like linear arrangement of Ta(V) atoms on its surface. Despite this both the catalysts show extremely similar trends in BD selectivity.

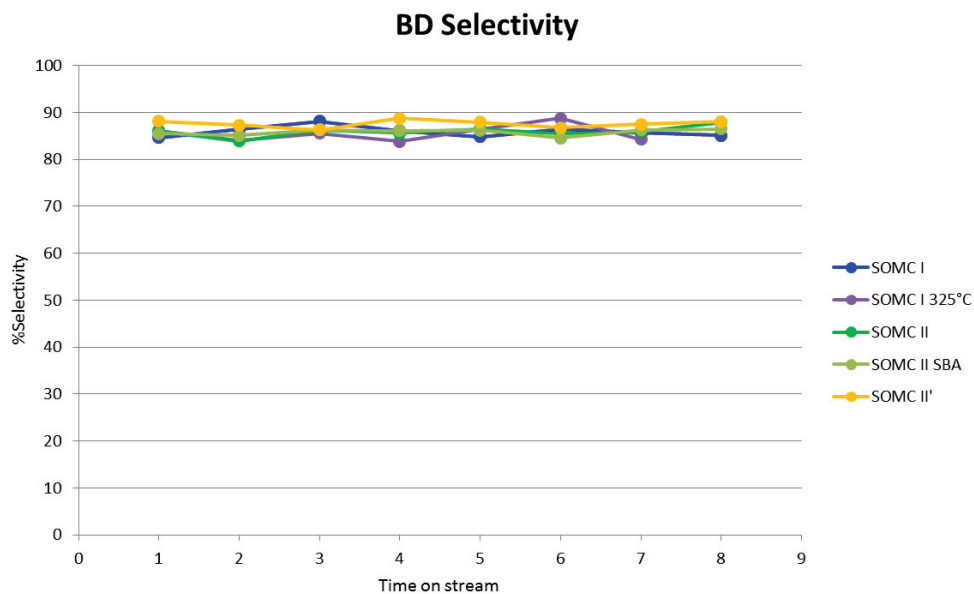


**Figure 4.7** - BD selectivity of SOMC-I and SOMC-II for 8 hrs time on stream

In **Figure 4.8** we see the product distributions for the catalysts in consideration.

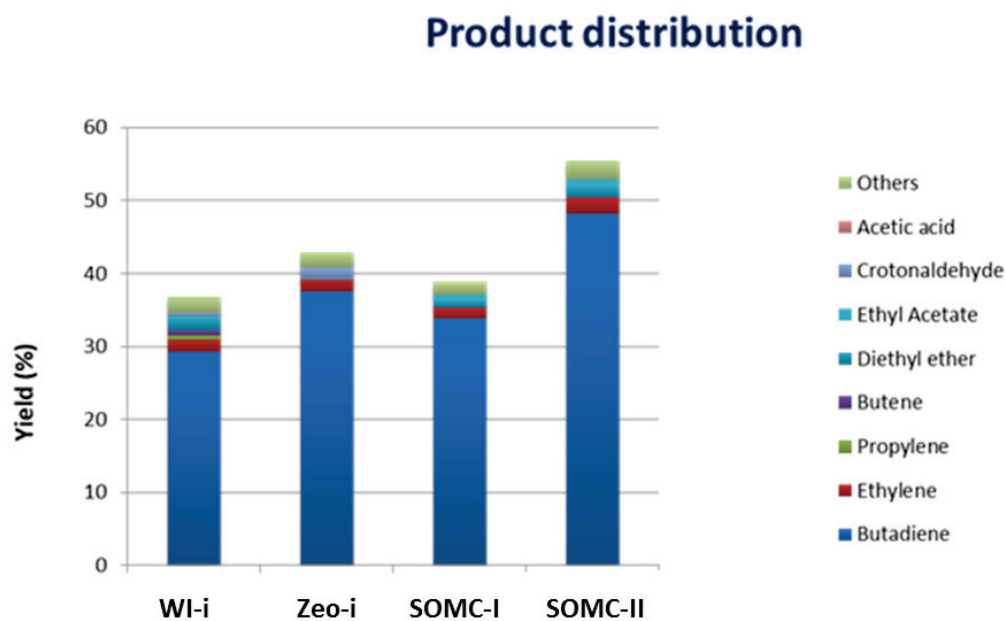


**Figure 4.8** - Product distribution of catalyst in consideration (i) WI-I (ii) Zeo-I (iii) SOMC-I (iv) SOMC-II

Both **SOMC-I** and **SOMC-II** exhibit extremely narrow product distributions. These catalysts represent systems with relatively well-defined and homogeneous surface species. The presence of such surface species can limit the number of alternate reaction pathways thereby suppressing the number of side products. This feature is significant for an industrial catalyst since it prevents wasting carbon in undesirable byproducts while also reducing the steps of separation.

The first observation is that for **WI-i**, a wide range of by-products is generated compared to the other three catalysts. This can be explained by considering the surface species populating the surface of the catalyst. By typical wetness impregnation technique of catalyst synthesis, dispersed metal ions with a variable number of M–O bonds between the support and the metal sites are formed. Such broad distribution of metal coordination environments leads to active sites with varying acid/base properties.<sup>15</sup> These sites can then catalyze numerous side reactions leading to a broad spectrum of reaction products.

#### **B4. Post-catalysis analysis**

Coke formation is believed to be the major culprit for catalyst deactivation in the ETB processes.<sup>5,16–18</sup> Few systematic studies for catalyst deactivation by coke formation could be found for the two step ETB process.

The amounts of coke formation for both spent **SOMC-I** and **SOMC-II** catalysts after 8 h reaction was also observed by TGA analysis (**Figure 4.7**). The weight losses measured by TGA analysis in the temperature range from 250 to 700 °C, which is temperature range for decoking<sup>5</sup>, were 1.53wt% and 1.38wt% for **SOMC-I** and **SOMC-II**, respectively. The lower propensity towards coke formation can be related to the fact that the catalytic reaction does not produce many heavy compounds and would mainly cause deactivation of the catalyst by creation of coke.<sup>16</sup>

Compared to the aforementioned catalysts, the TGA analysis of the spent **SOMC-II-SBA** after 8 hrs time stream evidenced 6.2% coke formation. Chae et al.<sup>5</sup> attributed such coking to the blockage of pores of the mesoporous material by the heavier byproducts produced in the reaction.

## C. General Conclusions

In conclusion, the family of silica supported TaO<sub>x</sub> catalysts synthesized by SOMC techniques were tested in the conversion of EtOH/AA to BD.

Isolated Ta (V) centers act as the primary active sites in the conversion of EtOH/AA to BD while the Ta atoms in a string like organization show considerable but reduced activity in the same transformation. The isolated  $[(\equiv\text{SiO})_2\text{Ta}(=\text{O})(\text{OH})]$  species tend to evolve into more stable tantalum aggregates, possibly with some string-like arrangements.

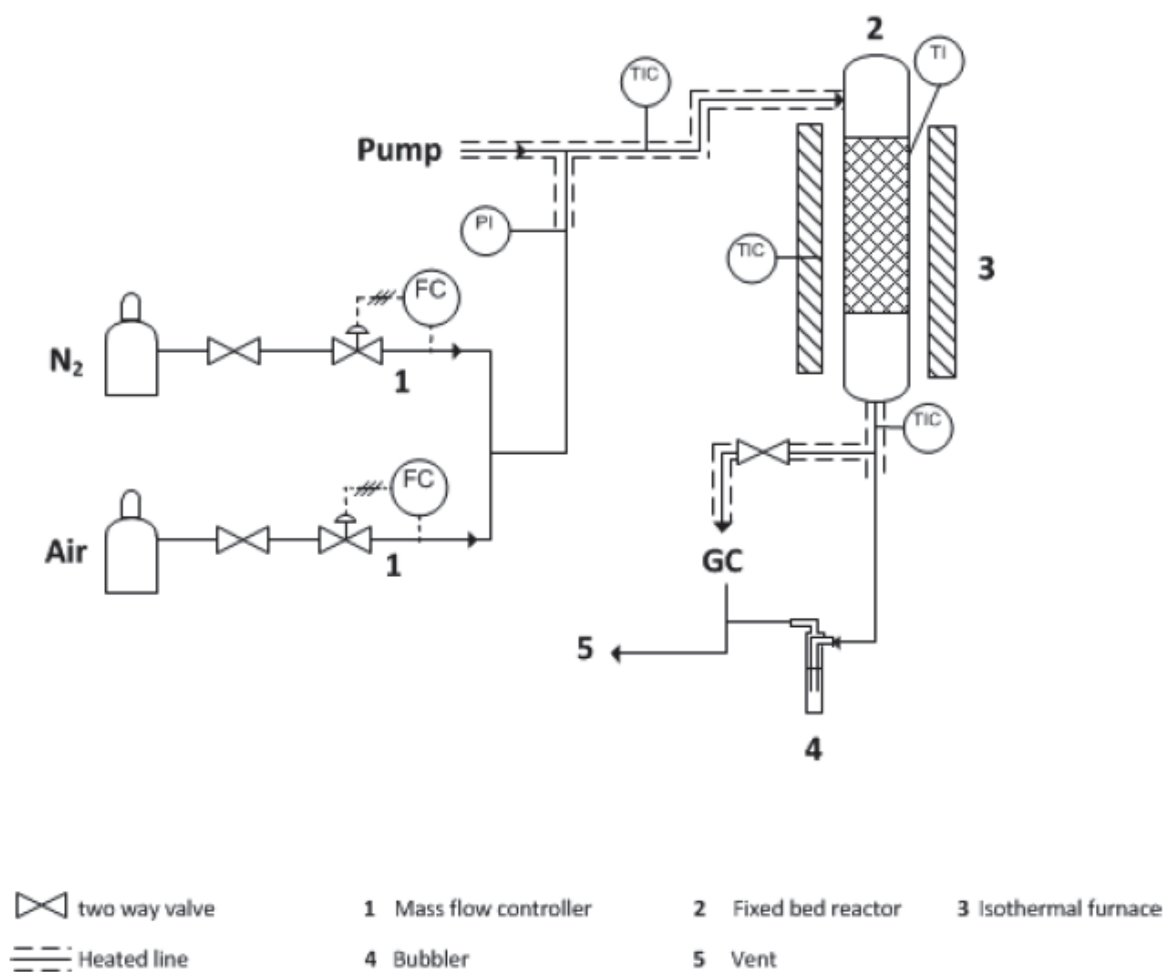
When tested under comparable catalytic testing conditions, SOMC based catalysts show excellent BD selectivity and yield as compared to the best performing Ta-based catalysts in literature. **SOMC-I** with isolated Ta(V) sites exhibits the best performance with BD selectivity of **86.9%** and BD yield of **48.2%**

Both **SOMC-I** and **SOMC-II** exhibit extremely narrow product distribution when compared with catalysts synthesized by conventional wetness impregnation techniques. This emphasizes the importance of molecular control over the surface species of the catalyst.

## D. Experimental details

### D1. General description of catalytic reactor

Reactivity experiments were carried out using a continuous flow reactor, operating under atmospheric pressure. For most of the experiments the Ethanol percent was fixed to a 2% in  $N_2$ . The catalyst amount and flux of the carrier were varied in order to achieve the desired residence time. Downstream products were continuously monitored by online gas chromatography (GC) using an Agilent-6890 instrument equipped with two columns (HP-5 50 m, 0.20 mm and HP-plot  $Al_2O_3$ -KCl 30 m, 0.50 mm) and two detectors (FID and TCD). Compounds were identified by means of GC-MS and then quantified by external standard calibration curve.



**D2. Analysis of coke by Thermo-gravimetric analysis (TGA)**

The thermogravimetric analysis used in this laboratory is a Q50 TGA from TA instruments. The temperature control system includes a circular environment chamber, a sample pan furnace, and a purge gas supply system. In the testing, polymer sample was heated up in the environment chamber which provides a stable temperature environment for a consistent measurement. Purging gas can be provided from both horizontal and vertical directions. The horizontal, 60ml/min flow can be either air or nitrogen depending on the type of decomposition and the specific testing purposes. The vertical, 40ml/min flow always supplies nitrogen to prevent oxidative degradation of the balance elements. In this lab, nitrogen gas was selected for the horizontal flow to prevent additional mass loss due to oxidization of the sample material. The mass loss of the sample was measured with a photodiode balance using a null-balance principle which measures the current required to return the meter to the null position.

## E. References

1. Makshina, E. V. *et al.* Review of old chemistry and new catalytic advances in the on-purpose synthesis of butadiene. *Chem. Soc. Rev.* **43**, 7917–7953 (2014).
2. Makshina, E. V., Janssens, W., Sels, B. F. & Jacobs, P. A. Catalytic study of the conversion of ethanol into 1,3-butadiene. *Catal. Today* **198**, 338–344 (2012).
3. Ochoa, J. V. *et al.* An analysis of the chemical, physical and reactivity features of MgO–SiO<sub>2</sub> catalysts for butadiene synthesis with the Lebedev process. *Green Chem.* **18**, 1653–1663 (2016).
4. Pomalaza, G., Capron, M., Ordonsky, V. & Dumeignil, F. Recent Breakthroughs in the Conversion of Ethanol to Butadiene. *Catalysts* **6**, 203 (2016).
5. Chae, H.-J. *et al.* Butadiene production from bioethanol and acetaldehyde over tantalum oxide-supported ordered mesoporous silica catalysts. *Applied Catal. B, Environ.* **150–151**, 596–604 (2014).
6. Kyriienko, P. I., Larina, O. V., Soloviev, S. O., Orlyk, S. M. & Dzwigaj, S. High selectivity of TaSiBEA zeolite catalysts in 1,3-butadiene production from ethanol and acetaldehyde mixture. *Catal. Commun.* **77**, 123–126 (2016).
7. Xu, Y., Liu, Z., Han, Z. & Zhang, M. Ethanol/acetaldehyde conversion into butadiene over sol–gel ZrO<sub>2</sub>–SiO<sub>2</sub> catalysts doped with ZnO. *RSC Adv.* **7**, 7140–7149 (2017).
8. Jones, M. D. *et al.* Investigations into the conversion of ethanol into 1,3-butadiene. *Catal. Sci. Technol.* **1**, 267–272 (2011).
9. W. M. Quattlebaum, W. J. T. A. J. T. D. *Deoxygenation of Certain Aldehydes and Ketones: Preparation of Butadiene and Styrene.* (1947).
10. Angelici, C., Velthoen, M. E. Z., Weckhuysen, B. M. & Bruijninx, P. C. A. Effect of Preparation Method and CuO Promotion in the Conversion of Ethanol into 1,3-Butadiene over SiO<sub>2</sub>–MgO Catalysts. *ChemSusChem* (2014).
11. Hayashi, Y. *et al.* Experimental and computational studies of the roles of MgO and Zn in talc for the selective formation of 1,3-butadiene in the conversion of ethanol. *Phys. Chem. Chem. Phys.* (2016).
12. Angelici, C., Weckhuysen, B. M. & Bruijninx, P. C. A. Chemocatalytic conversion of ethanol into butadiene and other bulk chemicals. *ChemSusChem* **6**, 1595–1614 (2013).

13. Bhattacharyya, S. K. & Sanyal, S. K. *Kinetic Study on the Mechanism of the Catalytic Conversion of Ethanol to Butadiene. Journal of Catalysis* **7**, (1967).
14. Quattlebaum, W. M., Toussaint, W. J. & Dunn, J. T. Deoxygenation of Certain Aldehydes and Ketones: Preparation of Butadiene and Styrene. *J. Am. Chem. Soc.* **69**, 593–599 (1947).
15. Copéret, C. *et al.* Surface Organometallic and Coordination Chemistry toward Single-Site Heterogeneous Catalysts: Strategies, Methods, Structures, and Activities. *Chemical Reviews* (2016).
16. Kim, T.-W. *et al.* Butadiene production from bioethanol and acetaldehyde over tantalum oxide-supported spherical silica catalysts for circulating fluidized bed. *Chem. Eng. J.* **278**, 217–223 (2015).
17. Liang Cheong, J. *et al.* Highly Active and Selective Zr/MCF Catalyst for Production of 1,3-Butadiene from Ethanol in a Dual Fixed Bed Reactor System. (2016).
18. Angelici, C. *et al.* Ex Situ and Operando Studies on the Role of Copper in Cu-Promoted SiO<sub>2</sub>-MgO Catalysts for the Lebedev Ethanol-to-Butadiene Process. *ACS Catal.* (2015).

# Chapter 5

## Towards catalyst structure activity relationship in transformation of ethanol and acetaldehyde to butadiene

*Chapter 5 attempts to bridge the catalyst characterization studies of the SOMC catalysts (discussed in Chapter 2 and Chapter 3) with their catalytic performance in Ostromyslensky's ethanol to butadiene transformation (studied in Chapter 4) to build a meaningful structure activity relationship.*

*This information has been used to hypothesize a reaction mechanism on the surface of the TaO<sub>x</sub>/SiO<sub>2</sub> SOMC catalysts.*



# Contents

<b>A. Introduction.....</b>	<b>113</b>
<b>B. Results and discussion .....</b>	<b>116</b>
B1. Evaluation of surface acidity of SOMC catalysts and its effect on catalytic performance .....	116
B2. Studying the influence of reaction parameters on catalytic activity .....	119
B2.1. Effect of feed composition on catalytic activity .....	119
B2.1 Effect of contact time on catalytic activity .....	120
B3. Proposed reaction mechanism for transformation of ethanol and acetaldehyde to butadiene .....	121
<b>C. Conclusions.....</b>	<b>124</b>
<b>D. Experimental details .....</b>	<b>125</b>
D1. Evaluation of surface acidity .....	125
D1.1. By Pyridine adsorption desorption.....	125
D1.1. By NH <sub>3</sub> Temperature programmed desorption (NH <sub>3</sub> -TPD).....	126
D2. Surface area by N <sub>2</sub> adsorption desorption isotherms .....	126
<b>E. References.....</b>	<b>130</b>



## A. Introduction

The long history of ETB process has resulted in numerous intensive studies and discussions on the reaction mechanism.<sup>1-5</sup> Early discussions were mostly based on reaction network studies based on the experimental results of catalytic tests using various feed combinations, temperatures and contact times as well as thermodynamic calculations of the proposed mechanisms.<sup>4,6</sup> Most of these studies did not take into consideration the structure of the catalyst in the proposition.<sup>7,8</sup> In the recent years with development in computational tools and spectroscopic characterization techniques there have been significant achievements in explaining the reaction mechanism by employing a combination of *in situ* DRIFT spectroscopy and DFT calculations<sup>1,2,9,10</sup>. Herein the surface of the catalyst has been taken into account to explain the adsorption and desorption of intermediate species involved in the transformation of ethanol to butadiene.

The one step process predominantly utilizes mixed oxide catalysts with a significant basic character and redox sites (for dehydrogenation of ethanol to acetaldehyde). Chiericato et al.<sup>1,2</sup> recently studied the one-step process over basic MgO suggesting a carbanion based mechanism for BD formation.

On the contrary, the two-step process is mostly performed over Lewis acid based catalysts<sup>7,8,11-14</sup>. These catalysts are mainly Group IV and Group V metal oxides supported on silica or zeolites. Though their functionality is not very efficient in dehydrogenation of ethanol to acetaldehyde, they show high activity and selectivity towards BD from mixture of ethanol and acetaldehyde. Lately, significant progress has been made in studying the reaction mechanism of Lewis acid catalyzed coupling of EtOH/AA mixture and more importantly, explaining the catalyst's structure activity relationship.

In 2016, Ivanova et al.<sup>15</sup> while studying Zr/SiBEA catalysts for ETB transformation, made an important observation that 'open' Zr(IV) Lewis acid sites- represented by isolated Zr atoms in tetrahedral positions of the zeolite crystalline structure connected to three -O-Si linkages and one OH group, were the active sites in the process of conversion of ethanol into

butadiene. The so called ‘closed’ sites represented by a Zr atom with four Zr-O-Si linkages contributed to lesser or no activity. (**Figure 5.1**)

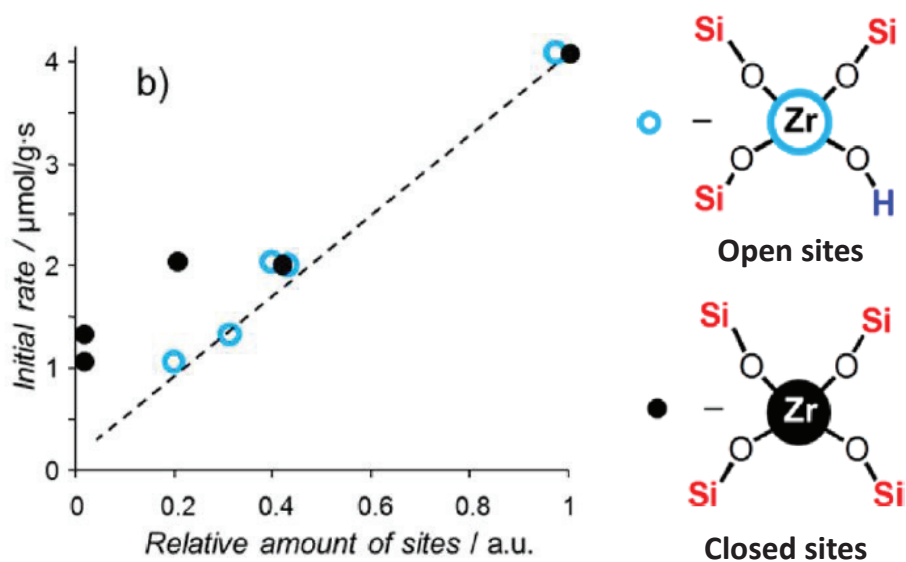


**Figure 5.1-** Relative amount of open and closed Lewis sites determined by FTIR spectroscopy of adsorbed CO versus initial rates of ethanol conversion

The same concept was extended to Ta/SiBEA system in EtOH/AA transformation to BD by Dzwigaj et al.<sup>13,16</sup> These catalysts which were prepared by tantalum incorporation into vacant T-atom sites of the SiBEA zeolites framework<sup>16</sup>, showed better selectivity to BD than conventional catalysts synthesized by wetness impregnation.<sup>14,17</sup> The high selectivity was attributed to the presence of Ta ‘open’ sites in higher concentration. However, DFT calculations on the structural and energy properties of these catalysts found that the substitution of tantalum into the zeolite structure results in numerous Ta reactive sites. (**Figure 5.2**)

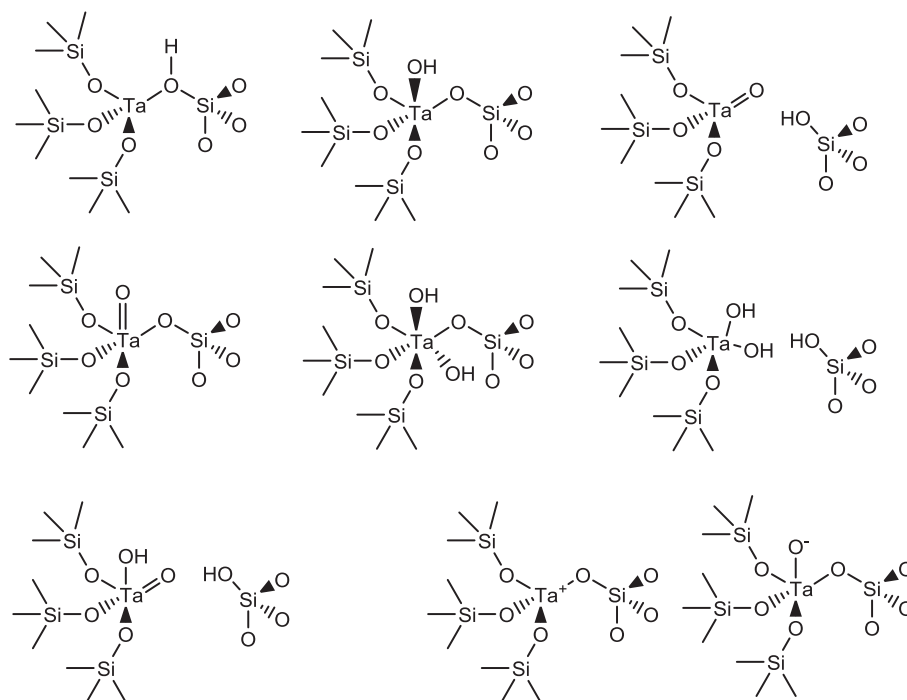


**Figure 5.2**-Environments of the reactive sites studied in on Ta/SiBEA system developed by Dzwigaj et al.<sup>13,16,18</sup>

Using the expertise of SOMC, in Chapter 2 we reported the synthesis of well-defined selectively single site Ta(V) pre-catalysts supported on silica, while in Chapter 3 we synthesized well-defined TaO<sub>x</sub> catalysts with mononuclear, di-nuclear and oligomer-like species. Their catalytic performances in EtOH/AA transformation to BD were evaluated and compared in Chapter 4. Based on this information in this chapter, we attempt to build a meaningful structure activity relationship for TaO<sub>x</sub>/SiO<sub>2</sub> catalysts in EtOH/AA transformation to BD.

## B. Results and Discussions

### B1. Evaluation of surface acidity of SOMC catalysts and its effect on catalytic performance

The spectroscopic study of adsorbed pyridine is an efficient way to determine a catalyst's surface acidity.<sup>19-21</sup> The type of interaction between the adsorbed pyridine and the acid sites on the catalyst surface produces several characteristic IR bands. The frequency of these bands enables one to distinguish between Bronsted (BPy) and Lewis acid sites (LPy). Typical IR absorption bands of pyridine adsorbed on Bronsted acid sites (BPy) are found at around 1491, 1545, 1578, and 1640  $\text{cm}^{-1}$ , while Lewis acidity gives rise to bands (LPy) around 1450, 1491, 1578, and 1612  $\text{cm}^{-1}$ .<sup>19,22,23</sup> The LPy bands at 1450 and 1612  $\text{cm}^{-1}$  are sensitive to the strength of the Lewis acidity.

For pyridine adsorption experiments, samples were pretreated at 150°C under the flow of helium for 30 mins and then a pyridine pulse (0.01 mL) was injected at 50 °C. The temperature was raised till 400 °C. DRIFT spectra were collected for every 100°C rise in temperature.

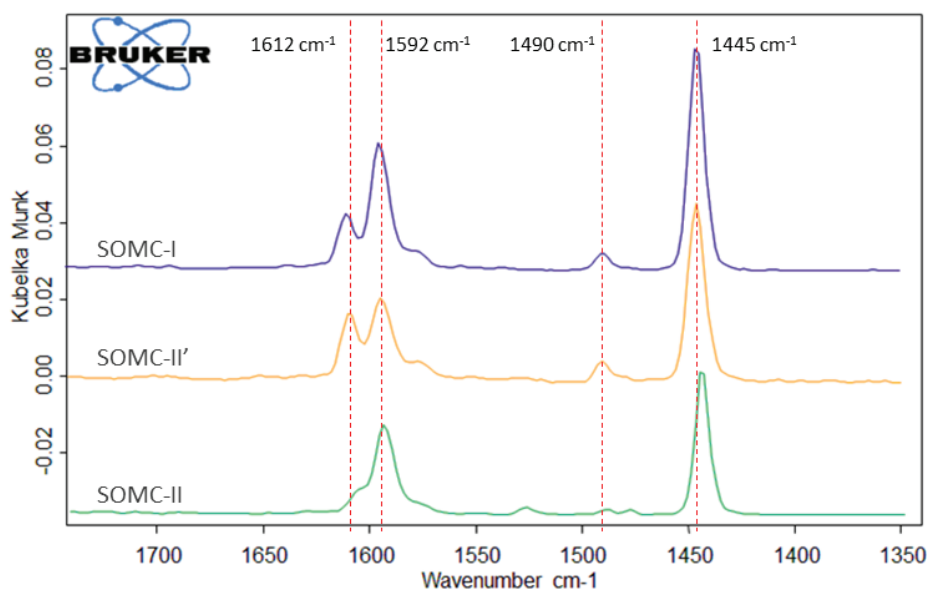


**Figure 5.3-** DRIFT spectra of adsorbed pyridine over SOMC-I, SOMC-II and SOMC-II' catalysts after desorption at 200°C

**Figure 5.3** shows the spectra during desorption on **SOMC-I**, **SOMC-II** and **SOMC-II'** at 200°C. It is clear that for all the catalysts, the dominant acid sites are Lewis type (1445 and 1592  $\text{cm}^{-1}$ ). The proportion of these Lewis acid sites is greater in the case of **SOMC-I** compared to the other two catalysts. **SOMC-I** and **SOMC-II'** also show a band at 1612  $\text{cm}^{-1}$  which can be attributed to the adsorption of pyridine on stronger Lewis sites.<sup>19</sup> In addition to the signals corresponding to Lewis acid sites, a small peak can be observed at 1490  $\text{cm}^{-1}$  for **SOMC-I** and **SOMC-II'**. This peak can be attributed either Lewis or Bronsted acid sites. This band is conspicuously absent in case of **SOMC-II**.

To establish the quantity of acid sites for **SOMC-I** compared to **SOMC-II** a thermal programmed desorption (TPD) using  $\text{NH}_3$  as probe molecule was performed. As shown in **Figure 5.4**,  $\text{NH}_3$  desorption signal was recorded in the range of 50°C to 350°C.

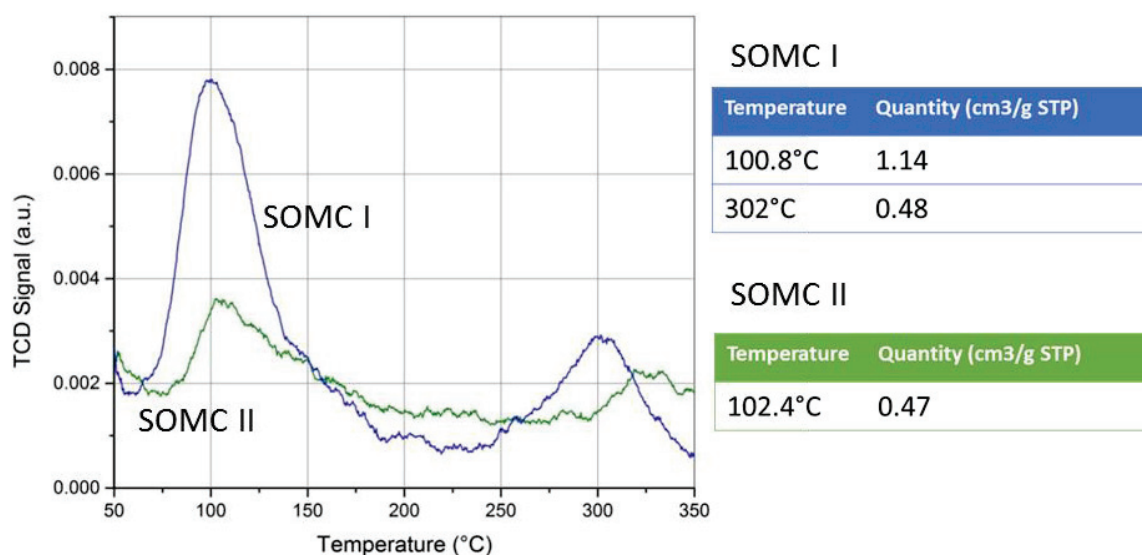


**Figure 5.4-**  $\text{NH}_3$  TPD profiles for SOMC-I (blue) and SOMC-II (green)

Observing the  $\text{NH}_3$ -TPD profiles of samples (**Figure 5.4**) it is possible to state that **SOMC-I** has greater acidity than **SOMC-II**, not only in terms of acid site density but also of strength. For **SOMC-II** a broad desorption band is observed around 100°C. Instead, for **SOMC** in addition to a more intense peak at 100°C, a peak at 302°C is observed. This peak can be indicative of the Bronsted Ta-OH sites on the surface of the catalyst.

The higher Lewis acidity can be attributed to the isolated nature of active sites on the surface of  $N_2O$ -oxidized **SOMC-I**. Indeed while studying a zirconium based system for ETB conversion, Ivanova et al. correlated the strength of Lewis acidity to the presence of isolated Zr atoms with one open hydroxyl functionality. It can be argued that the higher surface acidity can also be a result of better steric availability of the isolated Ta sites.

The difference in surface acidity of all the above mentioned catalysts was clearly reflected in the distribution of reaction by-products. **SOMC-I** and **SOMC-II'** both show markedly higher propensity towards formation of ethylene and diethylether when compared to **SOMC-II**. **Figure 5.5** shows the selectivity towards the different reaction by-products for 8 hrs time on stream in the EtOH/AA conversion to BD.

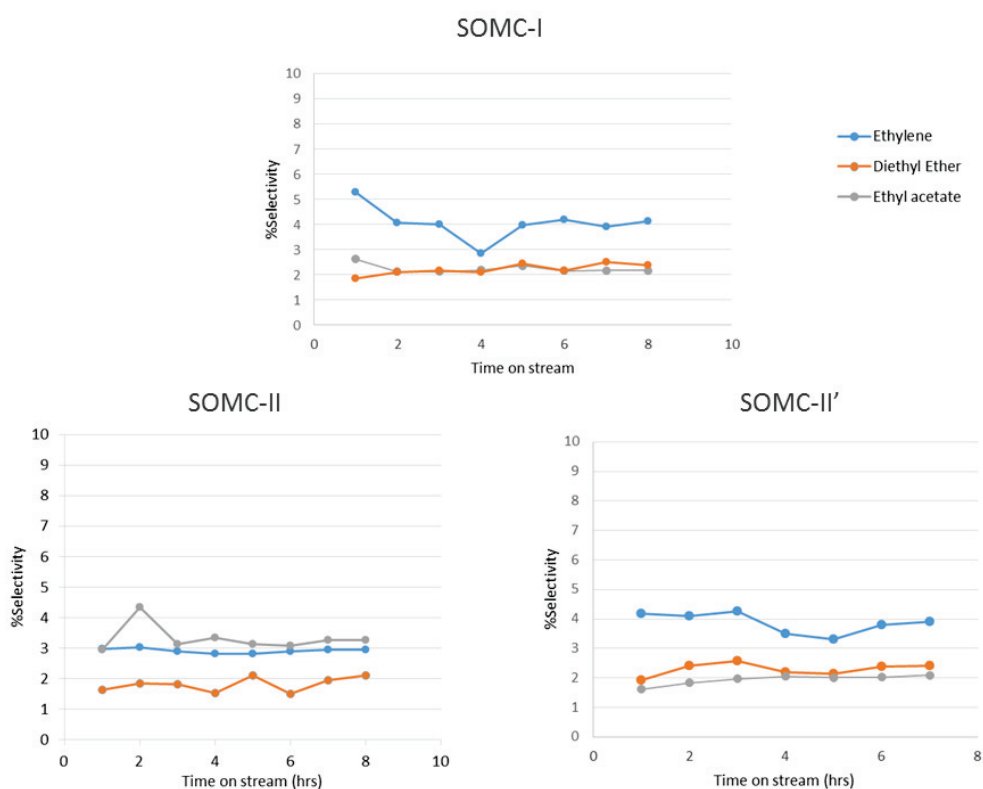


**Figure 5.5-** FTIR spectra of adsorbed pyridine over SOMC-I, SOMC-II and SOMC-II' catalysts after desorption at 200°C

It is notable that for all the above mentioned catalysts surface acidity can be directly correlated to the overall BD yield. **SOMC-I** and **SOMC-II'** which represent the catalytic systems with highest surface acidity perform significantly better compared to **SOMC-II**.

These findings illustrate the potential of SOMC technique in developing material with tunable surface properties via adjusting the nature and the number of surface active sites.

## B2. Studying the influence of reaction parameters on catalytic activity

### B2.1. Effect of feed composition on catalytic activity

The effect of molar ratio of EtOH/AA on the BD selectivity and yield was studied. (**Figure 5.6**)

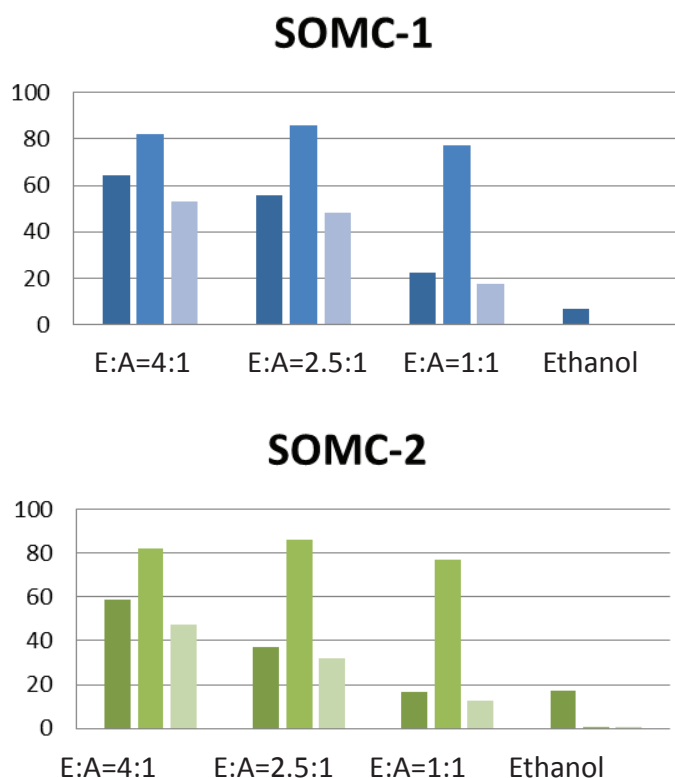


**Figure 5.6-** The effect of molar ratio of EtOH/AA on the BD selectivity and yield was studied

- For both the catalysts, increasing the EtOH/AA ratio, mostly led to decrease in BD selectivity. This can be explained by the fact that increasing the amount of ethanol in the feed accelerates its dehydration to ethylene and diethyl ether, thereby suppressing the overall selectivity towards butadiene.
- By feeding only EtOH, both the pre-catalysts SOMC-1 and SOMC-2 do not show significant conversion to BD. This is not surprising since the catalysts are predominantly acidic and lack sufficient basic character or redox sites to promote AA formation from EtOH.
- Reducing the EtOH/AA ration from 2.5:1 to 1:1 exhibited a slight decrease in BD selectivity. This observation is in tune with the studies in literature.<sup>24</sup> At EtOH:AA ratio of 1:1, the amount of EtOH in the feed is not enough to complete the MPV reduction of crotonaldehyde to crotyl alcohol (which will subsequently dehydrate to BD)

## B2.2. Effect of residence time on catalytic activity

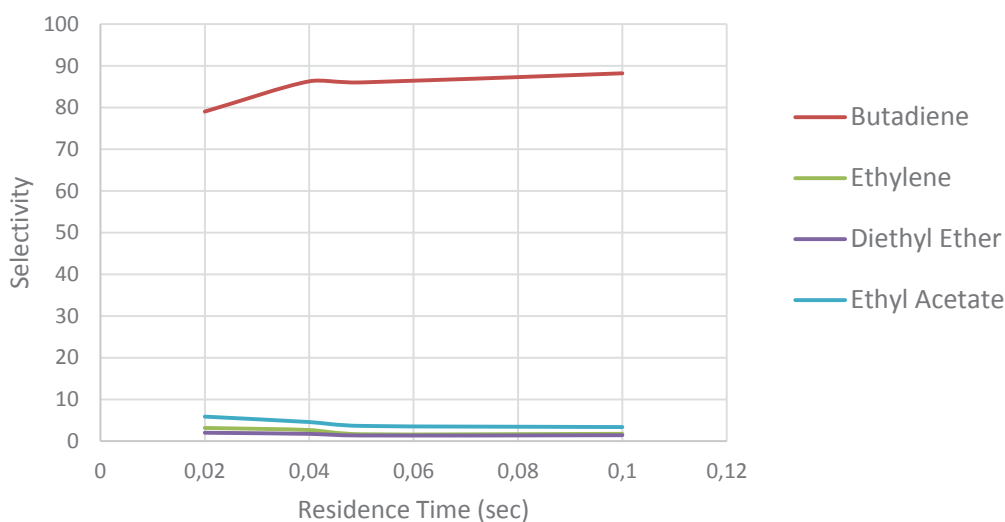


**Figure 5.7-** Effect of WHSV on EtOH/AA conversion to BD

The effect of residence time of EtOH/AA mixture was studied by changing the reactant flow rate. Generally stating, the change of residence time mostly led to a great difference of the conversion.<sup>24</sup> This law was consistent with our experiment. As showed in **Figure 5.7**, despite the increase of residence time, the selectivity of BD, ethylene, diethyl ether and ethyl acetate had little change, while the total conversion had a decreasing trend.

#### **B4. Proposed reaction mechanism for transformation of ethanol and acetaldehyde to butadiene**

The nature and distribution of active sites on the surface of TaO<sub>x</sub>/SiO<sub>2</sub> catalysts is not straightforward. However with the SOMC protocol we could tailor catalysts with well defined surface TaO<sub>x</sub> species. In Chapter 4 from the study of structure activity relationship of the catalysts, we proposed that isolated Ta (V) centres act as the primary active sites in conversion of EtOH/AA to BD by Ostromyslensky process. This conclusion was in line with the findings of Ivanova et al.<sup>15</sup> who while studying ZrO<sub>2</sub>/SiO<sub>2</sub> catalysts for the one step process proposed that isolated Zr atoms in tetrahedral positions of connected to three –O–Si linkages and one OH group, were the active sites in the process of conversion of ethanol into BD. Therefore for simplicity in discussing the possible mechanism, we consider [(≡SiO)<sub>2</sub>Ta(=O)(OH)] as the only active center for transformation.

In order to understand the interaction of ethanol with the surface of the catalyst, experiments were performed by adsorbing ethanol at 50 °C, heating it up to 350 °C. The spectrum of the catalyst was subtracted at each temperature, so that the observed bands correspond to the surface species created by ethanol adsorption and possibly transformation. (**Figure 5.8**)

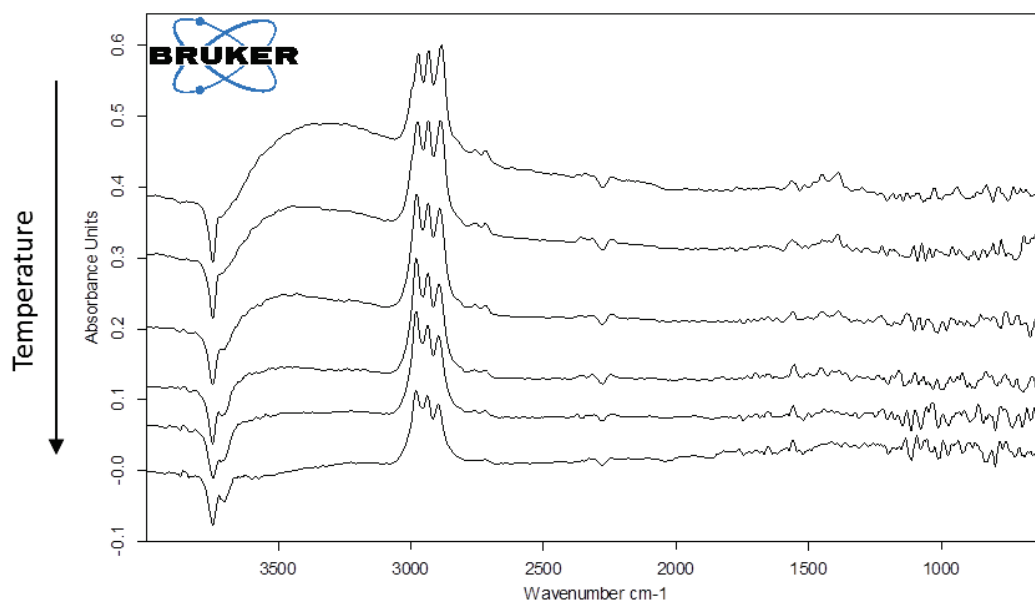


**Figure 5.8-** In situ DRIFTS spectra acquired of ethanol adsorbed on SOMC-I catalyst from 50-350°C in 3200 to 1000  $\text{cm}^{-1}$  spectral region

With increase in temperature, the spectra of the catalyst after ethanol adsorption clearly showed two negative peaks around  $3747\text{cm}^{-1}$  and  $3721\text{cm}^{-1}$ . These peaks can be attributed Si-OH and Ta-OH sites, signaling their consumption. Unfortunately, due to a low signal-to-noise ratio the peaks corresponding to the intermediates formed due to interaction of ethanol with the catalyst could not be observed.

Following this experiment, the same DRIFT study was repeated by adsorbing a EtOH/AA mixture (2.5:1 molar ratio), was adsorbed on the surface of the catalyst and then the catalyst was heated up to  $350^\circ\text{C}$ . As in the case of ethanol, two negative peaks appear in the OH region indicating consumption of both Si-OH and Ta-OH sites. Additionally in this case a broad peak is observed in the region of  $3200\text{cm}^{-1}$  to  $3600\text{cm}^{-1}$  suggesting formation of water. Upon desorption of the adsorbed ethanol and acetaldehyde at  $350^\circ\text{C}$ , two peaks became apparent at  $1562\text{cm}^{-1}$  and  $1461\text{cm}^{-1}$ . These vibrations could be from the reaction products of adsorbed ethanol and acetaldehyde. As previously assigned by Taifan et al.<sup>10</sup>, these two peaks could be attributed to C=C stretch ( $1575\text{ cm}^{-1}$ ) and the bending modes of  $\text{CH}_2$  or  $\text{CH}_3$

(1440  $\text{cm}^{-1}$ ) arising from the  $\text{C}_4$  intermediates with some contributions from surface enolates and polymerized acetaldehyde. (**Figure 5.9**)

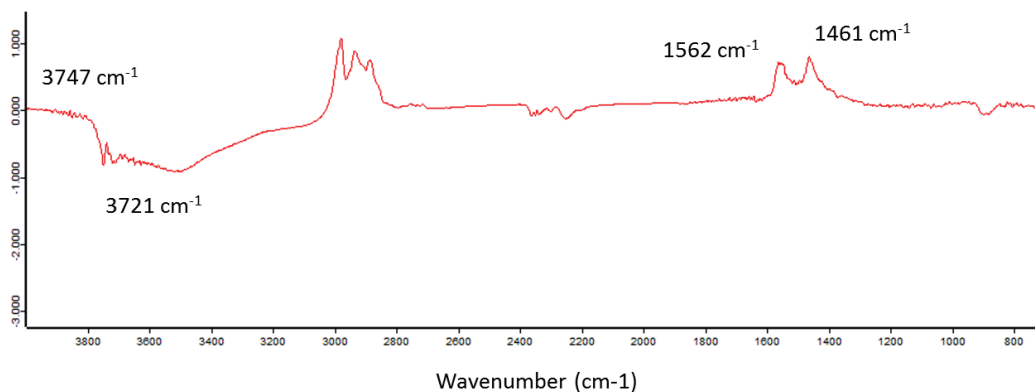


**Figure 5.9-** DRIFTS spectrum acquired of EtOH/AA (2.5:1) adsorbed on SOMC-I catalyst at 350°C

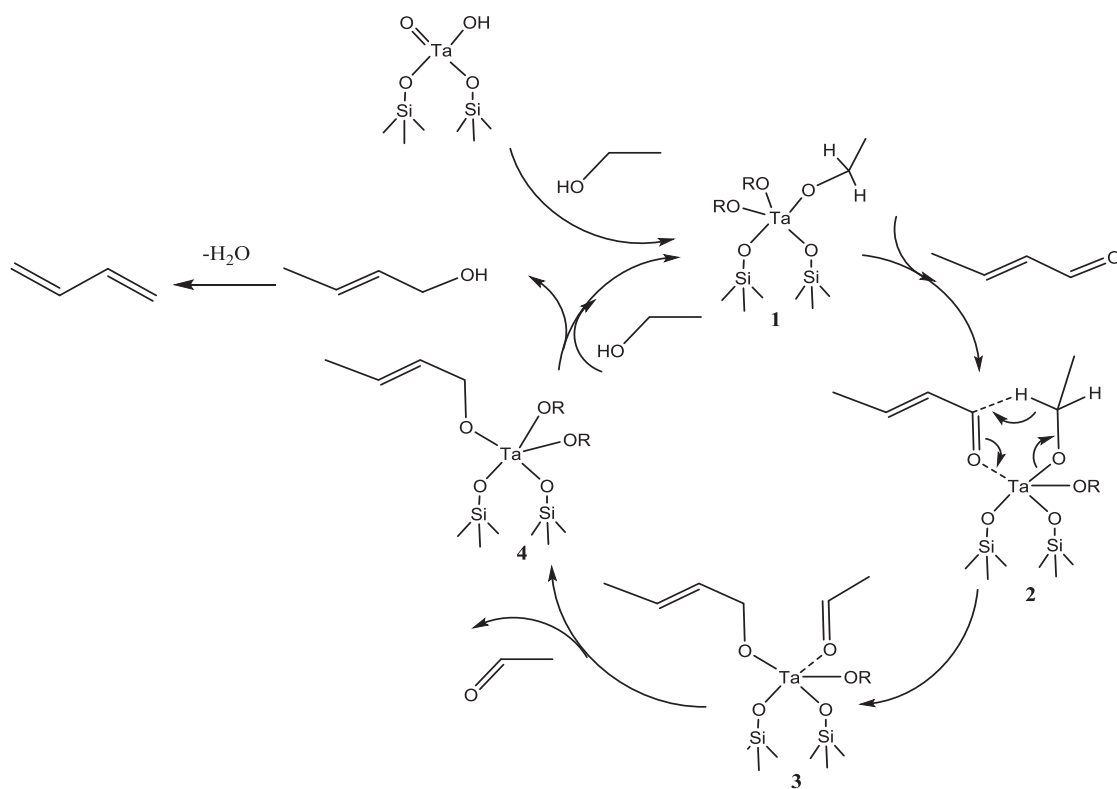
The next step was to investigate the C-C coupling reaction over the catalyst **SOMC-I** to form the  $\text{C}_4$  molecules. To this end a reaction a gas phase reaction between  $\text{CD}_3\text{OD}$  and  $\text{CH}_3\text{CHO}$  was studied over the catalyst at 325°C under batch conditions. After two hours, the gas phase was analysed by GC-MS. The mass spectra revealed the formation of mono-deuterated butadiene, showing that the  $\text{C}_4$  molecule is formed via coupling of two molecules of acetaldehyde. This is consistent with the generally accepted Kagan mechanism.

As discussed earlier the Kagan mechanism proceeds via five preliminary steps- (i) acetaldehyde formation from Ethanol (ii) aldol condensation of acetaldehyde to acetaldol (iii) dehydration of acetaldol to crotonaldehyde (iv) Meerwein-Ponndorf-Verley Reaction between crotonaldehyde and ethanol to obtain crotyl alcohol and acetaldehyde (v) dehydration of crotyl alcohol to butadiene.

Meerwein-Ponndorf-Verley Reaction between crotonaldehyde and ethanol is thought to be catalysed by tantalum.<sup>25,26</sup> It is known from the point of view of organometallic chemistry that ethanolsis of tantalum oxo hydroxo specie will generate ethoxy species on tantalum (**1**) and producing water as a byproduct. This could be seen by DRIFT study of ethanol

desorption. In the next step, crotonaldehyde can coordinate to the Ta site, leading to intermediate **2**. The reaction would then go through a six-membered ring transition state, where hydrogen transfer from ethanol leads to the generation of enolate specie (**3**) and an adsorbed acetaldehyde (which can then desorb from the site and potentially undergo coupling with another acetaldehyde). The formation of enolate specie was evidenced in the DRIFT spectra for EtOH/AA adsorption at 350°C.

An incoming ethanol molecule can then displace crotyl alcohol from the active site, closing the catalytic cycle. **Scheme 5.1** shows the proposed reaction mechanism for MPV reduction over the Ta(V) site of SOMC-I.



**Scheme 5.1-** Proposed and hypothesized reaction mechanism for MPV reduction over the Ta(V) site of SOMC-I

## C. General conclusion

In this chapter we focused on studying the effect of catalyst properties on catalytic activity. Studying the effect of type and amount of acidic sites on the catalyst surface, it was concluded that a small proportion of Bronsted acid sites along with the Lewis acid sites were beneficial in the conversion of EtOH/AA to BD. The most performing catalyst **SOMC-I** showed the highest acidity. The higher surface acidity could be a result of better steric availability of the isolated Ta sites.

The effect of molar ratio of EtOH/AA on the BD selectivity and yield was studied for SOMC-I and SOMC-II. For both the catalysts, increasing the EtOH/AA ratio, mostly led to decrease in BD selectivity. The catalysts did not show significant activity in transformation of only EtOH to BD.

Also, assuming isolated  $[(\equiv\text{SiO})_2\text{Ta}(=\text{O})(\text{H})]$  to be the active site in the transformation of EtOH/AA to BD, an attempt was made to understand the mechanism of the reaction on the surface of SOMC-I. The Meerwein-Ponndorf-Verley Reaction between crotonaldehyde and ethanol is thought to be catalysed by tantalum. Based on in-situ DRIFT experiments for adsorption of (i) ethanol and (ii) a mixture of ethanol and acetaldehyde on the surface of the catalyst at 350°C, a mechanism was hypothesized for the reduction of adsorbed crotonaldehyde by the hydrogen from ethanol on the isolated Ta (V) center.

## **D. Experimental details**

### **D1. Evaluation of surface acidity**

#### **D1.1. By Pyridine adsorption desorption**

For pyridine adsorption experiments, samples were pretreated and the pyridine pulse (0.01 mL) was injected at 50 °C, then temperature was raised to 400 °C. The IR apparatus used was a Bruker Vertex 70 with a Pike Diffuse IR cell attachment. Spectra were recorded using a MCT detector after 128 scans and 2 cm<sup>-1</sup> resolution. The mass spectrometer used was an EcoSys-P from European Spectrometry Systems.

#### **D1.2. By NH<sub>3</sub> Temperature programmed desorption (NH<sub>3</sub>-TPD)**

NH<sub>3</sub>-temperature-programmed desorption (TPD) measurements were obtained with a TPD/TPR/TPO Micromeritics instrument. 50–100 mg of catalysts were pre-treated at the calcination temperature for 1 h under a He flow. After cooling down to 80 °C, NH<sub>3</sub> was adsorbed by flowing of a 10% NH<sub>3</sub> in He gas mixture for 30 min (30 mL min<sup>-1</sup>, NTP), with subsequent He treatment at 80 °C for 15 min to remove physisorbed molecules.

Catalysts were then heated under He flow (50 mL min<sup>-1</sup>, NTP) at a heating rate of 10 °Cmin<sup>-1</sup> up to the calcination temperature.

### **D2. Surface area by N<sub>2</sub> adsorption desorption isotherms**

The specific surface area was measured applying the single point BET method. The instrument used for this analysis was a Carlo Erba Sorpty 1700. The BET method (Brunauer Emmet Teller) calculates the surface area of the sample from the volume of the gas corresponding to the monolayer adsorption. The single-point approximation consists in the measurement of the pressure of adsorption and the corresponding gas volume adsorbed. In the analysis around 0.5g of the sample was placed inside the sample holder and then heated at 150°C under vacuum (4 Pa) in order for it release the water, air or other molecules adsorbed. Afterwards the sample was put in liquid nitrogen and the adsorption of the gaseous N<sub>2</sub> was carried out.



## E.References

1. Chierigato, A. *et al.* On the Chemistry of Ethanol on Basic Oxides: Revising Mechanisms and Intermediates in the Lebedev and Guerbet reactions. *ChemSusChem* **8**, 377–388 (2015).
2. Ochoa, J. V. *et al.* An analysis of the chemical, physical and reactivity features of MgO–SiO<sub>2</sub> catalysts for butadiene synthesis with the Lebedev process. *Green Chem.* **18**, 1653–1663 (2016).
3. Sushkevich, V. L., Ivanova, I. I., Ordonsky, V. V. & Taarning, E. Design of a Metal-Promoted Oxide Catalyst for the Selective Synthesis of Butadiene from Ethanol. *ChemSusChem* (2014). doi:10.1002/cssc.201402346
4. Bhattacharyya, S. K. & Sanyal, S. K. Kinetic Study on the Mechanism of the Catalytic Conversion of Ethanol to Butadiene. *Journal of Catalysis* **7**, (1967).
5. Quattlebaum, W. M., Toussaint, W. J. & Dunn, J. T. Deoxygenation of Certain Aldehydes and Ketones: Preparation of Butadiene and Styrene. *J. Am. Chem. Soc.* **69**, 593–599 (1947).
6. Angelici, C., Weckhuysen, B. M. & Bruijninx, P. C. A. Chemocatalytic Conversion of Ethanol into Butadiene and Other Bulk Chemicals. *ChemSusChem* **6**, 1595–1614 (2013).
7. Makshina, E. V. *et al.* Review of old chemistry and new catalytic advances in the on-purpose synthesis of butadiene. *Chem. Soc. Rev.* **43**, 7917–7953 (2014).
8. Pomalaza, G., Capron, M., Ordonsky, V. & Dumeignil, F. Recent Breakthroughs in the Conversion of Ethanol to Butadiene. *Catalysts* **6**, 203 (2016).
9. Ordonsky, V. V, Sushkevich, V. L. & Ivanova, I. I. Study of acetaldehyde condensation chemistry over magnesia and zirconia supported on silica. *Journal Mol. Catal. A, Chem.* **333**, 85–93 (2010).
10. Taifan, W., Yan, G. X. & Baltrusaitis, J. Surface chemistry of MgO/SiO<sub>2</sub> catalysts during the ethanol catalytic conversion to 1,3-butadiene: in situ DRIFTS and DFT study. *Catal. Sci. Technol.* **7**, 4648–4668 (2017).
11. Jones, M. D. *et al.* Investigations into the conversion of ethanol into 1,3-butadiene. *Catal. Sci. Technol. Catal. Sci. Technol* **1**, 267–272 (2011).
12. Kyriienko, P. I. *et al.* Effect of the niobium state on the properties of NbSiBEA as bifunctional catalysts for gas- and liquid-phase tandem processes. *Journal Mol. Catal. A, Chem.* **424**, 27–36 (2016).
13. Kyriienko, P. I., Larina, O. V., Soloviev, S. O., Orlyk, S. M. & Dzwigaj, S. High selectivity of TaSiBEA zeolite catalysts in 1,3-butadiene production from ethanol and

- acetaldehyde mixture. *Catal. Commun.* **77**, 123–126 (2016).
14. Kim, T.-W. *et al.* Butadiene production from bioethanol and acetaldehyde over tantalum oxide-supported spherical silica catalysts for circulating fluidized bed. *Chem. Eng. J.* **278**, 217–223 (2015).
  15. Sushkevich, V. L., Palagin, D. & Ivanova, I. I. With Open Arms: Open Sites of ZrBEA Zeolite Facilitate Selective Synthesis of Butadiene from Ethanol. *ACS Catal.* **5**, 4833–4836 (2015).
  16. Dzwigaj, S., Yannick, M. & Che, M. Ta(V)-Single Site BEA Zeolite by Two-Step Postsynthesis Method: Preparation and Characterization. *Catal Lett.* **135**, 169–174 (2010).
  17. Kim, T. W. *et al.* Butadiene production from bioethanol and acetaldehyde over tantalum oxide-supported spherical silica catalysts for circulating fluidized bed. *Chem. Eng. J.* **278**, 217–223 (2015).
  18. Tielens, F., Shishido, T. & Dzwigaj, S. What Do Tantalum Framework Sites Look Like in Zeolites? A Combined Theoretical and Experimental Investigation. *J. Phys. Chem.* **114**, 9923–9930 (2010).
  19. Busca, G. The surface acidity of solid oxides and its characterization by IR spectroscopic methods. An attempt at systematization. *Phys. Chem. Chem. Phys.* **1**, 723–736 (1999).
  20. Barzetti, T., Selli, E., Moscotti, D. & Forni, L. *Pyridine and ammonia as probes for FTIR analysis of solid acid catalysts.*
  21. Chen, Y., Fierro, J. L. G., Tanaka, T. & Wachs, I. E. Supported Tantalum Oxide Catalysts: Synthesis, Physical Characterization, and Methanol Oxidation Chemical Probe Reaction. *J. Phys. Chem. B* **107**, 5243–5250 (2003).
  22. Datka, J., Turek, A. M., Jehng, J. M. & Wachs, I. E. *Acidic Properties of Supported Niobium Oxide Catalysts: An Infrared Spectroscopy Investigation.* *JOURNAL OF CATALYSIS* **135**, (1992).
  23. Baltes, M. *et al.* Supported Tantalum Oxide and Supported Vanadia-tantala Mixed Oxides: Structural Characterization and Surface Properties. *J. Phys. Chem. B.* **105**, 6211–6220 (2001).
  24. Han, Z., Li, X., Zhang, M., Liu, Z. & Gao, M. SI for Sol-gel synthesis of ZrO<sub>2</sub>-SiO<sub>2</sub> catalysts for the transformation of bioethanol and acetaldehyde into 1,3-butadiene. *RSC Adv.* 103982–103988 (2015).
  25. Corson, B. B., Jones, H. E., Welling, C. E., Hinckley, J. A. & Stahly, E. E. Butadiene from Ethyl Alcohol. Catalysis in the One-and Two-Stop Processes. *Industrial & Engineering Chemistry* **42**, (UTC, 1950).

## Chapter 1

26. Müller, P. *et al.* Mechanistic Study on the Lewis Acid Catalyzed Synthesis of 1,3-Butadiene over Ta-BEA Using Modulated Operando DRIFTS-MS. *ACS Catal.* **6**, 6823–6832 (2016).

## General Conclusions

Surface organometallic chemistry (SOMC) has provided valuable tools in bridging the gap between homogeneous and heterogeneous catalysts by designing well-defined single site heterogeneous surface complexes. In the past these well-defined catalysts have been known to catalyze various reactions like alkane metathesis, olefin metathesis, alkene polymerization etc with excellent results. The aim of this project was to utilize this expertise of SOMC to develop catalysts for the on-purpose synthesis of butadiene by Ostromyslensky's two step process.

Ta (V)/SiO<sub>2</sub> represents one of the most studied systems for this transformation i.e conversion of EtOH/AA to BD. Most of the prior catalytic systems studied in literature employ the conventional technique of solvent impregnation followed by calcination to generate TaO<sub>x</sub>/SiO<sub>2</sub> catalysts. By their nature such systems face the major drawback of having numerous kinds of surface species and in many cases low concentration of the active species. Therefore need was felt for a higher control over the surface structures that can lead to a more selective and active catalysis. Such study was anticipated to provide insights into identification of active specie in the transformation as well as in establishing the structure activity relationship for TaO<sub>x</sub>/SiO<sub>2</sub> systems.

In this endeavor our strategy was to synthesize and thoroughly characterize a family of well-defined Ta-based silica-supported catalysts through SOMC with varying tantalum nuclearity and to evaluate and analyze their performance in the EtOH/AA to BD conversion.

In **Chapter 2** a novel route to selectively tailor isolated single site Ta (V) species on the surface of silica was discussed. In this strategy, previously studied [(≡SiO)<sub>2</sub>Ta(H)<sub>x=1,3</sub>] were synthesized on the surface of silica dehydroxylated at 500°C according to the procedure discussed in literature. The formation of these species could be verified by IR and NMR spectroscopies. Also for the first time HRSTEM of microscopy of this material was conducted which provided an additional proof of the tantalum moieties being isolated and single site. These species were then subjected to mild oxidation with excess N<sub>2</sub>O at room temperature. The following material was characterized by IR and NMR spectroscopy as well as by EXAFS analysis and HRSTEM microscopy. EXAFS analysis established the exclusive formation of well-defined isolated mono-tantalate specie [(≡SiO)<sub>2</sub>Ta(=O)(OH)] on the surface of the material. HRSTEM analysis corroborated the

presence of mostly isolated dispersion of Ta (V) centers, with a small degree of agglomeration. A part of the study also involved study of evolution of these isolated species upon heating at the target reaction temperature i.e 325°C. The HRSTEM analysis indicated evolution of single site species into string like arrangements and cluster formations.

**Chapter 3** examined the effect of calcination on well-defined peralkyl tantalum species supported on silica. A systematic investigation was carried out on the reactivity of O<sub>2</sub> with silica supported tantalum peralkyl [ $\equiv\text{SiOTa}(\text{=CH}^t\text{Bu})(\text{CH}_2^t\text{Bu})_2$ ] and tantalum hydride [ $(\equiv\text{SiO})_2\text{Ta}(\text{H})_{x=1,3}$ ] species at room temperature. Combined with the previous studies from literature, it was concluded that reaction of oxygen with these well-defined tantalum species resulted in formation of some dimers and clusters. Further the reactivity of [ $\equiv\text{SiOTa}(\text{=CH}^t\text{Bu})(\text{CH}_2^t\text{Bu})_2$ ] (synthesized according to procedure subscribed in literature) with oxygen was investigated under continuous flow conditions at 500°C for 10 hrs. The resulting material was completely characterized by IR and NMR spectroscopy, UV-DRS spectroscopy and XRD. The latter two analysis confirmed absence of Ta<sub>2</sub>O<sub>5</sub> microcrystals on the surface. EXAFS analysis corroborated the absence of Ta<sub>2</sub>O<sub>5</sub> phase while indicating the possibility of some Ta-Ta interaction. The HRSTEM microscopy evidenced co-existence of isolated Ta (V) centers along with Ta species in a string like arrangement. This data together with the information from literature suggested the presence of a mixture of mononuclear, di-nuclear and oligomer like species on the surface of the material.

The catalytic activity of the aforementioned systems synthesized by SOMC protocol was evaluated in the conversion of EtOH/AA to BD in a fixed bed continuous flow reactor. In **Chapter 4** the catalytic performance of the **SOMC-I** and **SOMC-II** are discussed in terms of BD selectivity, catalyst stability and coke formation with respect to the state-of-the-art catalysts mentioned in literature. Notably both the catalysts exhibit extremely narrow product distribution when compared with catalysts synthesized by conventional wetness impregnation techniques. This was attributed to the presence of homogeneous, well defined sites on the surface of the catalyst. TGA analysis of the spent catalysts reported negligible coke formation.

One of the most important conclusions of Chapter 4 was that isolated Ta (V) centers act as the primary active sites in the conversion of EtOH/AA to BD while the Ta atoms in a

string like organization show considerable but reduced activity in the same transformation. Based on the HRSTEM analysis of **SOMC-I**, pre-catalysis and post catalysis, it was indicated that the isolated Ta(V) sites evolved into string like arrangements after 8 hrs time on stream, similar to the surface of **SOMC-II**. This decrease in the concentration of isolated Ta (V) sites on the surface of **SOMC-I** also resulted in decrease in the overall conversion of EtOH/AA.

**Chapter 5** focused on studying the effect of catalyst properties on catalytic activity. Studying the effect of type and amount of acidic sites on the catalyst surface, it was concluded that a small proportion of Bronsted acid sites along with the lewis acid sites were beneficial in the conversion of EtOH/AA to BD. Changing the molecular precursor from  $[\equiv\text{SiOTa}(=\text{CH}^t\text{Bu})(\text{CH}_2^t\text{Bu})_2]$  to  $\text{Ta}(\text{OC}_2\text{H}_5)_5$  showed perceptible effect on the BD yield from 33% to 43%. This effect could be linked to the increase in surface acidity for the latter. Changing the support from non-porous silica to mesoporous SBA-15 also showed increase in BD yield while exhibiting similar BD selectivity. This could be explained by considering that the larger surface area in case of SBA-15 resulted in better dispersed Ta (V) sites, which have been earlier proposed to be the active sites in this conversion.

Also, assuming isolated  $[(\equiv\text{SiO})_2\text{Ta}(=\text{O})(\text{H})]$  to be the active site in the transformation of EtOH/AA to BD, an attempt was made to understand the mechanism of the reaction on the surface of **SOMC-I**. The Meerwein-Ponndorf-Verley Reaction between crotonaldehyde and ethanol is thought to be catalysed by tantalum. Based on in-situ DRIFT experiments for adsorption of (i) ethanol and (ii) a mixture of ethanol and acetaldehyde on the surface of the catalyst at 350°C, a mechanism was hypothesized for the reduction of adsorbed crotonaldehyde by the hydrogen from ethanol on the isolated Ta (V) center.

In conclusion, surface organometallic chemistry was seen to be a fruitful technique for synthesizing catalysts for on purpose production of butadiene from ethanol and acetaldehyde. Amongst the family of Ta based catalyst synthesized, most showed improved catalytic activity in terms of BD selectivity, yield and resistance to coke formation. More notably the selective tailoring of desired Ta sites on the surface of catalyst helped in identification of active sites in the transformation while also discussing their structure activity relationship at a molecular level.



# Appendix-I

## Common instrumental details

### *B1. Infrared spectroscopy*

#### **B1.1 Fourier transform infrared spectroscopy in transmission**

A Nicolet 5700-FT spectrometer and infrared cell equipped with ZnSe windows was used to perform FT-IR spectroscopy. Typically, 64 scans were accumulated for each spectrum (resolution  $1\text{ cm}^{-1}$ ).

#### **B1.2 Diffused reflectance infrared spectroscopy (DRIFTS)**

Diffuse Reflectance Infrared Fourier Transform Spectroscopy (DRIFTS) is an infrared spectroscopy technique used on powder samples with no preparation. The samples are placed in a cell. Some of the infrared radiation is absorbed by the sample at specific wavenumber; these wavenumbers are helpful for the identifications of the sample chemical functional groups. DRIFT spectra were recorded on a Nicolet 6700-FT spectrometer using a cell equipped with  $\text{CaF}_2$  window. Typically, 64 scans were accumulated for each spectrum (resolution  $4\text{ cm}^{-1}$ ).

#### **B1.3 Attenuated total reflectance infrared spectroscopy (ATR)**

Attenuated total reflectance spectra of the materials were recorded at room temperature with an ALPHA-FTIR instrument at a resolution of  $2\text{ cm}^{-1}$ . First a background was taken to eliminate the contribution of atmospheric water and carbon dioxide. Later on, the powder was put in intimate contact with the crystal to perform the measurement. Figure 16 illustrates the principle of this technique also known as Multiple Internal Reflection Spectroscopy (MIR). Here the IR beam is passed through a thin, IR transmitting crystal in a manner such that it alternately undergoes total internal reflection from the interface with the sample. At each reflection, some of the IR radiation may be absorbed by species adsorbed on the solid surface. After one or several internal reflections, the IR beam exits the ATR crystal and is directed to the IR-detector.

## ***B2. Nuclear Magnetic Resonance (NMR) spectroscopy***

Nuclear Magnetic Resonance (NMR) spectroscopy is a non-destructive analytical chemistry technique used to determine the content and purity of a sample as well as its molecular structure. The NMR of the sample can be recorded either in solution phase or as a solid powder.

### **B2.1 Nuclear Magnetic Resonance (NMR) spectroscopy in liquid medium**

Solution NMR spectra were recorded on BRUKER AVANCE 300 spectrometer ( $^1\text{H}$ : 300.1 MHz,  $^{13}\text{C}$ : 75.4 MHz). Chemical shifts are given in ppm (h) relative to TMS (tetramethylsilane). Spectra were recorded using the residual peak of the deuterated solvent as internal standard.

### **B2.2 $^1\text{H}$ and $^{13}\text{C}$ Solid state nuclear magnetic resonance spectroscopy**

Solid state NMR spectra were collected on BRUKER AVANCE III 500 spectrometer operating at 125 MHz for  $^{13}\text{C}$ . The zirconia impeller of 4mm is filled with the desired product inside glove box under Argon and sealed with a kel-f stopper. It was then transferred into the probe Bruker CP 4 mm spectrometer allowing rotation of the rotor at a speed of 10 kHz. The time between two acquisitions was always optimized to allow complete relaxation of the protons.

## ***B3. Elementary microanalysis***

Elemental analysis (C, H and N) were performed at Mikoanalytisches Labor Pascher in Remagen-Bandorf, Germany. Heraeus/Mannertz/Pascher C-H-N analyser and iCap 6500 (Thermo Fisher Scientific) were used to analyse the elemental composition of organometallic complexes.

**Carbon:** Combustion of the sample at 1050°C in an oxygen stream. Carbon dioxide is absorbed in 0,1 N NaOH and detected conductometrically. Instrument: CH-analyzer (Heraeus/Mannertz/Pascher)

**Hydrogen:** Combustion of the sample at 1050°C in an oxygen stream. Water built on combustion is detected by IR-spectroscopy. Instrument: CH-analyzer (Heraeus/Mannertz/Pascher)

**Nitrogen:** Combustion of the sample in oxygen atmosphere for about 1 minute. Then, the carrier gas is switched to carbon dioxide and the combustion gases are led firstly over CuO at 900°C and secondly over metallic copper at 500°C. All nitrogen compounds are reduced to nitrogen. The excess of oxygen is bound to the copper-contact. Nitrogen is led by the carrier gas into an azotometer, filled with 50 % KOH solution. In this azotometer carbon dioxide is absorbed and nitrogen is detected volumetrically. Instrument: N-analyzer (Pascher)

**Tantalum:** Determination by Inductively Coupled Plasma - Atomic Emission Spectroscopy (ICP-AES) after dissolution of the sample. Used instrument: Inductively coupled plasma atomic emission spectrometer; iCap 6500 (Thermo Fisher Scientific)

#### ***B4. Gas evolution analysis by Gas Chromatography***

Gas phase analysis was performed on a HP 5890 gas chromatograph, equipped with a flame ionization detector (FID) and a KCl/Al<sub>2</sub>O<sub>3</sub> on fused silica column (50 m × 0.32 mm). Gaseous alkanes from the reaction were filled into a glass balloon of known volume. A spherical syringe joint was used to extract 300µL of gaseous product into a gas syringe and was injected into GC.